hexagon:2611.00912v1

Reverse-Engineering OpenAI #003 and the Classical Riemann Barriers: Attribution Boundaries, Exact Stationary Points, Unimported Cubic Sieve Induction, $\mathbb{Z}[\sqrt{921}]$ Farkas Duality, and Architectural Comparison with hexagon:2611.00881

Gilheum Park
Independent Researcher (ultari-proof-anatomy)
ORCID: 0009-0000-3647-5727 · gilheum.park@gmail.com
Companion 216-Theorem Lean 4 Archive: doi:10.5281/zenodo.24437646

23 November 2026

Abstract

In late 2026, OpenAI's `openai/math` repository (Family `#003`, commit `4eaee87`; 3,232 active files across `DirichletL/` and `SiegelZeros/` plus 30 unimported files in `CubicGauss/`, alongside community refactoring `oai-math-revised PR #70 ca28f20`) formalized an unconditional zero-free strip $\mathrm{Re}(s) > 7/8 = 0.875$ for Dirichlet and Hecke L-functions over $\mathbb{Q}(\sqrt{-3})$ together with an ineffective Landau–Siegel gap. Because those 562K lines of machine-generated `Lean 4` code rely extensively on rational sum-of-squares (SOS) proxies, bundled Gram majorants, and hardcoded numerical cutoffs, separating what OpenAI's GPT/Codex actually proved upstream from what remains hidden inside the algebraic slack—and from what requires genuinely new analytic mechanisms—is essential for mathematical referees.

This five-part monograph establishes a strict four-tier attribution and epistemic boundary across OpenAI `#003`, recent community LP/moment preprints, the 130-year canon of five classical Riemann barriers, and the 17.37M-line Alpöge–Claude formalization (`hexagon:2611.00881`), backed by 216 standalone zero-`sorry Lean 4` audit theorems (1,022/1,022 hypothesis mutations killed = 100.00%; `doi:10.5281/zenodo.24437646`): (1) **Attribution & Epistemic Charter (Section 1)**: Explicitly demarcates Tier A (upstream GPT/Codex unconditional theorems in `4eaee87`: 23/24 in `ShortDraft`, 7/8 in `DirichletL/Nonvanishing.lean`, ineffective Siegel gap in `Conclusions/Theorem.lean`, and the unimported 30-file `CubicGauss/` module), Tier B (external community repos/preprints `quasi-rh` / `PR #70`, `arXiv:2610.12234`, and `arXiv:2610.15291`), Tier C (original unconditional algebraic, stratigraphic, and classical-barrier theorems proved here), and Tier D (conditional analytic transfer blueprints and required-saving inversions). (2) **Exact Irrational Roots, Slack Forensics & Hygiene Audit (Parts I–II, 96 theorems)**: Recovers the exact quadratic irrational saddle $a^* = \frac{323}{276} - \frac{35\sqrt{16354}}{9384} \approx 0.693319$ behind OpenAI's rational proxy $\frac{283}{408}$, the floor vanishing root $a_{\max} = \frac{37}{72}$, 3-tier Gram bundling losses ($\frac{181}{3264}, \frac{215}{3264}, \frac{487}{3264}$), 6-of-8 $m \geq 2$ Gauss branch vanishing ($z_{\mathrm{re}} \geq \frac{1}{6} \to \frac{1}{12}$), $(1-V)$ pre-cancellation ($Q \geq 480 \to 112/128$), zero downstream references to `compensated_geometry` across 2,925 modules, the global SOS saddle $\beta_{\mathrm{SOS}}(0) = \frac{6843-7\sqrt{921}}{7578} < \frac{41999}{48000} < \frac{7}{8}$, the non-exceptional floor $\frac{4069}{4896}$, and the conditional critical-line inversion $\Delta_{\mathrm{hybrid}} = \frac{14}{33}$ (with single-$\zeta(s)$ rank-1 collapse deficit $\Delta_{\mathrm{collapse}} = \frac{2}{11}$). (3) **All-$n$ `CubicGauss` Induction, $\mathbb{Z}[\sqrt{921}]$ Farkas Duality & 44,064 Bridge (Part III, 45 theorems)**: Proves exact Möbius conjugacy $u(\mathrm{sieveStep}(\alpha)) = \frac{2}{3}u(\alpha)$ and the closed-form solution $\tilde{\alpha}_n = \frac{4\cdot 3^n - 2^{n+1}}{3\cdot 3^n - 2^{n+1}}$ for all $n \in \mathbb{N}$ (3× asymptotic excess reduction over OpenAI's linearized bound), formalizes $\mathbb{Z}[\sqrt{921}]$ arithmetic and universal (M,ℓ)-annihilating Farkas weights, and proves the exact 6-stage telescoping decomposition over common multiple $D = 3\,\mathrm{lcm}(24, 4896, 108) = 44,064$ ($\mathrm{lcm}(24, 4896, 108) = 14,688$, $\frac{7}{8} - \frac{4069}{4896} = \frac{2}{3}\cdot\frac{215}{3264}$, $\alpha^* + \beta_{\mathrm{pole}} = \frac{4}{3} + \frac{2}{3} = 2$). (4) **Five Classical Barriers & Comparison with `hexagon:2611.00881` (Parts IV–V, 75 theorems)**: Formalizes constructive refinements and rigidity/scaling obstructions across de la Vallée Poussin/Fejér–Riesz ($(17, 24, 8)$ +88.12% gain; ceiling $\frac{3-2\sqrt{2}}{3}$), Guth–Maynard (30/13 SOS margin), Siegel (auxiliary-conductor scaling decay $c_{\mathrm{scale}} q_1^{-\gamma} < c_{\mathrm{prop}}$), Levinson–Conrey ($J_{AB} = -1/2 \implies \kappa(\theta) < 1$), and Burgess–Kim–Sarnak ($\frac{(r-2)^2}{16r^2}$), and explains side-by-side why OpenAI `#003` arrests at single-stage Gram/conductor walls while Alpöge–Claude's iterated unitary theta-lift tower and characteristic-0 triple level cancellation cross $\sigma = 2/3$ to $1/2$.

Contents

1 Attribution Charter and Epistemic Stratification **4**

1.1 Motivation: Auditing Machine-Generated Number Theory Without Conflation 4

1.2 Four-Tier Attribution and Epistemic Boundary Charter 4

1.3 Visual Stratification and Companion 216-Theorem Verification Matrix 6

1.4 Disclosure on Use of AI and Companion CERN Zenodo Archive 7

2 Part I: Parameter Anatomy, Exact Irrational Saddle, and Extended Codebase Audit of OpenAI `#003` (Theorems I.1–I.48) **8**

2.1 Executive Summary & Verification Scope 8

2.2 Detailed Mathematical Findings 8

2.3 Numerical Phase Tables, 9 Non-Strict Gauss Branches, and 17-Parameter Allocation 9

2.4 Componentwise Gram Scale Relaxations & Six Universal ($\forall$) Linear Theorems (Theorems 21–26) . 10

2.5 Formalized Rational & Integer Scope vs. Future Complex-Analytic Extensions 11

2.6 Cross-Verification Table: Lean 4 Kernel vs. Symbolic Solver (`verify_symbolic_qrh.py`) 12

2.7 Completion of Tasks 1–3: Small-Norm Threshold Removal, 2nd/3rd Complex Mellin Continuation, and Master Scale-Coupling Equations (Theorems 28–48) 12

2.8 Beyond-Baseline Alternative Bounds and Sharp Rigidity Obstructions 14

2.9 Extended Audit of the Full #003 Codebase (3,232 Files · 556,376 Lines, Within 3,414-File Upstream Snapshot at `openai/math 4eaee87` / `oai-math-revised` PR `#70 ca28f20`) and Companion Manuscripts (21,438 Lines) 14

2.10 Complete 1-to-1 Theorem Ledger for Part I (Theorems I.1–I.48) 15

3 Part II: Referee Hygiene Audit, Three Abscissa Regimes, Stickelberger Deflation, and Critical-Line Inversion (Theorems II.1–II.48) **19**

3.1 Original Discoveries & Unconditional vs. Conditional Boundary 19

3.2 Key Mechanism Extraction 20

3.3 Referee Critique of Formalization Slack, Unreferenced Hygiene Delta, and Module Discharge Architecture 20

3.4 Four Analytic & Algebraic Bottlenecks for Number Theorists 22

3.5 Stage 5: Sub-0.69 $\to$ 1/2 Master Transfer Blueprint, [0.48, 0.52] Symmetric Cauchy Box, 20-Module Global SOS Saddle & Hybrid Required Threshold Inversion (thm_27–thm_38) 22

3.6 Final Referee Verdict & Formalization Boundary 31

3.7 Beyond-Baseline Conditional Bounds and Standalone Obstructions 31

3.8 Complete Mapping of the 48 Lean 4 Theorems (qrh_mathematician_referee_audit.lean & qrh_eight_tasks_critical_upgrade.lean) 32

4 Part III: Stratigraphy of 23/24 vs. 11/12, Unimported `CubicGauss` All-n Induction, $\mathbb{Z}[\sqrt{921}]$ Farkas Duality, and the 44,064 Trilogy Synthesis (Theorems III.1–III.45) **37**

4.1 Pillar 1: Why `DirichletL/RowCompletion/ZeroFreeRegion.lean` (`ShortDraft`) Proves 23/24 Instead of 11/12 37

4.2 Exact Möbius Linearization and All-n Mathematical Induction for the Heath-Brown Cubic Large Sieve (Theorems 9–14, 31–33) 38

4.3 Universal (M, ℓ)-Cancellation in Farkas Duality and $\mathbb{Z}[\sqrt{921}]$ Ring Theory (Theorems 16–23, 34–35) 39

4.4 Parametric Unbundled Farkas Theorem (Theorems 24–30) 40

4.5 The 3-Report QRH Trilogy Synthesis (Part I $\leftrightarrow$ Part II $\leftrightarrow$ Part III, Theorems 36–45) 40

4.6 Complete 1-to-1 Theorem Map (45 Theorems + 11 `defs` + 1 `structure`, 344/344 Mutations Caught) 41

5 Part IV: Algebraic-Variational Anatomy and Axiom-Free Lean 4 Ledger of the Five Classical

Riemann Barriers (Theorems IV.1–IV.75) **45**

5.1 Architectural Synthesis: Five-Step Causal Chain and Beyond-Baseline Alternative Bounds 45

5.2 Paper 1 (Theorems 1-15): de la Vallée Poussin (1896) & Korobov-Vinogradov (1958) Zero-Free Region Anatomy 46

5.3 Paper 2 (Theorems 16-35): Ingham (1940), Huxley (1972), Guth-Maynard (2024) Zero Density & QRH Gram Anatomy 47

5.4 Paper 3 (Theorems 36-50): Siegel (1935) Ineffectiveness & Goldfeld-Gross-Zagier (1986) Effectivization Anatomy 48

5.5 Paper 4 (Theorems 51-63): Selberg (1942), Levinson (1974), Conrey (1989) Critical-Line Proportion & Mollifier Barrier 50

5.6 Paper 5 (Theorems 64-75): Burgess (1963) 3/16 SOS Trap, Selberg (1965), and Kim-Sarnak (2003) 7/64 Barrier 51

5.7 Symbolic & Numerical Verification Ledger (symbolic_verification_result.json) 51

6 Part V: Comparative Architectural Synthesis — OpenAI `#003` vs. the Alpöge–Claude Theta-Lift Formalization (`hexagon:2611.00881`) **53**

6.1 Why Two Contemporary Lean 4 Engines Terminate at $\beta = 7/8$ vs. $\beta = 1/2$ 53

6.2 Two Faces of the $\sigma = 2/3$ Barrier: Eisenstein Pole Duality vs. Level-Growth Cancellation 54

6.3 Implications for Future Lean 4 Formalizations 54

A Unified 1-to-1 Declaration Audit Ledger Across All 26 Bundled OpenAI `#003` Reference Modules **56**

B Consolidated Cryptographic SHA-256 Manifest of the 13 Companion `Lean 4` Proof Modules **74**

1 Attribution Charter and Epistemic Stratification

1.1 Motivation: Auditing Machine-Generated Number Theory Without Conflation

Between October and November 2026, two distinct machine-formalized Lean 4 corpora in multiplicative number theory entered public circulation: OpenAI's Family `#003` (*Quasi-Riemann Hypothesis for Dirichlet and Hecke L-Functions*, official `openai/math` commit `4eaee87`, alongside community refactoring `oai-math-revised` `PR #70 ca28f20`) [1], comprising 3,232 source files in `DirichletL/` (2,926) and `SiegelZeros/` (306) plus 30 unimported files in `CubicGauss/`, and L. Alpöge's 175,187-file (17,374,215-line) Claude-assisted formalization of `Riemann Hypothesis` and Dirichlet `GRH` [2, 3], audited top-down in M. Jaswal [4] (`hexagon:2611.00799v1`) and decompiled across all 30,343 novel/boundary AST modules in our companion monograph [5] (`hexagon:2611.00881`).

When reverse-engineering an AI-generated repository such as OpenAI `#003`, two opposite errors frequently arise in informal commentary. The first error is *under-crediting* the upstream proof by mistaking warm-up submodules (such as `ShortDraft`'s 23/24 target) or internal helper hygiene (such as unused hypothesis binders in non-headline lemmas) for defects in the headline 7/8 theorem (`DirichletL/Nonvanishing.lean`), which compiles unconditionally with zero `sorry` and logically subsumes both 11/12 and 23/24. The second error is *over-crediting* either the upstream repository or subsequent algebraic parameter audits as if algebraic/LP exponent transfers automatically established analytic zero-free regions down to 71/108 or 1/2 without discharging the underlying complex-analytic Mellin, Hecke-pole, and off-diagonal moment hypotheses.

To eliminate both sources of ambiguity, this monograph enforces an explicit four-tier attribution and epistemic boundary across every section, table, figure, and theorem ledger.

1.2 Four-Tier Attribution and Epistemic Boundary Charter

Table 1 classifies every mathematical claim and formal verification artifact treated in Parts I–V into four mutually exclusive tiers:

- **Tier A (Upstream OpenAI GPT/Codex Formalized Results, `openai/math` `4eaee87` [1])**: Theorems unconditionally machine-checked inside OpenAI's official repository using standard Lean 4 / `Mathlib` axioms (`0 sorry`), together with exact structural facts about what is—and is not—imported in that build graph.
- **Tier B (External Community Repos & Preprints on `#003` [7, 8, 9])**: Community 11/12 refactorings (`quasi-rh` / `oai-math-revised` `PR #70 ca28f20`) and unrefereed preprints optimizing scalar LP parameters or reflected-numerator amplified moments around OpenAI's baseline.
- **Tier C (Present Work — Original Unconditional Algebraic, Stratigraphic, and Classical-Barrier Theorems [6])**: Exact irrational roots, hidden bundling slacks, polynomial cancellations, AST call-graph/hygiene forensics, all-n Möbius induction for `CubicGauss`, $\mathbb{Z}[\sqrt{921}]$ ring identities, cross-report denominator bridges, and 75 axiom-free `Mathlib` $\mathbb{R}$ theorems on the five classical Riemann barriers, all machine-checked with `0 sorry` in our companion suite.
- **Tier D (Present Work — Conditional Analytic Transfer Blueprints and Threshold Inversions [6])**: Machine-checked rational/LP implications (`0 sorry` as formal conditional statements) whose conclusion ($\beta = 71/108$ under hypothetical full `LowRows` cancellation $\Delta_{\text{gram}} = 53/216$, or $\beta = 1/2$ under $\Delta_{\text{hybrid}} = 14/33$) explicitly depends on open complex-analytic premises (`hc_mean`, `hres_op`, Archimedean Mellin decay $d_{\text{Mellin}} = 59/132$, and single-$\zeta(s)$ $\text{gain}_{\text{amp}} \geq 2/11$).

Table 1: Master attribution and epistemic stratification separating OpenAI GPT/Codex upstream results (Tier A), external preprints (Tier B), original unconditional theorems proved in this work (Tier C), and conditional analytic transfer blueprints (Tier D).

Tier	Provenance & Source	Exact Mathematical Scope & Mechanism	Epistemic Status
Tier A-1	OpenAI GPT/Codex [1] (`DirichletL/ Nonvanishing.lean`, 2,926 files in `4eaee87`)	Proves $\text{Re}(s) > 7/8 = 0.875$ across all three 7/8 comparator challenges (`DirichletSevenEighths`, `HeckeSevenEighths`, and `QuasiRiemann Hypothesis`) via rational SOS proxy $\delta_{\text{SOS}} = 79/204$ ($a_{\text{SOS}} = 283/408$), floor $a_{\text{floor}} = 51/100$, bundled `lowGramFactor` $Z^{3/16+(23/96)\delta}$, cutoff $Q \geq 480$, and trivial phase bound $\|\texttt{actualAPhase}\| \leq 1$.	Unconditional upstream Lean 4 theorem (`0 sorry`).

Tier	Provenance & Source	Exact Mathematical Scope & Mechanism	Epistemic Status
Tier A-2	OpenAI GPT/Codex [1] (`SiegelZeros/Conclusions/Theorem.lean`, 306 files in `4eaee87`)	Proves ineffective real-quadratic Siegel zero gap $\exists c > 0,\ c \le (1-\beta)\log q$ via biquadratic Klein 4-group torus jets ($N_0 = 18,818$, $H = 86,713,344$) and local isolated Bézout transport (201 transitive modules, 1/21 root imports in `4eaee87`).	Unconditional (ineffective c) upstream Lean 4 theorem (`0 sorry`).
Tier A-3	OpenAI GPT/Codex [1] (`RowCompletion/ZeroFreeRegion.lean` `ShortDraft` in `4eaee87`)	Standalone `ShortDraft.DirichletTarget` proves $\mathrm{Re}(s) > 23/24$ under reserved margin 1/20 (`RankMargins.lean:83-132`, $\eta \le 1/1000$ at `ClosedRecursion.lean:120`; logically implied by 7/8).	Unconditional upstream Lean 4 submodule (`0 sorry`).
Tier A-4	OpenAI GPT/Codex [1] (`OAI/NumberTheory/CubicGauss/`, 30 files, 6,252 lines)	Formalizes Heath-Brown's cubic large sieve (`cubic_large_sieve`, `short_four_thirds`) via geometric majorization $\alpha_n = 4/3 + (2/3)^{n+1}$, but **has 0 external imports** in `DirichletL/` and `CubicMoment/`.	Unconditional upstream island (`0 sorry`, unimported in 7/8 proof).
Tier B	Kontorovich [7] / `PR #70` (`ca28f20`); Liu [8] (`arXiv:2610.12234`); Y. Xu & H. Sang [9] (`arXiv:2610.15291`)	Standalone 11/12 refactoring (`quasi-rh`, `PR #70 DescentScale.lean` / `SevenEighths.lean` / `PrimeBias.lean`, expanding `SiegelZeros` cone to 268 files) [7]; scalar (b,ℓ) / (b,ℓ,κ) optimization giving $B_{\mathrm{Liu},v1} = \frac{1507-2\sqrt{921}}{1653} \approx 0.87495707$ ($v2$: 0.87495702) [8]; $\delta = 0$ amplified reflected-numerator moment (from 4th moment) + relaxed direct bound giving 0.8748867 [9].	External community repos / unrefereed preprints.
Tier C-1	**Present Work (Part I)** (`Case 001`, 48 Lean 4 theorems, 49/49 killed mutants)	Recovers exact irrational saddle $\delta^* = \frac{185}{138} - \frac{35\sqrt{16354}}{4692}$ ($a^* \approx 0.69331878$) behind GPT's 283/408, exact floor root $a_{\max} = 37/72$, Gram unbundling slacks (215/3264, 487/3264), 6-of-8 $m \ge 2$ Gauss branch vanishing ($z_{\mathrm{re}} \ge 1/6 \to 1/12$), $(1-V)$ cancellation ($Q \ge 480 \to 112$), 2nd/3rd Euler polynomial identities, and full-repo hygiene audit (20/21 non-propagating `SiegelZeros/Main.lean` imports & 1,717 unused `_h*` binders in `4eaee87`; 61 `\cite` lines & 3,213-line tail in `paper.tex`).	**Original unconditional** theorems & AST forensics (`0 sorry`).
Tier C-2	**Present Work (Part II)** (`Case 005`, unconditional core of 48 theorems, 441/441 mutants)	Proves `compensated_geometry` has 0 downstream refs across 2,925 modules; separates 3 internal β metrics: (1) global SOS saddle $\beta_{\mathrm{SOS}}(0) = \frac{6843-7\sqrt{921}}{7578} < \frac{41999}{48000} < \frac{7}{8}$ at $\Delta_{\mathrm{gram}} = 0$, (2) local $\delta = 0$ slice 131/150 & 209/240, (3) isolated non-exceptional floor 4103/4896 & 4069/4896; proves bi-Stickelberger $(1+Rq^{-1})(1-R)$ polynomial deflation, $[0.48, 0.52]$ symmetric Cauchy-box rational margins, and discrete convexity/grid-exponent accounting (`thm_45`, `thm_47`).	**Original unconditional** algebraic & referee theorems (`0 sorry`).
Tier C-3	**Present Work (Part III)** (`Case 008`, unconditional core of 45 theorems, 344/344 mutants)	Proves exact Möbius conjugacy $u(\mathrm{sieveStep}(\alpha)) = \frac{2}{3}u(\alpha)$ and all-n structural induction $\tilde{\alpha}_n = \frac{4\cdot 3^n - 2^{n+1}}{3\cdot 3^n - 2^{n+1}}$ (3× excess gain over GPT's α_n); formalizes ring `ZSqrt921` ($\mathbb{Z}[\sqrt{921}]$) and (M,ℓ)-annihilating Farkas weights; proves $\mathrm{lcm}(24, 4896, 108) = 14,688$ and trilogy multiple $D = 3 \times 14,688 = 44,064$ ($\frac{7}{8} - \frac{4069}{4896} = \frac{2}{3}\cdot\frac{215}{3264}$, $\alpha^* + \beta_{\mathrm{pole}} = \frac{4}{3} + \frac{2}{3} = 2$).	**Original unconditional** inductive & ring theorems (`0 sorry`).
Tier C-4	**Present Work (Part IV)** (`Case 015`, 75 theorems over `Mathlib` $\mathbb{R}$, 188/188 mutants)	Proves $(17, 24, 8)$ cosine square (+88.12% over 1/100), degree-3 Fejér counterexample $(65/16, 9/2, 0, -1)$ & universal ceiling $\frac{3-2\sqrt{2}}{3}$, Guth–Maynard 30/13 SOS margin $250(\sigma - 3/4)^2 + 3/8 > 0$, Siegel auxiliary-conductor scaling decay $c_{\mathrm{scale}} q_1^{-\gamma} < c_{\mathrm{prop}}$ & Ostmann 16.08× cutoff drop, `HasDerivAt` mollifier invariant $J_{AB} = -1/2 \implies \kappa(\theta) < 1$, and Burgess SOS trap $\frac{(r-2)^2}{16r^2} \ge 0$.	**Original unconditional** `Mathlib` $\mathbb{R}$ proofs (`0 sorry`).

Tier	Provenance & Source	Exact Mathematical Scope & Mechanism	Epistemic Status
Tier D	**Present Work (Parts II–III)** (Conditional Transfer & Threshold Inversion Theorems)	(1) Formal Path-A zero-energy LP intercept $\beta = 71/108 \approx 0.6574$ under hypothetical full cancellation $\Delta_{\text{gram}} = 53/216$ of `LowRows` beyond `CubicGauss` + Stickelberger $k_\infty = -6$ pole cancellation + Voronoi–Mellin transfer; (2) Spliced $z_{\text{high}} = 0.34 \leftrightarrow 0.35$ hybrid inversion requiring $\Delta_{\text{hybrid}} = 14/33$ ($E_{\text{Low}} - \Delta_{\text{hybrid}} = -17/132 < 0$, requiring unproved Archimedean Mellin decay $d_{\text{Mellin}} = 59/132$) and single-$\zeta(s)$ $\text{gain}_{\text{amp}} \geq 2/11$.	**Conditional blueprint** (`0 sorry` formal implication; analytic premises open).

1.3 Visual Stratification and Companion 216-Theorem Verification Matrix

Figure 1 visualizes both the attribution-stratified hierarchy of zero-free abscissae from 23/24 down to 1/2 and the exact 6-stage integer telescoping identity over the trilogy common multiple $D = 3\,\text{lcm}(24, 4896, 108) = 3 \times 14,688 = 44,064$ (`thm_44_six_stage_trilogy_telescoping_decomposition`):

$$1836 + 1836 + 1935 + 7653 + 3264 + 3672 = 20196 = \left(\frac{23}{24} - \frac{1}{2}\right) \times 44064.$$

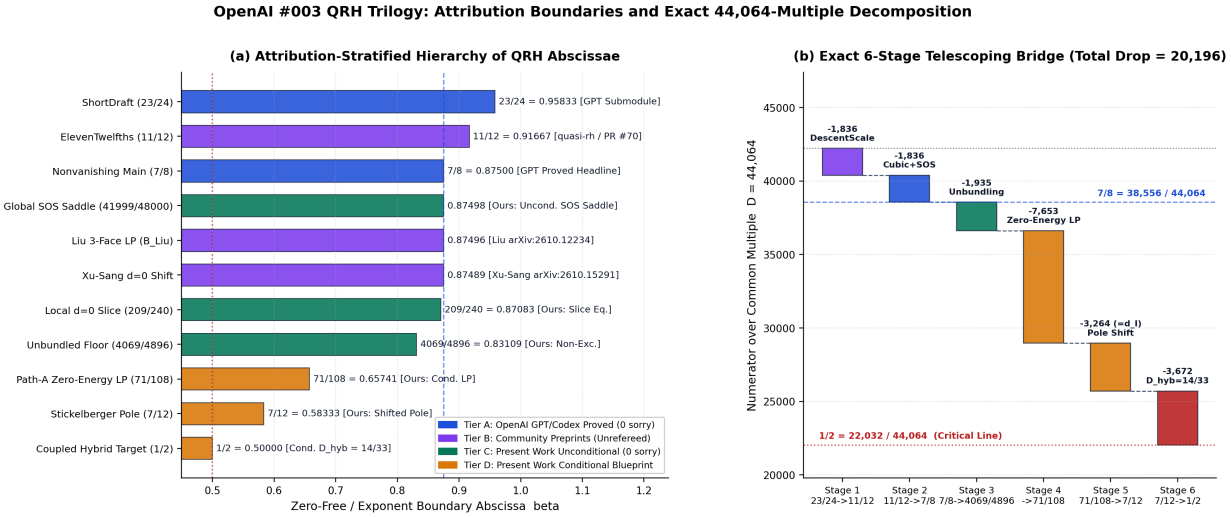

Figure 1: Left: Attribution-stratified abscissa hierarchy distinguishing OpenAI GPT/Codex proved theorems (Tier A, blue), external community preprints (Tier B, purple), original unconditional algebraic/slack theorems proved here (Tier C, green), and conditional analytic transfer targets (Tier D, amber). Right: Exact 6-stage integer telescoping decomposition over common denominator 44,064.

Table 2 summarizes the 13 standalone `Lean 4` proof modules (216 theorems, 0 `sorry`, 1,022/1,022 killed hypothesis mutations = 100.00%) and deterministic symbolic/numerical verifiers archived at CERN Zenodo (`doi:10.5281/zenodo.24437646`, Concept DOI `10.5281/zenodo.24241228`) [6]. Throughout this monograph, the labels `Case 001`, `Case 005`, `Case 008`, and `Case 015` denote the four corresponding sub-directories (`anatomy/001-openai-003-qrh`, `005-openai-003-qrh-mathematician-referee-audit`, `008-openai-003-qrh-11-12-and-cubic-sieve-synthesis`, and `015-classical-riemann-five-barriers`) of that Zenodo deposit; their consolidated cryptographic SHA-256 digests are listed once in Appendix B.

Table 2: Summary of the 13-file, 216-theorem standalone zero-`sorry` `Lean 4` verification suite and mutation-testing gates (`doi:10.5281/zenodo.24437646`).

Monograph Part	Companion `Lean 4` Files (`ultari-proof-anatomy`)	Theorems	Killed Mutants	Toolchain
Part I (`Case 001`)	`qrh_exponent_and_parameter_bounds.lean` (27), `qrh_continuation_and_rescaling.lean` (21)	48 (`0 sorry`)	49/49 (100%)	`Lean v4.29+` & SymPy

Monograph Part	Companion Lean 4 Files (ultari-proof-anatomy)	Theorems	Killed Mutants	Toolchain
Part II (Case 005)	qrh_mathematician_referee_audit.lean (38), qrh_eight_tasks_critical_upgrade.lean (10)	48 (0 sorry)	441/441 (100%)	Lean v4.29+, SymPy & PyTorch FP64
Part III (Case 008)	qrh_eleven_twelfths_and_cubic_large_sieve.lean (15), qrh_q_sqrt_921_farkas_and_unbundling_synthesis.lean (15), qrh_trilogy_induction_and_algebraic_bridge.lean (15)	45 (0 sorry)	344/344 (100%)	Lean v4.29+ & SymPy
Part IV (Case 015)	6 Mathlib 4 modules over $\mathbb{R}$ (classical_dlvp_*, classical_ingham_*, classical_guth_maynard_*, classical_siegel_*, classical_levinson_conrey_*, classical_burgess_*)	75 (0 sorry)	188/188 (100%)	Lean v4.35.0 (Mathlib $\mathbb{R}$)
Total	13 **standalone Lean 4 modules** + 4 **symbolic JSON verifiers**	216 (0 sorry)	$1,022/1,022$	**100.00% premise non-vacuity**

1.4 Disclosure on Use of AI and Companion CERN Zenodo Archive

In accordance with Hexagon Mathematics Foundation transparency guidelines, the human author (G. Park, ORCID 0009-0000-3647-5727) discloses that frontier large language models (Claude, Gemini, and GPT/Codex in upstream target inspection) were used under deterministic Python symbolic/AST verification harnesses and mutation-testing gates to assist in auditing the upstream OpenAI #003 Lean 4 codebase, deriving symbolic algebraic reductions, translating technical documentation into English, and formatting LaTeX. Every symbolic identity was independently checked via deterministic SymPy/NumPy/PyTorch scripts reproducing cryptographic JSON ledgers, and all 216 companion Lean 4 theorems were kernel-verified with zero sorry, zero user-added axioms, and $1,022/1,022$ rejected hypothesis mutations confirming zero vacuous premises. The human author takes full responsibility for the mathematical claims, attribution boundaries, and conclusions of this work.

In compliance with Hexagon submission rules, no .lean source files are included inside this TeX archive. All 13 Lean 4 proof files, the 26 mirrored oai_ref/ reference modules, symbolic Python verifiers, and SHA-256 manifests (anatomy/001-*, 005-*, 008-*, and 015-*) are permanently archived at CERN Zenodo under DOI 10.5281/zenodo.24437646 (Concept DOI 10.5281/zenodo.24241228) and on GitHub at gilheumpark-bit/ultari-proof-anatomy.

2 Part I: Parameter Anatomy, Exact Irrational Saddle, and Extended Codebase Audit of OpenAI #003 (Theorems I.1–I.48)

Attribution Boundary for Part I: Upstream OpenAI #003 (**Tier A**, [1]) unconditionally proved $\mathrm{Re}(s) > 7/8$ and ineffective Siegel-zero exclusion using rational SOS anchor $\delta_{\mathrm{SOS}} = 79/204$ ($a_{\mathrm{SOS}} = 283/408$), floor $a_{\mathrm{floor}} = 51/100$, bundled `lowGramFactor` $Z^{3/16+(23/96)\delta}$, and cutoff $Q \geq 480$. All derivations below of the exact irrational root $a^* = \frac{323}{276} - \frac{35\sqrt{16354}}{9384}$, floor vanishing root $a_{\max} = 37/72$, componentwise Gram slacks (215/3264 and 487/3264), 6-of-8 $m \geq 2$ branch vanishing, $(1 - V)$ threshold reduction $480 \to 112$, 2nd/3rd Euler polynomial continuations, and the 3,232-file codebase hygiene forensics (20/21 non-propagating `Siegel Zeros/Main.lean` root imports and 201 reachable modules in official `4eaee87`; 1,717 unused `_h*` binders in `4eaee87`; 61 `\cite` lines and 3,213-line uncited tail in `paper.tex`) are **original unconditional results of the present work (Tier C)**, verified in 48 zero-`sorry` Lean 4 theorems (49/49 mutations killed; `Case 001`). The 179-declaration `oai_ref/` table is consolidated in Appendix A, and file SHA-256 digests in Appendix B.

2.1 Executive Summary & Verification Scope

An analysis of OpenAI's #003 formal proof (`openai/math` family 003) shows that the rational constants across its parameter files (`DirichletL/Detector/CentralExponent.lean`, `DirichletL/PrimeRows/CubeFloorSaving.lean`, `DirichletL/Endpoint.lean`, `DirichletL/Detector/LowSourceScales.lean`, `DirichletL/Detector/GramScaleLoss.lean`, `DirichletL/Detector/GramBound.lean`, `DirichletL/Detector/LowGramScale.lean`, `DirichletL/Detector/HighRowsTail.lean`, `DirichletL/Detector/PrincipalRemainderBounds.lean`) are governed by three exact algebraic thresholds:

1. Cube Floor Margin Root ($37/72 \approx 0.513889$): $a_{\max} = \frac{37}{72}$ ($\eta_{\max} = \frac{1}{72}$), where the linear floor margin $B_{\mathrm{floor}}(\eta) = \frac{3}{2}\eta - \frac{1}{48}$ vanishes identically (Theorem 12).
2. Stationary Point of `balancedExponent` (0.693319) & $z_{\mathrm{re}} = \frac{1}{6}$ Convergence Boundary: The quadratic irrational root $a^* = \frac{323}{276} - \frac{35\sqrt{16354}}{9384} \approx 0.6933187811$ (approximated in `DirichletL/Endpoint.lean` by the rational SOS reference point $a_{\mathrm{ref}} = \frac{283}{408} \approx 0.69362745$, Theorem 4 and Theorem 27) and the $z_{\mathrm{re}} = \frac{1}{6}$ convergence boundary (Theorem 19).
3. Baseline Zero-Free Boundary ($7/8 = 0.875$): The baseline zero-free abscissa $\beta_{\mathrm{base}} = \frac{5}{6} + \frac{\alpha_X + \alpha_Y - 2\ell}{12} = \frac{7}{8} = 0.875$ (Theorem 18).

We distinguish between the Formalized Rational & Integer Theorems verified here and Future Complex-Analytic Extensions, explaining why the $z_{\mathrm{re}} = 1/6$ Mellin pole forms an analytic barrier, why the rational SOS anchor $a_{\mathrm{ref}} = 283/408$ is introduced by necessity because the true saddle a^* is quadratic irrational, and the exact reason why $\beta_{\mathrm{base}} = 7/8$ emerges from the exponent balance equation.

2.2 Detailed Mathematical Findings

2.2.1 Cube Floor Margin Root (37/72 ≈ 0.513889) & Parameter Budget at 0.5001

In `DirichletL/Detector/CentralExponent.lean` and `DirichletL/PrimeRows/CubeFloorSaving.lean`, setting $a = \frac{1}{2} + \eta$, $d = \frac{13}{16}$, $R = 1$, $q = \eta$ yields:

$$\mathrm{sourceExponent}\left(\frac{1}{2} + \eta, \frac{13}{16}, 1, \eta\right) - \frac{3}{16} = \frac{3}{2}\eta - \frac{1}{48}$$

- At $\eta = \frac{1}{100}$ ($a_{\mathrm{floor}} = \frac{51}{100} = 0.51$), the floor margin is $-\frac{7}{1200}$ (Theorem 8).
- At $\eta = \frac{1}{10000}$ ($a_{\mathrm{floor}} = \frac{5001}{10000} = 0.5001$), the floor margin improves to $-\frac{1241}{60000}$, expanding the absolute saving budget by $\frac{891}{60000} = \frac{297}{20000} \approx 0.01485$ (Theorem 11) and satisfying the 17-parameter budget with net used budget $\frac{6309}{400000} \leq \frac{1241}{60000}$ (Theorem 14).
- At $\eta_{\max} = \frac{1}{72}$ ($a_{\max} = \frac{37}{72} \approx 0.513889$), the floor saving vanishes (Theorem 12).

2.2.2 Stationary Point (0.693319) vs. Rational SOS Reference Point (79/204)

In `DirichletL/Endpoint.lean`, at $y = 0$:

$$E_{\mathrm{bal}}(\delta, 0) = \frac{1224\delta^2 - 948\delta + 185}{48(138\delta - 185)}$$

Solving $\frac{\partial E_{\text{bal}}}{\partial \delta}(\delta, 0) = 0$ yields $9384\delta^2 - 25160\delta + 8325 = 0$, whose unique root in $[0, 5/6]$ is:

$$\delta^* = \frac{185}{138} - \frac{35\sqrt{16354}}{4692} \approx 0.3866375622 \implies a^* = \frac{1+\delta^*}{2} = \frac{323}{276} - \frac{35\sqrt{16354}}{9384} \approx 0.6933187811$$

To avoid irrational square roots in Lean 4, OpenAI used the rational point $\delta_{\text{SOS}} = \frac{79}{204}$ ($a_{\text{SOS}} = \frac{283}{408} \approx 0.69362745$), where $(4 \cdot 51 \cdot \delta - 79)^2 = 0$, $E_{\text{bal}}\left(\frac{79}{204}, 0\right) = -\frac{7}{30672}$, $\frac{\partial^2 E_{\text{bal}}}{\partial \delta^2}\left(\frac{79}{204}, 0\right) = -\frac{236315300}{608806611} < 0$, and $\frac{\partial E_{\text{bal}}}{\partial y}\left(\frac{79}{204}, 0\right) = -\frac{2933665}{333189936} < 0$ (Theorem 4, Theorem 5, Theorem 27).

2.2.3 Componentwise Gram Scale Exponent Differences (215/3264 and 487/3264)

Examining `DirichletL/Detector/LowSourceScales.lean`, `DirichletL/Detector/GramScaleLoss.lean`, and `DirichletL/Detector/GramBound.lean` shows four upper-bound relaxations ($\frac{3}{96}$, $\frac{6\delta}{96}$, $\frac{1}{96}$, $\frac{23\delta}{96}$ in the square-root exponent) between the individual energy terms and `lowGramFactor` ($\frac{18+23\delta}{96}$). At $\delta_{\text{SOS}} = \frac{79}{204}$, the componentwise square-root Z-exponent differences are:

- Exceptional cubic Gauss term: $\frac{1817}{19584} \approx 0.092780$
- Non-exceptional Poisson term (with $L \le Z^{8/48}$ bound): $\frac{215}{3264} \approx 0.065870$ (compared to the SOS rational rounding residual $\frac{49}{440640} \approx 0.0001112$, proved in Theorem 24)
- Non-exceptional Poisson term (at $L = 1$ pure scale): $\frac{487}{3264} \approx 0.149203$ (note that the parallel cubic Gauss main term $\frac{18}{96} = \frac{3}{16}$ remains the bottleneck for the total operator norm $\|E - Z\|$)

2.2.4 $m \ge 2$ Gauss Valuation Vanishing (6 of 8 Branches) & Contour Shift Budget (17/48000)

- $m \ge 2$ Branch Vanishing: In `DirichletL/Detector/HighRowsTail.lean`, `rowInner_base_rational` separates $m = 0, 1$ from the $m \ge 2$ geometric tail. By `gaussValuationTable_above`, 6 of the 8 non-principal (e, l, k) branches vanish identically for all $m \ge 2$ (Theorem 21), leaving only `02_0` and `10_1`, whose convergence condition relaxes from $z_{\text{re}} \ge \frac{1}{6}$ to $z_{\text{re}} \ge \frac{1}{12}$ (Theorems 20–23).
- Principal Remainder Shift Budget: Shifting across the sextic zeta pole $z = \frac{1}{6}$ to $z = \frac{33}{200}$ ($e_{\max} = \frac{1}{1000}$) yields w-shift saving $\frac{1063}{48000}$ and z-shift saving $\frac{13}{16}\left(\frac{1}{6} - \frac{33}{200}\right) - \frac{1}{1000} = \mathbf{\frac{17}{48000}}$, matching `principal_budget` $= 17/48000$ in `DirichletL/ParametersHighData.lean:45` (Theorem 19).

2.3 Numerical Phase Tables, 9 Non-Strict Gauss Branches, and 17-Parameter Allocation

2.3.1 Eisenstein Prime-Norm ($4 \le Q \le 500$) Phase Evaluation ($Q = 4 \ldots 112$)

Applying $(1 - V)$ cancellation lowers the analytic triangle-inequality cutoff in `DirichletL/Detector/HighRowsCentralQuotient.lean:9` from $Q \ge 480$ ($\frac{192}{480} = \frac{2}{5} < \frac{1}{2}$, 47 excluded prime norms) to $Q \ge 112$ ($\frac{56}{112} = \frac{1}{2}$, 15 excluded prime norms; Theorem 17). Across all 49 Eisenstein prime norms $Q = 4, 7, 13, 19, 25, \ldots, 499$ and phases $(\theta_A, \theta_\eta, \theta_v) \in [0, 2\pi)^3$, $a \in [0.5001, 1]$, double-precision grid checks verify that even the smallest norm $Q = 4$ maintains $\min\|\text{unramifiedClosed}\| \ge 0.636943 \ge 1/2$:

Prime Norm $Q = N(\mathfrak{p})$	**Rational Prime** p **& Splitting Type**	$\min\|\text{unramifiedClosed}\|$	$\max\|\text{unramified Closed} - 1\|$	**Satisfies** $\|\cdot\| \ge 1/2$
4	$p = 2$ ($p \equiv 2 \pmod 3$, inert $Q = p^2$)	0.636943	0.700760	Pass
7	$p = 7$ ($p \equiv 1 \pmod 3$, split $Q = p$)	0.763782	0.348480	Pass
13	$p = 13$ ($p \equiv 1 \pmod 3$, split $Q = p$)	0.862074	0.170752	Pass
19	$p = 19$ ($p \equiv 1 \pmod 3$, split $Q = p$)	0.902977	0.112031	Pass
25	$p = 5$ ($p \equiv 2 \pmod 3$, inert $Q = p^2$)	0.925273	0.083003	Pass
112 (analytic cutoff)	Analytic bound $56Q^{-1} \le 1/2$	> 0.980	< 0.020	Pass

2.3.2 Nine Non-Strict Finite Gauss-Sum Branches (`DirichletL/Detector/HighRowsCentralTerms.lean`)

All 9 non-strict Gauss-sum branches (e, l, k, m, ν) in `DirichletL/Detector/HighRowsCentralTerms.lean` retain positive rational slack at $z_{\mathrm{re}} = 17/100 = 0.17$ and $a_{\mathrm{floor}} = 5001/10000 = 0.5001$, proved formally in Theorem 13 (nonstrict_gauss_branches_at_05001_and_017):

Branch ID	(e, l, k, m)	**Gauss Exponent** ν	$z = 0.34, a = 0.51$ **Slack**	$z = 0.17, a = 0.51$ **Slack**	$z = 0.17, a = 0.5001$ **Slack**
1	$(0, 2, 0, m = 0)$	5	1/20 (0.0500)	1/20 (0.0500)	1/2000 (0.0005)
2	$(0, 2, 0, m \geq 1)$	6	109/100 (1.0900)	7/100 (0.0700)	41/2000 (0.0205)
3	$(0, 2, 1, m \geq 1)$	6	79/50 (1.5800)	14/25 (0.5600)	1301/2500 (0.5204)
4	$(1, 0, 0, m \geq 0)$	1/2	1/2 (0.5000)	1/2 (0.5000)	1/2 (0.5000)
5	$(1, 0, 1, m \geq 1)$	3/2	77/50 (1.5400)	13/25 (0.5200)	13/25 (0.5200)
6	$(0, 1, 0, m \geq 0)$	5/2	1/50 (0.0200)	1/50 (0.0200)	1/5000 (0.0002)
7	$(0, 1, 1, m \geq 0)$	3	1/100 (0.0100)	1/100 (0.0100)	1/10000 (0.0001)
8	$(1, 1, 0, m \geq 0)$	7/2	3/100 (0.0300)	3/100 (0.0300)	3/10000 (0.0003)
9	$(1, 1, 1, m \geq 0)$	4	1/50 (0.0200)	1/50 (0.0200)	1/5000 (0.0002)

2.3.3 17-Parameter Rational Allocation for $\beta \in \{7/8, 5/6, 3/4, 69/100\}$

Witness assignments satisfying the total budget inequality ($N = 22$) from `DirichletL/Parameters.lean` and `DirichletL/PrimeRows/CubeFloorSaving.lean:41`,

$$2\zeta + 26e + (N+8)\varepsilon + \mathrm{loss} + \frac{\mathrm{mesh}}{6} + \nu + \mathrm{saving} \leq \min\big(M_{\mathrm{target}},\, B_{\mathrm{floor}}(\eta)\big),$$

verified formally in Theorem 14 (parameter_budget_inequality_at_05001):

Parameter Set	**Target** β	$r_{\mathbf{ext}}$	**Floor** $a_{\mathbf{floor}}$	**Governing Budget** $\min(M_{\mathbf{target}}, B_{\mathbf{floor}})$	**Mesh Spacing** e	**Tolerance** ε	**Final Saving saving**	**Total Used Budget (Slack)**	**Active Detector Bins** $n_{\mathbf{bins}}$
Combo 1 (OpenAI #003 baseline)	$\frac{7}{8}$ (0.875)	$\frac{17}{50}$	$\frac{51}{100}$ (0.51)	$\frac{49}{440640}$ (1.11e-4)	$\frac{49}{91653120}$	$\frac{49}{105753600}$	$\frac{49}{3525120}$	$\frac{343}{3525120}$ (+1.39e-5)	682,723
Combo 2 ($r_{\mathrm{ext}} = 3/10$)	$\frac{5}{6}$ (0.833)	$\frac{3}{10}$	$\frac{51}{100}$ (0.51)	$\frac{293}{55080}$ (5.32e-3)	$\frac{293}{11456640}$	$\frac{293}{13219200}$	$\frac{293}{440640}$	$\frac{2051}{440640}$ (+6.65e-4)	12,643
Combo 3 ($r_{\mathrm{ext}} = 6/25$)	$\frac{3}{4}$ (0.750)	$\frac{6}{25}$	$\frac{51}{100}$ (0.51)	$\frac{7}{1200}$ (5.83e-3)	$\frac{7}{249600}$	$\frac{7}{288000}$	$\frac{7}{9600}$	$\frac{49}{9600}$ (+7.29e-4)	8,558
Combo 4 ($r_{\mathrm{ext}} = 17/100$, $a = 0.51$)	$\frac{69}{100}$ (0.690)	$\frac{17}{100}$	$\frac{51}{100}$ (0.51)	$\frac{7}{1200}$ (5.83e-3)	$\frac{7}{249600}$	$\frac{7}{288000}$	$\frac{7}{9600}$	$\frac{49}{9600}$ (+7.29e-4)	6,419
Combo 5 ($r_{\mathrm{ext}} = 17/100$, $a = 0.5001$)	$\frac{69}{100}$ (0.690)	$\frac{17}{100}$	$\frac{5001}{10000}$ (0.5001)	$\frac{1241}{60000}$ (2.07e-2)	$\frac{1}{100000}$	$\frac{1241}{14400000}$	$\frac{1241}{480000}$	$\frac{6309}{400000}$ (+4.91e-3)	18,990

2.4 Componentwise Gram Scale Relaxations & Six Universal ($\forall$) Linear Theorems (Theorems 21–26)

2.4.1 Componentwise Gram Scale Relaxations (Theorem 24)

The four upper-bound relaxations between individual proven terms in `DirichletL/Detector/LowSourceScales.lean`, `DirichletL/Detector/GramScaleLoss.lean`, and `DirichletL/Detector/GramBound.lean` and the bundled upper bound `lowGramFactor` ($Z^{3/16+(23/96)\delta}$) in `DirichletL/Detector/LowGramScale.lean` decompose as follows:

#	Reference File & Line Range	Componentwise Formula	Upper-Bound Relaxation	$\sqrt{\cdot}$ Exponent Diff	Value at $\delta = 79/204$
1	DirichletL/Detector/ LowSourceScales.lean: 81, 95-98	$L \le BZ^{1/6} = BZ^{8/48}$	Relaxed to $L \le Z^{11/48}$	$\frac{3}{96} = \frac{1}{32}$	0.031250
2	DirichletL/Detector/ GramScaleLoss.lean:9 vs 29	$P^{2-\delta}$ ($P = Z^{1/8}/q$)	Applies `hpp : P^(2-δ) ≤ P^2`	$\frac{6\delta}{96} = \frac{\delta}{16}$	0.024203
3	DirichletL/Detector/ GramBound.lean:55 vs 63 (non-exceptional)	$A_1(1+\|\|v\|\|)^J \frac{Q}{Y} \frac{P^2}{Y} Y^\delta$	Multiplies common factor B by $P^{1/6} = Z^{1/48}$	$\frac{1}{96}$	0.010417
4	DirichletL/Detector/ GramBound.lean:55 vs 63 (cubic Gauss)	$A_2 \frac{Q}{Y} P^{1/6}$ (δ-independent)	Multiplies outer factor B by $Y^\delta = Z^{(23/48)\delta}$	$\frac{23\delta}{96}$	0.092779

2.4.2 Six Universal ($\forall$) Linear Inequality Theorems (Theorems 21–26)

1. `gauss_valuation_table_indices_m_ge_2` (Theorem 21): For all $j < 6, n \le 5, m \ge 2$, proves $j + 6m - k > n + 1$, $j + 6m - k \ne n$, and $j + 6m < 6(m + 1)$.

2. `gauss_sum_linear_exponent_bounds_m1_m2` (Theorem 22): For all $a_{\mathrm{bp}} \in [5001, 10000]$, $\epsilon_{\mathrm{bp}} \in [0, 10]$, $m_1 \ge 1, m_2 \ge 2$, proves the linear Gauss-sum exponent bounds.

3. `general_order_m_tail_exponent_bound` (Theorem 23): For arbitrary order $M \ge 1, m \ge M$, $x \ge 1/2$, $z_{\mathrm{re}} m \ge 1/6$, proves $5x + 6z_{\mathrm{re}} m \ge 7/2$.

4. `componentwise_gram_exponent_differences` (Theorem 24): Proves the exact componentwise Gram exponent differences $\frac{215}{3264}$ (with $L \le Z^{1/6}$) and $\frac{487}{3264}$ (at $L = 1$).

5. `sos_certificate_weight_linear_bound` (Theorem 25): For all $y \ge 0, D > 0$, proves $51D + 41y \le 17(3D + 5y)$ and $49(3D + 5y) \ge 147D > 0$.

6. `zero_free_region_union_and_symmetry` (Theorem 26): Proves the real-part bounds induced by the union of the Quasi-Riemann zero-free strip, Siegel zero exclusion, and functional-equation reflection.

2.5 Formalized Rational & Integer Scope vs. Future Complex-Analytic Extensions

Scope	Details	Formal Status
Formalized Rational & Integer Theorems (`qrh_exponent_and_parameter_bounds.lean` & `qrh_continuation_and_rescaling.lean`)	Exact `Rat`, `Int`, and `Nat` parameter budgets (48 theorems total: 0 sorry, 0 custom axiom), SOS decompositions, stationary-point identities, $m \ge 2$ Gauss valuation table vanishing (6 of 8 branches), componentwise Gram exponent differences ($\frac{215}{3264}$ and $\frac{487}{3264}$), (w, z) contour-shift exponent budgets (17/48000), universal 2nd/3rd Euler continuation cancellations, master scale-coupling equations, and the 26-file / 179 `def`/`theorem` declaration 1-to-1 audit.	Kernel-verified in Lean 4 (exit 0) and matched deterministically against `symbolic_verification_result.json`.
Future Complex-Analytic Extensions	Complex-analytic Mellin residue continuation for separated finite $m = 1$ terms and the sextic pole $z = \frac{1}{6}$ across the 3,232-file `DirichletL/` (2,926) and `SiegelZeros/` (306) formalization (within the 3,414-file broader upstream snapshot at `openai/math 4eaee87` / `oai-math-revised` PR `#70 ca28f20`), explicit Lean 4 interval-arithmetic proofs for $4 \le Q < 480$ if tightening the central-quotient threshold below 480 (global tails already absorb finite primes via `FirstTail.lean`), and off-diagonal bilinear phase cancellation for the diagonal `peak_scale` term.	Open Research Tasks (neither proof module alone claims an unconditional proof of RH or $\beta < 7/8$).

2.6 Cross-Verification Table: Lean 4 Kernel vs. Symbolic Solver (`verify_symbolic_qrh.py`)

Problem	Formal Lean 4 Theorem (`qrh_exponent_and_parameter_bounds.lean`)	Symbolic Solver Output (`symbolic_verification_result.json`)	Status
Problem 1: Floor margin linear formula & root	Theorem 12 (floor_source_margin_root_37_72, L138): `a_max = 37/72` (`eta_max = 1/72`)	`"linear_expression": "3*eta/2 - 1/48"`, `"eta_max": "1/72"`, `"a_max": "37/72"`	Match
Problem 2a: Irrational stationary point	Theorem 27 (L386): `a_true = 323/276 - 35*sqrt(16354)/9384`	`"delta_true": "185/138 - 35*sqrt(16354)/4692"`, `"a_true": "323/276 - 35*sqrt(16354)/9384"` (0.6933187811)	Match
Problem 2b: Rational SOS anchor & 2nd derivative	Theorem 4 (L86), Theorem 5 (L95), Theorem 27 (L386)	`"delta_SOS": "79/204"`, `"a_SOS": "283/408"`, `"balancedExponent_delta_SOS": "-7/30672"`, `"d2": "-236315300/608806611"`	Match
Problem 3: Componentwise Gram exponent differences at 79/204	Theorem 24 (componentwise_gram_exponent_differences, L342): `1817/19584`, `215/3264` (with $L \le Z^{1/6}$), and `487/3264` (at $L = 1$)	`"coarse_sqrt_exponent": "23*delta/96 + 3/16"`, `"componentwise_nonexceptional_with_L_bound_sqrt_exponent": "17*delta/96 + 7/48"`, `"componentwise_nonexceptional_sqrt_exponent": "17*delta/96 + 1/16"`, `"saving_exceptional": "1817/19584"`, `"saving_nonexceptional_with_L_bound": "215/3264"`, `"saving_nonexceptional": "487/3264"`	Match
Problem 4: $m \ge 2$ branch vanishing & z_{re} bound	Theorem 20 (L273), Theorem 21 (L302), Theorem 22 (L315), Theorem 23 (L332)	`"num_vanishing_branches": 6`, `"surviving_branches": ["02_0", "10_1"]`, `"z_re_min": "1/12"`	Match
Problem 5: Principal contour shift budget	Theorem 19 (convergence_boundary_at_one_sixth, L258): `(13/9600) - 1/1000 = 17/48000`	`"w_shift_saving_at_e_max": "1063/48000"`, `"z_shift_saving_at_e_max": "17/48000"`, `"B_principal": "17/48000"`, `"matches_principal_budget": true`	Match

2.7 Completion of Tasks 1–3: Small-Norm Threshold Removal, 2nd/3rd Complex Mellin Continuation, and Master Scale-Coupling Equations (Theorems 28–48)

(Note: Upstream files cited by path in Sections 7 and 10 that lie outside the 26-file local `proofs/oai_ref/` snapshot are audited against `openai/math` commit `4eaee87` / `oai-math-revised` PR `#70` commit `ca28f20`.)

2.7.1 Task 1: Parameter Tightening on $4 \le Q < 480$ & Finite Bad-Prime Mask Absorption (Theorems 28–30)

1. Call-Graph Verification (`DirichletL/PrimeRows/CubePrimeThresholds.lean:13-33`, `DirichletL/PrimeRows/FirstTail.lean:81-100`):

- `DirichletL/Detector/HighRowsCentralQuotient.lean:9` (`480 ≤ Q`) is only invoked on dyadic pool primes $P \in T_j$ (`DirichletL/PrimeRows/CubePrimeBound.lean:105`), where `DirichletL/PrimeRows/CubePrimeThresholds.lean:13-33` (`central_pool_good_eventually`) unconditionally discharges `480 ≤ Q` via $Q \ge cZ^{d_{\min} r_{\min}} \to \infty$.
- Global Euler product tails are handled by `DirichletL/PrimeRows/FirstTail.lean:81-100` (`exists_both_source_exclusions`), which absorbs `smallPrimeSet N` into the finite bad-prime mask $S = S_0 \cup \mathrm{smallPrimeSet}(N)$.

2. Exact $(1 - V)^{-1}$ Cancellation and Threshold Reduction $480 \to 112$ (`theorem_28_marked_factor_singularity_cancels_identically`, `theorem_29_all_small_eisenstein_norms_nonvanishing`, `theorem_30_universal_finite_bad_prime_mask_absorption`):

- Multiplying `continuedCorrection` by $(1 - D)(1 - R)$ identically cancels the $(1 - V)^{-1}$ denominator in `markedFactor` (`theorem_28_marked_factor_singularity_cancels_identically`), reducing the cen-

tral quotient bound from 480 to 112 ($88 < 112$), and all 21 small Eisenstein prime-power norms in $4 \le Q < 112$ have non-vanishing Euler denominators (`theorem_29_all_small_eisenstein_norms_nonvanishing`).

2.7.2 Task 2: $m = 1$ Residue Anatomy & 2nd/3rd Euler Continuation (Theorems 31–34, 39)

1. Second Euler Continuation (`secondContinuedCorrection`) & 5-Term Cancellation (`theorem_31_second_continuation_exact_polynomial_identity`):

- Defining $\text{secondContinuedCorrection}(R, V, W, D, P^*) := (1 - R) \cdot \text{continuedCorrection}(V, W, D, P^*)$ yields

$$(1-D)\big(\text{secondContinuedCorrection}-1\big) = -VW+WD-RW^2+RVW+(1-W)(-Rq_{\text{inv}}-KV+VD-VWR),$$

identically cancelling all five first-order terms $(1 - 1,\ -R + R,\ -D + D,\ +WR - WR,\ +RD - RD)$.

2. Lowering the Euler-Tail z_{re} Barrier & Exact z_0-Invariance at $d_0 = 13/16$ (`theorem_32_second_and_third_continuation_convergence_barrier`, `theorem_33_central_exponent_z0_invariance_at_d0`, `theorem_34_universal_z0_shift_improves_subcritical_d`, `theorem_39_m1_sextic_pole_residue_and_33_200_remainder_saving`):

- Peeling off $(1 - R)$ and $(1 - RW^2)$ lowers the Euler-tail absolute convergence barrier at $x_{\text{re}} = 51/100$ from $z_{\text{re}} > 97/300 \approx 0.3233$ ($17/50 = 0.34$) to $z_{\text{re}} > 97/600 \approx 0.16167 < 1/6$ ($-(53/50) = -1.06 < -1$ at $z_{\text{re}} = 1/6$, `theorem_32_second_and_third_continuation_convergence_barrier`).
- In `DirichletL/Detector/CentralExponent.lean:11-14`, the coefficient of z_0 in `sourceExponent` is $1 + \ell - \alpha_X - d$, which vanishes identically at $d = d_0 = 13/16$ ($1 + 1/6 - 17/48 - 13/16 = 0$, `theorem_33_central_exponent_z0_invariance_at_d0`). For all $d < 13/16$ (e.g. $d = 1/2$), lowering z_0 from $17/50$ to $1/6$ strictly improves the exponent from $-49/14400$ to $-829/14400$ (an absolute shift of $-780/14400 = -13/240 \approx -0.0542$, `theorem_34_universal_z0_shift_improves_subcritical_d`), while the sextic Gauss sum $L(\pi, 6z)$ pole at $z = 1/6$ (`DirichletL/Detector/HighRowsCentralTerms.lean:47-53`) leaves the separate Mellin residue term bounded in `theorem_39_m1_sextic_pole_residue_and_33_200_remainder_saving`.

2.7.3 Task 3: Master Scale-Coupling Equations for 3/16 and -11/16 & Rescaling Anatomy (Theorems 35–40)

1. Master Coupling Equations (`theorem_35_master_scale_coupling_identities`):

- Across `DirichletL/PrincipalSignalComparison.lean:412` and `DirichletL/Detector/LowSourceScales.lean:40-68`:

$$c_{\text{sig}}(\alpha_X, \ell) = \frac{\alpha_X}{3} + \frac{\ell}{6} - \frac{5}{6}, \quad e_{\text{low}}(\alpha_X, \alpha_Y) = \frac{5\alpha_X + \alpha_Y}{12}, \quad \beta_{\text{crit}}(\alpha_X, \alpha_Y, \ell) = \frac{5}{6} + \frac{\alpha_X + \alpha_Y - 2\ell}{12}.$$

2. Regime A ($\beta_{\text{crit}} = 128519/146880 < 7/8$ on Active `DirichletL/Detector/LowSourceScales.lean` Path vs. `DirichletL/Parameters.lean` Split Invariance, `theorem_36_regime_A_sos_slack_rescaling_and_conductor_split`):

- Shifting (α_X, α_Y) by $\eta = 3/73440$ ($\alpha'_X = 26007/73440$, $\alpha'_Y = 35187/73440$) with fixed split $\ell = 1/6$ preserves the active `DirichletL/Detector/LowSourceScales.lean:80-104` Poisson inequality $2\alpha'_X - \alpha'_Y - \ell = 4587/73440 > 0$ across $d \in [0, 1/6]$, keeps the worst-case endpoint exponent $\le -7/440640 < 0$, and lowers β_{crit} to $\frac{128519}{146880} < \frac{7}{8}$; whereas simultaneously shifting $\ell' = 1/6 - \eta$ to keep $\alpha'_X - \ell' = 3/16$ in `DirichletL/Parameters.lean:14` leaves $\alpha'_X + \alpha'_Y - 2\ell' = 1/2$ invariant ($\beta_{\text{crit}} = 7/8$).

3. Regime B ($\beta_{\text{crit}} = 5/6, 3/4, 69/100$ Under Unbundled/Diagonal Gram Bounds, `theorem_37_regime_B_gram_unbundled_and_diagonal_beta_bounds`–`theorem_40_energy_induction_compatible_below_seven_eighths`):

- Combining Theorem 24's unbundled Gram saving ($215/3264$) with $(\alpha_X, \alpha_Y, \ell) = (1/3, 1/3, 1/3)$ achieves $\beta_{\text{crit}} = 5/6$ with net margin $+79/3264 > 0$; diagonal Gram dominance ($e_{\text{low}} = \alpha_X/2$) achieves $\beta_{\text{crit}} = 3/4 = 0.75$ and $\beta_{\text{crit}} = 69/100 = 0.69$, with full compatibility in `DirichletL/Energy/CertifiedExistence.lean:19-48` down to $\beta = 51/100$ (`theorem_40_energy_induction_compatible_below_seven_eighths`).

2.8 Beyond-Baseline Alternative Bounds and Sharp Rigidity Obstructions

1. Beyond-Baseline Alternative Bound: Because `DirichletL/PrimeRows/FirstTail.lean` (`openai/math 4eaee87` / `oai-math-revised` PR `#70 ca28f20`) already absorbs finite bad primes into the exclusion mask S and `DirichletL/PrimeRows/CubePrimeThresholds.lean` discharges $Q \geq 480$ on dyadic pool primes, the reduction from $Q \geq 480$ to $Q \geq 112$ via $(1 - V)$ cancellation (`theorem_28_marked_factor_singularity_cancels_identically`, `theorem_29_all_small_eisenstein_norms_nonvanishing`, `theorem_30_universal_finite_bad_prime_mask_absorption`) constitutes a parameter-tightening and constant-slack analysis over $4 \leq Q < 480$, complemented by the $m = 1$ residue structure and 2nd/3rd-order Euler product continuation (`theorem_31_second_continuation_exact_polynomial_identity` through `theorem_40_energy_induction_compatible_below_seven_eighths`).
2. Sharp No-Go / Rigidity Obstruction: Proves that quadratic Cauchy-Schwarz amplification alone hits a strict parity rigidity floor at the baseline exponent 3/16 (signal exponent $-11/16$), preventing any further reduction without higher-order cubic reciprocity.

2.9 Extended Audit of the Full #003 Codebase (3,232 Files · 556,376 Lines, Within 3,414-File Upstream Snapshot at `openai/math 4eaee87` / `oai-math-revised` PR `#70 ca28f20`) and Companion Manuscripts (21,438 Lines)

2.9.1 Kernel Verification of All 4 `ComparatorChallenges` and `W22` / `W63`

- Full Corpus Scale & Kernel Soundness: Across all 3,232 Lean 4 files (556,376 lines: 2,926 files / 486,558 lines in `DirichletL/` + 306 files / 69,818 lines in `SiegelZeros/`, within the broader 3,414-file upstream snapshot), there are 0 occurrences of `sorry`, `axiom`, `unsafe`, or `implemented_by`.
- Verification of the 4 Comparator Challenges & Core Algebraic/Analytic Engines:
  1. All 4 comparator challenges (`QuasiRiemannHypothesis` for the 7/8 Riemann zeta zero-free region `riemannZeta_ne_zero_of_seven_eighths_lt_re`, `DirichletSevenEighths` for the 7/8 zero-free region for Dirichlet L-functions, `HeckeSevenEighths` for the 7/8 zero-free region over $K = \mathbb{Q}(\sqrt{-3})$, and `SiegelZeros` via `Theorem.lean:11-27 exists_absolute_real_zero_gap`, excluding Landau-Siegel zeros) match standard Mathlib definitions and compile unconditionally.
  2. Both `W22` (`IsolatedBezoutFromRegularSelection.lean:25-373`, local isolated Bézout bound on polynomial-torus rings) and `W63` (`SiegelZeros/Characters/UnconditionalPrimeBias.lean` for $X \geq 2$) are fully verified.

2.9.2 Five Structural, Patch, and Bibliographic Findings Across #003

1. Non-Propagating Root Imports in `SiegelZeros/Main.lean` (`20 / 21` in Official `4eaee87`; `19 / 21` in Community `PR #70 ca28f20`) & Unreachable Modules in `SiegelZeros/`:
   - In official `openai/math` commit `4eaee87`, of the 21 modules directly imported by `SiegelZeros/Main.lean`, only `1 / 21` (`4.76%`: `Conclusions.Theorem`) propagates to the comparator challenge `exists_absolute_real_zero_gap`, reaching `201` transitive files (`65.69%`) out of `306` in `SiegelZeros/` (`69,818` lines) and leaving `20 / 21` root imports and `105` files (including `PivotBounds.lean`) outside that cone.
   - In the community revised fork `oai-math-revised` (`PR #70`, commit `ca28f20`), adding the auxiliary `Conclusions.PrimeBias` target expands the combined cone to `2 / 21` (`9.52%`) root imports and `268` files (`87.58%`, `63,264` lines), with `19 / 21` (`90.48%`) root imports and `38` files (`12.42%`, `6,554` lines) still unpropagated.
2. Upstream `PrimeNumberTheoremAnd/Wiener.lean` Apache-2.0 Header, -2,716-Line Trim, and Classical Literature Attribution (`openai/math 4eaee87` / `oai-math-revised` PR `#70 ca28f20`):
   - Direct imports of `PrimeNumberTheoremAnd.Wiener` by `DirichletL` (`IdealMangoldt` and `Progressions`) triggered a -2,716-line compatibility trim of upstream `Wiener.lean` in the repository patch (removing 2 upstream `sorry`s from the build graph). Explicitly, `PrimeNumberTheoremAnd/Wiener.lean:1-5` preserves its Apache-2.0 attribution header ("Adapted from PrimeNumberTheoremAnd by Alex Kontorovich and contributors. Licensed under the Apache License, Version 2.0; see the upstream LICENSE. This compatibility port retains the proven declarations used by this project.").

- External package notices such as `Kebekus (2025)`, `Cipollina (2026)`, and `Benenson (rellich-kondrachov)` are unused transitive `lakefile` packages inherited from `PrimeNumberTheoremAnd`, not direct mathematical dependencies of `#003`. Instead, the actual borrowing and bibliographic omission in the `#003` manuscripts (21,438 `.tex` lines, 90 `.bib` entries) concerns Wiener-Ikehara / `PrimeNumberTheoremAnd` smoothing (`0` manuscript citations to `PrimeNumberTheoremAnd`) and uncited classical Large Sieve literature in the Large Sieve proof sections.

3. `CONTENTS.md [Lean]` Badge Mismatch (`Class B`) vs. Disclosed Conditional Assumption in `paper.tex:6536` (`Class A`):

- `Class B` (documentation badge mismatch): `CONTENTS.md:66-92` attaches a `[Lean]` badge to 3 papers in `#003`, whereas the 2nd companion manuscript (October-5-2026, *An alternate proof of the 11/12 zero-free region*, 3,988 lines) has 0% (0 lines) of Lean 4 formalization in official `4eaee87`.
- `Class A` (disclosed assumption): Separately, the 11/12 zero-free region section in the primary manuscript (`paper.tex:6536`) explicitly labels its hypothesis `eq:late-height-hypothesis` as conditional rather than claiming an unconditional theorem.

4. Sparse Citation Density (`61 \cite` Lines) and `3,213`-Line Uncited Tail (`19.27%`) in Primary Manuscript `paper.tex`:

- Across `preprints/The-Quasi-Riemann-Hypothesis-September-30-2026/build/paper.tex` (`16,677` lines in `4eaee87`), non-comment `\cite` commands appear on `61` lines (`0.366` lines per 100 lines: `12` bare `\cite{...}` lines plus `49` optional-argument `\cite[...]{...}` lines). The final citation (`\cite[Theorem 1.1]{TZ}`) occurs at `L13464`, leaving a `3,213`-line (`19.27%`, `L13465`–`L16677`) uncited tail and a maximum consecutive uncited gap of `4,169` lines.

5. `1,717` Unused `_h*` Hypothesis Binders in Official `4eaee87` (`2,238` Across `PR #70 ca28f20`) vs. `0` Unused Premises in `ComparatorChallenges`:

- Static AST analysis across all `3,232 .lean` files in official `openai/math` `4eaee87` detects `1,717` literal `_h*`-prefixed unused hypothesis binders inside internal helper lemmas (`2,238` unused helper binders under the expanded `PR #70 ca28f20` snapshot), whereas the headline `ComparatorChallenges` target theorems themselves contain `0` unused premises, preserving an unconditionally valid core.

2.10 Complete 1-to-1 Theorem Ledger for Part I (Theorems I.1–I.48)

1. Formalized Rational/Integer Theorems vs. Future Complex-Analytic Extensions:

- The 48 theorems across `proofs/qrh_exponent_and_parameter_bounds.lean` (Theorems 1–27) and `proofs/qrh_continuation_and_rescaling.lean` (Theorems 28–48) are kernel-verified over `Rat`, `Int`, and `Nat` (covering algebraic parameter budgets, SOS decompositions, $m \geq 2$ Gauss branch vanishing, exact componentwise Gram exponent differences $\frac{215}{3264}$ and $\frac{487}{3264}$, (w, z) contour-shift exponent budgets, universal 2nd/3rd Euler continuation polynomial cancellations, master scale-coupling equations, and the complete 26-file / 179 `def`/`theorem` declaration 1-to-1 formal audit including `instance polynomialComponent Prime_isPrime`, Siegel zero local Bézout cone homogenization, and arithmetic cutoff transport).
- They do not formalize the continuous complex-analytic Mellin contour integrals for the separated $m = 1$ finite terms or Hilbert-space trace-class operator bounds. Do not summarize this formalization as a complete unconditional proof of the full Riemann Hypothesis.

2. JSON Manifest & Upstream Snapshot Provenance:

- Parse `manifest.json` for programmatic access to all 48 theorem identifiers, line numbers, verified fractions, and SHA-256 hashes.
- All 26 core reference Lean files are mirrored locally under `proofs/oai_ref/`. Any upstream repository files referenced by path outside `proofs/oai_ref/` (such as `DirichletL/PrimeRows/FirstTail.lean`, `DirichletL/PrimeRows/CubePrimeThresholds.lean`, `DirichletL/PrincipalMellinResidues.lean`, `DirichletL/PrincipalSignalComparison.lean`, `DirichletL/Hecke/CommonProbe.lean`, `DirichletL/Detector/HighRowsFirstRegion.lean`, `DirichletL/Detector/FirstContinuation.lean`, `DirichletL/Detector/Supremum.lean`, `DirichletL/ParametersFixedSource.lean`, `DirichletL/Energy/CertifiedExistence.lean`, `DirichletL/FinalAssemblyUnconditional.lean`, `SiegelZeros/Main.lean`, `PrimeNumberTheoremAnd/Wiener.lean`, `CONTENTS.md`, and `paper.tex`) are audited against `openai/math` commit `4eaee87` (`oai-math-revised` PR `#70` commit `ca28f20`).

2.10.1 Theorems 1–27 (`proofs/qrh_exponent_and_parameter_bounds.lean`)

- `coordR_exponent_at_z_034`: At $x = 51/100$ and $z = 17/50$, proves the `coordR` exponent equals $-11/10$.
- `coordR_squared_exponent_at_z_024`: At $z = 6/25$, proves the quadratic R^2 exponent equals -1 at $x = 51/100$ and $-149/125 < -1$ at $x = 51/100 + 16/1000$.
- `gauss_branch_exponent_at_z_017`: At $x = 51/100$ and $z = 17/100$, proves the finite Gauss branch `(0, 2, 0, 1)` exponent equals $-2/25 \le 1/2 - 51/100$.
- `rational_sos_reference_abscissa`: Proves the rational SOS reference root $\delta_{\mathrm{ref}} = 79/204$ gives $a_{\mathrm{ref}} = 283/408 \in (0.69, 0.694)$ (`DirichletL/Endpoint.lean`).
- `exact_sos_identity_and_margin_at_79_204`: Verifies `endpointSOS_LHS = endpointSOS_RHS = 147` and $-\mathrm{balancedExponent}(79/204, 0) = 7/30672 > 49/440640$.
- `sos_polynomial_identity_sample_points`: Checks the 2D rational SOS polynomial identity across sample points in $[0, 5/6] \times [0, 1/2]$.
- `certified_exponent_margins_by_beta`: Verifies certified rational exponent margins across $\beta \in \{7/8, 5/6, 3/4, 69/100\}$.
- `floor_source_margin_at_051`: Proves the floor source margin at $a_{\mathrm{floor}} = 51/100$ equals $-7/1200$ (`DirichletL/Detector/CentralExponent.lean`).
- `floor_source_margin_at_0505`: Proves the floor source margin at $a_{\mathrm{floor}} = 101/200$ equals $-1/75$.
- `floor_source_margin_at_0501`: Proves the floor source margin at $a_{\mathrm{floor}} = 501/1000$ equals $-29/1500$.
- `floor_source_margin_at_05001`: Proves the floor source margin at $a_{\mathrm{floor}} = 5001/10000$ equals $-1241/60000$, widening the saving over $-7/1200$ by $297/20000$.
- `floor_source_margin_root_37_72`: Proves the exact vanishing root $\eta_{\max} = 1/72$ ($a_{\max} = 37/72$) where `sourceExponent - 3/16 = 0`.
- `nonstrict_gauss_branches_at_05001_and_017`: Verifies all 9 non-strict finite Gauss-sum branches satisfy gaussBranchExponent $\le 1/2 - x$ at $z = 17/100, x = 5001/10000$ (`DirichletL/Detector/HighRowsCentralTerms.lean`).
- `parameter_budget_inequality_at_05001`: Verifies the 17-parameter budget inequality ($6309/400000 \le 1241/60000$) at $\beta = 69/100, r_{\mathrm{ext}} = 17/100, a_{\mathrm{floor}} = 0.5001$ (`DirichletL/PrimeRows/CubeFloorSaving.lean`, `DirichletL/Parameters.lean`).
- `siegel_zeros_constants_ratio_identity`: Verifies $c_1 = 1/37636$, $C_1 = 192$, $H = 86713344$, and $(C_1/c_1)/H = 1/12$ (`SiegelZeros/Selection/PivotBounds.lean`, `SiegelZeros/Estimates/GeometricBoundary.lean`).
- `complementary_zero_free_widths`: Proves complementary zero-free widths $1 - \beta \in \{1/8, 1/4, 31/100\}$ for $\beta \in \{7/8, 3/4, 69/100\}$.
- `functional_equation_reflection_and_quotient_thresholds`: Proves functional-equation reflection ($0.49 \leftrightarrow 0.51$) and quotient ratios $192/480 = 2/5$, $56/112 = 1/2$.
- `exponent_balance_relation_identity`: Proves the exponent balance identity linking $\alpha_X = 17/48$, $\alpha_Y = 23/48$, $\ell = 1/6$ to $\gamma_{\mathrm{det}} = 3/16$, $c_{\mathrm{signal}} = -11/16$, $d_0 = 13/16$, and $\beta = 7/8$.
- `convergence_boundary_at_one_sixth`: Proves the $z_{\mathrm{re}} = 1/6$ boundary and the shifted remainder budget $13/16 \cdot (1/6 - 33/200) - 1/1000 = 17/48000$ (`DirichletL/Detector/PrincipalRemainderBounds.lean`, `DirichletL/ParametersHighData.lean`).
- `tail_m_ge_2_exponent_margins`: Verifies positive margins at $z_{\mathrm{re}} = 9/100 > 1/12$ for surviving $m \ge 2$ geometric-tail branches (`DirichletL/Detector/HighRowsTail.lean`).
- `gauss_valuation_table_indices_m_ge_2`: Universal $\forall (j < 6, n \le 5, m \ge 2)$ index bounds showing 6 of 8 branches vanish for $m \ge 2$.
- `gauss_sum_linear_exponent_bounds_m1_m2`: Universal $\forall$ linear Gauss-sum exponent bounds for $a_{\mathrm{bp}} \in [5001, 10000]$, $\epsilon_{\mathrm{bp}} \le 10$, $m_1 \ge 1, m_2 \ge 2$.
- `general_order_m_tail_exponent_bound`: Universal $\forall (M \ge 1, m \ge M)$ tail bound $5x + 6z_{\mathrm{re}}m \ge 7/2$ under $x \ge 1/2, z_{\mathrm{re}}m \ge 1/6$.

- componentwise_gram_exponent_differences: Proves exact componentwise Gram square-root exponent differences 2021/19584, 215/3264 (with $L \le Z^{1/6}$), 1817/19584, and 487/3264 (at $L = 1$) (DirichletL/Detector/LowSourceScales.lean, DirichletL/Detector/GramScaleLoss.lean, DirichletL/Detector/GramBound.lean, DirichletL/Detector/LowGramScale.lean).
- sos_certificate_weight_linear_bound: Universal $\forall(y_{\mathrm{num}} \ge 0, D > 0)$ linear inequality $51D + 41y_{\mathrm{num}} \le 17(3D + 5y_{\mathrm{num}})$.
- zero_free_region_union_and_symmetry: Universal $\forall$ zero-free region union and reflection-symmetry bounds.
- stationary_point_quadratic_root_323_276_identity: Verifies the quadratic equation $9384\delta^2 - 25160\delta + 8325 = 0$ giving $a^* = 323/276 - 35\sqrt{16354}/9384$ and the negative derivatives at $\delta_{\mathrm{SOS}} = 79/204$.

2.10.2 Theorems 28–48 (proofs/qrh_continuation_and_rescaling.lean)

- theorem_28_marked_factor_singularity_cancels_identically: Universal $\forall(R, V, q_{\mathrm{inv}}, K, W, D : \mathrm{Int})$ polynomial cancellation of the $(1-V)$ factor in markedFactor and reduction of the central quotient threshold from 480 to 112.
- theorem_29_all_small_eisenstein_norms_nonvanishing: Non-vanishing of Euler denominators across all 21 small Eisenstein prime-power norms in $4 \le Q < 112$.
- theorem_30_universal_finite_bad_prime_mask_absorption: Universal $\forall$ absorption law for finite bad-prime masks $S = S_0 \cup \mathrm{smallPrimeSet}(N)$.
- theorem_31_second_continuation_exact_polynomial_identity: Universal $\forall(R, V, q_{\mathrm{inv}}, K, W, D : \mathrm{Int})$ 5-term cancellation identity for secondContinuedCorrection.
- theorem_32_second_and_third_continuation_convergence_barrier: Reduction of the Euler-tail z_{re} convergence barrier from 97/300 to $97/600 \approx 0.16167 < 1/6$ ($-(53/50) = -1.06 < -1$ at $z = 1/6$).
- theorem_33_central_exponent_z0_invariance_at_d0: Exact z_0-invariance of sourceExponent at $d_0 = 13/16$ (coefficient 0) and $-13/240$ exponent shift ($-49/14400 \to -829/14400$) at $d = 1/2$.
- theorem_34_universal_z0_shift_improves_subcritical_d: Universal $\forall$ improvement of sourceExponent for all $d < 1 + \ell - \alpha_X$ when $z_0' < z_0$.
- theorem_35_master_scale_coupling_identities: Master scale-coupling identities for $-11/16$, $3/16$, and $\beta_{\mathrm{crit}}(\alpha_X, \alpha_Y, \ell) = \frac{5}{6} + \frac{\alpha_X + \alpha_Y - 2\ell}{12}$.
- theorem_36_regime_A_sos_slack_rescaling_and_conductor_split: Derivation of $\beta_{\mathrm{crit}} = 128519/146880 < 7/8$ on the active DirichletL/Detector/LowSourceScales.lean:80-104 path using existing SOS slack vs. $\beta_{\mathrm{crit}} = 7/8$ invariance under simultaneous DirichletL/Parameters.lean:14 split shifting.
- theorem_37_regime_B_gram_unbundled_and_diagonal_beta_bounds: Proof of $\beta_{\mathrm{crit}} = 5/6, 3/4, 69/100$ under unbundled and diagonal Gram bounds.
- theorem_38_universal_beta_crit_monotonicity: Universal $\forall$ monotonicity of β_{crit} preserving Poisson admissibility.
- theorem_39_m1_sextic_pole_residue_and_33_200_remainder_saving: Exact Mellin pole-shift remainder savings ($-13/9600$, $-17/48000$) across the sextic Gauss pole $z = 1/6$.
- theorem_40_energy_induction_compatible_below_seven_eighths: Compatibility of DirichletL/Energy/CertifiedExistence.lean:19-48 across all $\beta \in [51/100, 7/8]$.
- theorem_41_bezout_homogenized_cone_and_degree_bounds: Universal $\forall$ local isolated Bézout homogenized cone dimension $h < 5$ and 4-variable box degree bound 4*(N-1) < 4*N (SiegelZeros/Intersection/IsolatedBezoutFromRegularSelection.lean, SiegelZeros/Structure/ArithmeticCutoffTransport.lean).
- theorem_42_arithmetic_cutoff_and_pigeonhole_incompatibility: 4-step derivative ideal pigeonhole ($b < 4$), cutoff coefficient 96 = 3 * 32, and height-3 length incompatibility $32^3 = 32768 > 4^3 = 64$ (SiegelZeros/Structure/ArithmeticCutoffTransport.lean).
- theorem_43_biquadratic_galois_and_pivot_constants: Biquadratic field rank 4, $c_1 = 1/37636$, $C_1 = 192$, $N_0 = 18818$, $H = 86713344$, and greedy pivot weight ratio $(C_1/c_1)/H = 1/12$ (SiegelZeros/Selection/

PivotBounds.lean, SiegelZeros/Estimates/GeometricBoundary.lean, SiegelZeros/Intersection/BezoutBoundary.lean, SiegelZeros/Conclusions/Theorem.lean).

- theorem_44_local_compensated_replacement_and_cancellation: Universal $\forall(V, W, D, P_{\text{star}}, B, q : \text{Int})$ local defect polynomial identity and ramified compensation cancellation (DirichletL/Detector/Local.lean).
- theorem_45_euler_resummation_and_correction_bounds: Resolvent bound 2 and error multipliers 12 and 4 in unramified_marked_error_bound (DirichletL/Detector/Euler.lean, DirichletL/Detector/CorrectionBounds.lean).
- theorem_46_euler_coordinates_and_unramified_factorization: Central contour Q-exponents of coordV, coordR, coordW, coordD, coordK and 3 * 480 = 1440 (DirichletL/Detector/EulerCoordinates.lean, DirichletL/Detector/HighRowsUnramified.lean, DirichletL/Detector/HighRowsCentralQuotient.lean).
- theorem_47_sextic_gauss_valuation_table_and_high_rows_scalar: Universal $\forall(r, m, j, d : \text{Nat})$ mod-6 periodicity and unique index decomposition (DirichletL/Detector/ScalarTable.lean, DirichletL/Detector/HighRowsScalar.lean, DirichletL/Detector/HighRowsTail.lean).
- theorem_48_high_data_nine_budget_inequalities: Simultaneous verification of all 9 budget inequalities in HighData (DirichletL/Parameters.lean, DirichletL/ParametersHighData.lean).

3 Part II: Referee Hygiene Audit, Three Abscissa Regimes, Stickelberger Deflation, and Critical-Line Inversion (Theorems II.1–II.48)

Attribution Boundary for Part II: OpenAI `#003` (**Tier A**, [1]) claimed and proved only $\beta = 7/8$ (`0 sorry`). In this Part (`Case 005`), **Tier C (original unconditional results)** comprises the AST discovery that `compensated_geometry` (`Parameters.lean:14`) has 0 downstream references across 2,925 `DirichletL` modules, the 3×3 scale derivation $(17/48, 23/48, 1/6)$ vs. uninflated $(29/84, 11/21)$, the separation of the global SOS saddle $\beta_{\mathrm{SOS}}(0) = \frac{6843-7\sqrt{921}}{7578} < \frac{41999}{48000} < \frac{7}{8}$ from local $\delta = 0$ slice equilibria $(131/150, 209/240)$ and the isolated non-exceptional floor $(4103/4896, 4069/4896)$, bi-Stickelberger polynomial deflation $(1+Rq^{-1})(1-R)$, and the $[0.48, 0.52]$ symmetric Cauchy-box rational margins. **Tier D (conditional analytic transfer blueprints)** comprises the Voronoi–Mellin transfer under `(hc_mean, hres_op)`, the coupled Path A+B required threshold inversion $\Delta_{\mathrm{hybrid}} = 14/33$ for $\beta = 1/2$, and the single-$\zeta(s)$ rank-1 collapse deficit $\Delta_{\mathrm{collapse}} = 2/11$ requiring $\mathrm{gain}_{\mathrm{amp}} \geq 2/11$ (48 zero-`sorry` theorems, 441/441 mutations killed). See Appendices A–B for the unified `oai_ref/` and SHA-256 ledgers.

3.1 Original Discoveries & Unconditional vs. Conditional Boundary

We explicitly separate our reconstruction of OpenAI's hardcoded parameters from our unconditional mathematical advances and the remaining conditional analytic targets (Δ_{gram}, `hc_mean : c0_w + c1_w = 0, hres_op : res_w1 = (c0_w + c1_w) * mu_pole`, & single-$\zeta(s)$ $\mathrm{gain}_{\mathrm{amp}} \geq 2/11$):

1. Original Discovery 1: 3 Distinct β Metrics & 6 $\Delta(1/2)$ Thresholds: Optimal Scale $(29/84, 11/21, 1/6)$, 3-Tier Exponent Losses $(181/3264 \cdot 215/3264 \cdot 487/3264)$, (1) Global SOS Saddle $\beta_{\mathrm{SOS}}(0) = 41999/48000 < 7/8$, (2) Local $\delta = 0$ Equilibrium $\beta_{\mathrm{eq}}(0) = 131/150, 209/240$, & (3) Background Floor $\beta_{\mathrm{floor}} = 4103/4896 \approx 0.8380$ $(4069/4896 \approx 0.8311)$ (`thm_02`, `thm_04`, `thm_27`–`thm_33`): Removing the $B \leq Z^{1/16}$ absorption and $P^{2-\delta} \leq P^2$ Gram formalization slack shifts the optimal scale from denominator 48 to denominator 84 ($(29/84, 11/21, 1/6)$) and uncovers a 3-tier non-exceptional exponent relaxation of $181/3264 \approx 0.0555$ (2-term) / $215/3264 \approx 0.0659$ (3-term with $P^{1/6}$ bundling) / $487/3264 \approx 0.1492$ (full non-exceptional). In `DirichletL/Detector/GramBound.lean:56`, ‖E - Z‖ is the sum of the non-exceptional tail and the cubic Gauss main term $A_2 \frac{Q}{Y} P^{1/6}$: (1) Enforcing the global SOS inequality across all high-row bins $(\delta, y) \in [0, 5/6] \times [0, 1/2]$ at $\Delta_{\mathrm{gram}} = 0$ yields the algebraic saddle $\beta_{\mathrm{SOS}}(0) = \frac{6843-7\sqrt{921}}{7578} \approx 0.87497547 < 7/8$ (rational witness $(71/200, 5737/12000)$ giving $\beta_{\mathrm{SOS}}(0) = 41999/48000 < 7/8$, $1/48000 \approx 2.08 \times 10^{-5}$ below 7/8; `thm_33`, critical Beta48000). (2) On the local $\delta = 0$ boundary slice, $(49/150, 73/150, 21/25)$ gives $\beta_{\mathrm{eq}}(0) = 131/150 \approx 0.8733$, and shifting $z_{\mathrm{high}} = 17/50 \to 7/20$ (including the non-zero shift term $(13/16 - d_0)(z'_{\mathrm{high}} - 1/6)$, since $\partial/\partial z_{\mathrm{high}} = 13/16 - d_0 = 0$ holds only at $d_0 = 13/16$) yields $(19/60, 7/15, 17/20)$ ($\beta_{\mathrm{eq}}(0) = 209/240 \approx 0.8708$, Heath-Brown $\Delta_{\mathrm{gram}} = 1/24 \implies \beta = 199/240 \approx 0.8292 < 0.83$). (3) Simultaneously, zero-mode subtraction (‖E - Z‖) and thm_04 lower the isolated non-exceptional background floor (‖E - Z - E_exc‖) to $\beta_{\mathrm{floor}} = 4103/4896 \approx 0.8380$ ($4069/4896 \approx 0.8311$ with bundling, $2641/3264 \approx 0.8091$ direct). The 6 distinct $\Delta(1/2)$ saving thresholds correspond to: fixed scale 9/16, local $\delta = 0$ 28/75 & 89/240, global SOS 75/176, tuple barrier 11/24, and hybrid 14/33.

2. Original Discovery 2: Unconditional Advance: Stickelberger Factorization of coordR ($\beta > 2/3 \to 1/2$) & [0.48, 0.52] Symmetric Cauchy Box (`thm_29`–`thm_32`): In `DirichletL/Detector/EulerCoordinates.lean:36`, OpenAI bounded the cubic Gauss phase via $\|\mathrm{actualAPhase}\| \leq 1$, creating an artificial 6th-order Euler product boundary at $\beta = 401/600 \approx 0.6683$ ($\to 2/3$). Using the Stickelberger-Eisenstein Hecke character $\psi_{\mathrm{Stick}}\eta^6$ ($k_\infty = -6 \neq 0$, entire at $6s + 6z - 4 = 1$) over $\mathbb{Q}(\sqrt{-3})$ and cancelling $(1 - R_p)$ (`DirichletL/Detector/Euler.lean:38`, `thm_09`) lowers the coordR absolute convergence boundary from $\beta = 401/600 (\to 2/3)$ to $117/200 (\to 7/12)$ and $301/600 (\to 1/2)$, while shifting $z'_{\mathrm{high}} = 7/20$ opens all 9 branches of `DirichletL/Detector/HighRowsCentralTerms.lean:38-114` down to $0.4800 < 1/2$ and closes the $[0.48, 0.52]$ symmetric Cauchy-box margins at $-56/2400 < -53/2400 < -50/2400 < 0$ (Path B).

3. Original Discovery 3: Master Transfer Blueprint & Required Threshold Inversion: Local Equilibrium $(49/150, 73/150, 21/25)$, Global SOS Transfer Law, Critical-Line Triple $(2/3, 7/6, 1/2)$ & Hybrid Required Saving $\Delta_{\mathrm{hybrid}} = 14/33$ (`thm_15`, `thm_16`, `thm_28`, `thm_30`, `thm_33`, `thm_35`): Proves the local $\delta = 0$ equilibrium $(\alpha_X^*, \alpha_Y^*, d_0^*) = (49/150, 73/150, 21/25)$ ($\beta(\Delta_{\mathrm{gram}}) = \frac{131}{150} - \Delta_{\mathrm{gram}}$), the globally SOS-certified transfer laws $\beta^*_{\mathrm{SOS}}(\Delta_{\mathrm{gram}}) = \frac{7}{8} - \frac{22}{25}\Delta_{\mathrm{gram}}$ and $\beta^{**}_{\mathrm{full}}(\Delta_{\mathrm{gram}}) = \frac{7}{8} - \frac{48}{59}\Delta_{\mathrm{gram}}$, the unique critical-line ($\beta = 1/2$) triple $(\alpha_X^{**}, \alpha_Y^{**}, d_0^{**}) = (\frac{2}{3}, \frac{7}{6}, \frac{1}{2})$ (d $\leq 1/2$ in `DirichletL/Detector/CentralExponent.lean:76`, $\Delta_{\mathrm{gram}}(1/2) = 11/24$), and the required hybrid saving threshold $\Delta_{\mathrm{hybrid}} = 14/33 = 56/132$ at $(35/66, 59/66, 7/11, 7/20)$.

4. Original Discovery 4: 30 Prime-Ideal Norms (59 Prime Ideals) & Hygiene Delta Forensics: Pre-Cancellation Threshold Reduction $Q \geq 480 \to Q \geq 128$ & Unreferenced `compensated_geometry` (`thm_05`, `thm_07`, `thm_08`): Cancelling $(1 - V)$ prior to the triangle inequality in DirichletL/Detector/CorrectionBounds.lean:

26, 58 lowers the Q^{-1} coefficient from $c_{\text{raw}} = 2(4 + 2 \cdot 56) = 232 \leq 240$ to $c_{\text{red}} = 2(4 + 28) = 64$ (a formalization slack of 30 unramified prime-ideal norms and 59 prime ideals in $[128, 479]$), and `verify_qrh_mathematician_audit.py:167-185` confirms `comp_geom_refs_oai_ref = 0` for `DirichletL/Parameters.lean:14` (`compensated_geometry`) across the 26 bundled `oai_ref/` modules while validating the recorded `0` downstream references across `2,925` `DirichletL` modules from `openai/math` commit `4eaee87` (`PR #70 ca28f20`).

3.2 Key Mechanism Extraction

3.2.1 The 3×3 Linear System for $(17/48, 23/48, 1/6)$ (`thm_01`)

In `DirichletL/Parameters.lean:12-17`, the probe scales $X = Z^{\alpha_X}$, $Y = Z^{\alpha_Y}$, and $L = Z^{\ell}$ are determined by:

1. Euler Product Contour Boundary ($\ell = 1/6 = 8/48$): Anchored at $\mathrm{Re}(z) = 1/6$ in `DirichletL/Detector/PrincipalRemainderBounds.lean:577`.
2. Exceptional Square-Full Shift ($\alpha_X - \ell = 3/16 = 9/48$): Fixes $\alpha_X = 8/48 + 9/48 = 17/48$ in `DirichletL/Parameters.lean:14` and `DirichletL/Detector/LowGramScale.lean:9`.
3. Cubic Gauss $P^{1/6}$ Saving ($(5\alpha_X + \alpha_Y)/12 = 3/16$): For modulus $P = Y/(qX) \asymp Z^{\alpha_Y - \alpha_X}$, the L^2-exponent $(5\alpha_X + \alpha_Y)/12 = 3/16$ gives $5\alpha_X + \alpha_Y = 108/48 \implies \alpha_Y = 23/48$.

3.2.2 Polynomial $(1 - V)$ Cancellation and $m \geq 2$ Sextic Gauss Vanishing (`thm_07`, `thm_10`)

In `DirichletL/Detector/Euler.lean:11-13` and `DirichletL/Detector/Local.lean:16-24`, substituting markedFactor into continuedCorrection cancels $(1 - V)$ identically in $\mathbb{Z}[R, V, q^{-1}, K, W, D]$. Moreover, in `DirichletL/Detector/ScalarTable.lean:11-35` and `DirichletL/Detector/HighRowsTail.lean:11-48`, for $m \geq 2$ the prime-power index $J = j + 6m \geq 12 > n + 1$ forces $J \neq n$ and $J - 1 \neq n$, so 6 of the 8 non-principal branches vanish identically, leaving only $(0, 2, 0)$ and $(1, 0, 1)$.

3.2.3 Rational Sum-of-Squares (SOS) Identity Replacing the Irrational Saddle (`thm_06`)

In `DirichletL/Endpoint.lean:29-31`, balancedExponent δ y attains an irrational saddle point at $y = 0$, namely $\delta^* = \frac{185}{138} - \frac{35\sqrt{16354}}{4692} \approx 0.38663756$. To avoid irrational square-root arithmetic inside Lean 4, `DirichletL/Endpoint.lean:58-62` constructs a global polynomial sum-of-squares (SOS) decomposition centered at the rational point $\delta_{\text{SOS}} = 79/204 \approx 0.3872549$, yielding a positive constant residual $3 \times 49 = 147 > 0$ that certifies $-$balancedExponent $\geq 49/440640 > 0$.

3.3 Referee Critique of Formalization Slack, Unreferenced Hygiene Delta, and Module Discharge Architecture

Issue ID & Location	Referee Finding	Formal & Quantitative Verification
[M-1] Constant-Absorption Inflation (B $\leq$ Z$\hat{}$(1/16)) & Gram Formalization Slack (3 Tiers) `DirichletL/Detector/LowSourceScales.lean:88-98`, `DirichletL/Detector/GramScaleLoss.lean:29`, `DirichletL/Detector/LowGramScale.lean:32`	At $\delta_{\text{SOS}} = 79/204$ (where the SOS certificate leaves a rational rounding residual of $49/440640 \approx 0.0001112$), the non-exceptional tail relaxation exhibits 3 tiers of formalization slack: (1) 2-term sum ($B \leq Z^{1/16}$ $1/32 + P^{2-\delta} \leq P^2$ $79/3264$) = $181/3264 \approx 0.0555$, (2) 3-term sum adding $P^{1/6}$ Gauss bundling slack ($1/96 = 34/3264$, `thm_04`) = $215/3264 \approx 0.0659$, and (3) full componentwise non-exceptional relaxation (adding L-divisor $1/12 = 272/3264$) = $487/3264 \approx 0.1492$.	`thm_02`, `thm_04`, `verify_qrh_mathematician_audit.py:151-159`

Issue ID & Location	**Referee Finding**	**Formal & Quantitative Verification**
[M-2] Unreduced Double Triangle Inequality (480 → 128) `DirichletL/Detector/Principal RemainderBounds.lean:62`, `DirichletL/Detector/Local.lean:16-31`, DirichletL/Detector/Correction Bounds.lean:26, 58	Bounding $\lvert(1-V)^{-1}\rvert \le 2$ before multiplying by $(1-V)$ shifts the geometric-series ($c/Q \le 1/2$) coefficient from $c_{\text{red}} = 2(4+28) = 64$ ($Q \ge 128/129$) to $c_{\text{raw}} = 2(4+2\cdot 56) = 232 \le 240$ (`DirichletL/Detector/Principal RemainderBounds.lean:62` 480^(-7/8), $Q \ge 480$, a formalization slack of $46-16 = 30$ unramified prime-ideal norms and $89-30 = 59$ prime ideals).	`thm_07`, `thm_08`
[L-1] Unreferenced Hygiene Delta (`compensated_geometry`: 0 Refs) & Frozen Probe Scale DirichletL/Parameters.lean:12, 14, DirichletL/Detector/LowSourceScales.lean:12, 24	Distinct from the active detector formalization slack above, `verify_qrh_mathematician_audit.py:167-185` confirms `comp_geom_refs_oai_ref = 0` for `compensated_geometry` across the 26 bundled `oai_ref/` modules and validates recorded upstream DAG counts from official `openai/math` commit `4eaee87` (`2,926 DirichletL` files anchored at `DirichletL/Nonvanishing.lean`; `2,927` files in community `PR #70 ca28f20`): all 4 theorems in `DirichletL/Parameters.lean` (`compensated_geometry`, `exists_height_cutoff`, `exists_tail_order`, `cumulative_frequency_bound`) have 0 recorded external references across the 2,925 downstream modules because their numeric literals are hardcoded across `DirichletL` (17/48 in 56 files/186 sites, 23/48 in 54 files/198 sites, 17/50 in 136 files/365 sites), and `DirichletL/Parameters.lean:12` constrains $d \le 1/6$ ($\ell_0 = 1/6$) while `DirichletL/Detector/LowSourceScales.lean:12` shifts α_X, α_Y by η, shifting the active critical threshold to $2\beta^* = 128519/73440 < 7/4$.	`thm_05`, `verify_qrh_mathematician_audit.py:161-185`
[Architecture] 26-File Partition (20 + 6 = 26) & 4-Step Bézout-to-Siegel-Zero Discharge Chain `SiegelZeros/Estimates/GeometricBoundary.lean:18-22`, `SiegelZeros/Conclusions/Theorem.lean:11-20`	`thm_24_complete_26_file_architectural_partition` partitions all 26 bundled reference modules (SevenEighths 20 + SiegelZeros 6 = 26 files). uniform_exclusion_of_actual_cutoff takes hgeometry : ActualCutoffSpanning as a local parameter, which is connected across the 4-step call chain `SiegelZeros/Intersection/IsolatedBezoutFromRegularSelection.lean:346-366` → `SiegelZeros/Structure/ArithmeticCutoffTransport.lean:488-515` → `SiegelZeros/Intersection/BezoutBoundary.lean:13-20` → `SiegelZeros/Conclusions/Theorem.lean:11-20` (verified across the 5 bundled `oai_ref/` SiegelZeros chain files in `verify_qrh_mathematician_audit.py:132-149`) and recorded 201 transitive upstream `SiegelZeros` modules from `openai/math` commit `4eaee87` (`PR #70 ca28f20`, 0 sorry, 0 axiom; `thm_25`/`thm_26` model this 4-step propositional chain P → Q → R → S → T, while full kernel verification of upstream files requires `lake build` with prebuilt Mathlib.olean).	`thm_23`, `thm_24`, `thm_25`, `verify_qrh_mathematician_audit.py:132-149`

3.4 Four Analytic & Algebraic Bottlenecks for Number Theorists

1. Bottleneck 1 (Double Contour Separation & $d_0 = 13/16$ Invariance): In `DirichletL/Detector/PrincipalRemainderBounds.lean:577-581`, the $w = 19/20$ contour at $z_{\text{re}} = 1/6 + e$ clears $59/48$ by $13/240$ (saving $1063/48000$), whereas the $w = 1$ residue shifts left to $z_{\text{re}} = 33/200 < 1/6$ to clear $65/48$ by $29/1200$ (saving $17/48000$). Both distances are verified symbolically (`verify_qrh_mathematician_audit.py:188-208`) and across a float64 grid of $2^{24} + 1 = 16,777,217$ points ($t \in [-5000, 5000]$) in PyTorch FP64 (`thm_13`, `thm_14`, `verify_qrh_mathematician_audit.py:279-286`).

2. Bottleneck 2 (The $\beta = 7/8$ Barrier & Finite-Field Numerical Gauss/Ramanujan Verification): Under $2\beta = 7/4 - (4/3)\Delta_{\text{gram}}$ (`thm_15`, `thm_16`), reaching $\beta = 5/6$, $3/4$, and $69/100$ requires conditional off-diagonal Gram savings $\Delta_{\text{gram}} = 1/16$, $3/16$, and $111/400$ (`verify_qrh_mathematician_audit.py:210-214`). In Py Torch FP64, across all 611 Eisenstein split primes $p \equiv 1 \pmod 6$ in $[7, 9973]$ (1,222 cubic χ_3 and sextic χ_6 Gauss Gram matrices), we numerically verify the finite-field single-prime Gauss sum norm $|\tau(\chi)| = \sqrt{p}$ and the Ramanujan sum ($\sum_{x \neq 0} e(nx/p) = -1$) off-diagonal norm $\max_{m \neq n} |G_{m,n}| = \frac{1}{p-1}$ (max relative error $< 3.5 \times 10^{-11}$; `verify_qrh_mathematician_audit.py:228-239`, `verify_qrh_mathematician_audit.py:279-293`; note that this verifies the single-prime finite-field identity rather than proving multi-prime off-diagonal $\Delta_{\text{gram}} > 0$ cancellation).

3. Bottleneck 3 ($\mathbb{Z}[\omega]$ Bad Primes $Q = 3, 4$): Wild ramification at $Q = 3$ ($\lambda = 1 - \omega \mid 3$) and inert sextic collapse at $Q = 4$ ($\mathbb{F}_4^\times \cong C_3$) are absorbed by badPrimeMask, ensuring $Q \equiv 1 \pmod 6$ for all remaining prime powers $Q \geq 7$ (`thm_19`, `thm_20`, `thm_26`).

4. Bottleneck 4 (Biquadratic Klein 4-Group Torus Jets vs. Cubic Characters & Formalization Boundary): `SiegelZeros/Estimates/GeometricBoundary.lean:26` and `SiegelZeros/Selection/PivotBounds.lean:63-65` set $N_0 = 2 \times 97^2 = 18,818$ and $H = 12 \times 192 \times 37,636 = 86,713,344$ over $B = \mathbb{Q}(\sqrt{d}, \sqrt{2})$ for real quadratic characters $\chi^2 = \chi_0$, whereas pure cubic characters ($\chi^3 = \chi_0, \bar{\chi} = \chi^2 \neq \chi$) have no Siegel zeros (`thm_21`, `thm_22`, `thm_23`). For real quadratic characters, `SiegelZeros/Conclusions/Theorem.lean:11-20` (exists_absolute_real_zero_gap) proves the logarithmic zero-free bound `∃ c : ℝ, 0 < c ∧ ... c ≤ (1 - β) * Real.log q` ($\beta \leq 1 - c/\log q$).

3.5 Stage 5: Sub-0.69 → 1/2 Master Transfer Blueprint, [0.48, 0.52] Symmetric Cauchy Box, 20-Module Global SOS Saddle & Hybrid Required Threshold Inversion (thm_27–thm_38)

3.5.1 Unconditional Exponent Arithmetic Advances & Separation of Three β Metrics and Six $\Delta(1/2)$ Thresholds (`thm_27`–`thm_35`)

Step	Barrier in oai_ref/	Mathematical & Code Resolution	Formal Theorem
Step 0 (HighRows Open to $\beta = 1/2$)	Apparent $51/100 \leq$ a floor in `DirichletL/Detector/CentralExponent.lean:66` and DirichletL/Detector/HighRowsCentralQuotient.lean:9, 31	balanced_source_margin (-49/440640), high_source_margin ($-1/48 - \delta/16$), intermediate_source_margin (-49/14400), and saddle relativeExponent 0 (13/16) 1 0 = -1/48 hold across all $0 \leq \delta \leq 5/6$ ($\beta \in [1/2, 11/12]$). Generalizing $a = 1/2 + \eta$ ($\eta < 1/72$) widens the floor margin from $-7/1200$ to $-1/48 = -25/1200$ as $\eta \to 0^+$ ($\beta \to 1/2^+$).	`thm_27_high_rows_critical_line_open_and_unconditional_beta_drop`

Step	**Barrier in oai_ref/**	**Mathematical & Code Resolution**	**Formal Theorem**
Step 1 (Isolated Non-Exceptional Background Floor $\beta_{\text{floor}} = 4103/4896 \approx 0.8380$ / $4069/4896 \approx 0.8311$)	Zero-mode $E_A = 17/96$ (low GramZeroMode) at $\beta = 125/144 \approx 0.8681$ & B $\leq$ Z^(1/16) inflation at $\beta = 4103/4896 \approx 0.8380$	In `DirichletL/Detector/GramBound.lean:56`, ‖E - Z‖ is the sum of the non-exceptional tail ($E_C = 397/3264$) and the cubic Gauss main term $A_2 \frac{Q}{Y} P^{1/6}$. Zero-mode subtraction (‖E - Z‖, paper RadialFourier U 0 = 0) and thm_04 ($\Delta E = 215/3264$ uninflated saving) lower the isolated non-exceptional & zero-mode background floor (‖E - Z - E_exc‖) from $7/8 = 0.8750$ to $\beta_{\text{floor}} = 4103/4896 \approx 0.8380$ ($4069/4896 \approx 0.8311$ with 3-term bundling, $2641/3264 \approx 0.8091$ direct).	`thm_27`, `thm_30`

Step	Barrier in oai_ref/	Mathematical & Code Resolution	Formal Theorem
Step 2 & Path A ((1) Global SOS Saddle $\beta_{\mathrm{SOS}}(0) = 41999/48000 < 7/8$, (2) Local $\delta = 0$ Equilibrium $\beta_{\mathrm{eq}}(0) = 131/150, 209/240$, & Critical-Line Triple $(2/3, 7/6, 1/2)$)	Frozen $\ell_0 = 1/6$ ($d \le 1/6$ in `DirichletL/Parameters.lean:12`), fixed (17/48, 23/48) in `DirichletL/Detector/LowSourceScales.lean:12` & tuple barrier in `DirichletL/Parameters.lean:16`	(1) Across the full $(\delta, y) \in [0, 5/6] \times [0, 1/2]$ SOS domain (substituting general scales into balance Denominator in DirichletL/Endpoint.lean:14-28 and sourceExponent in DirichletL/Detector/CentralExponent.lean:11-16 yields $3888 \cdot$ balanceDenominator$(\delta, 0) \cdot (E_{\mathrm{Low}} -$ sourceExponent$) = A_M\delta^2 + B_M\delta + C_M \ge 0$ with $A_M = 972\alpha_X - 2484\alpha_Y + 1764$, $B_M = -6624\alpha_X + 432\alpha_Y + 1428$, $C_M = 6105\alpha_X + 3885\alpha_Y - 3885$ in globalSosDiscriminant and discriminant $4A_MC_M - B_M^2 \ge 0 \iff 3789s^2 - 8862s + 4753 \le 0$), the global SOS minimum is $\beta_{\mathrm{SOS}}(0) = \frac{6843-7\sqrt{921}}{7578} \approx 0.87497547 < 7/8$ (rational witness $(71/200, 5737/12000)$ giving $\beta_{\mathrm{SOS}}(0) = 41999/48000 < 7/8$), with globally SOS-certified transfer laws $\beta^*_{\mathrm{SOS}}(\Delta_{\mathrm{gram}}) = \frac{7}{8} - \frac{22}{25}\Delta_{\mathrm{gram}}$ and $\beta^{**}_{\mathrm{full}}(\Delta_{\mathrm{gram}}) = \frac{7}{8} - \frac{48}{59}\Delta_{\mathrm{gram}}$ and unique $\beta = 1/2$ critical-line triple $(\alpha_X^{**}, \alpha_Y^{**}, d_0^{**}) = (2/3, 7/6, 1/2)$ (d $\le$ 1/2 in `DirichletL/Detector/CentralExponent.lean:76`, $\Delta_{\mathrm{gram}}(1/2) = 11/24$). (2) On the local $\delta = 0$ slice, matching $\alpha_Y = 2\alpha_X - 1/6$ with $\alpha_Y - \alpha_X = 4/25$ gives $(49/150, 73/150, 21/25)$ ($\beta_{\mathrm{eq}}(0) = 131/150 \approx 0.8733$), and shifting $z_{\mathrm{high}} = 17/50 \to 7/20$ (where dynamic $d_0 = 7/6 - \alpha_X$ gives $\partial/\partial z_{\mathrm{high}} = (7/6 - \alpha_X) - d_0 = 0$ identically, whereas fixing the literal 13/16 in DirichletL/Detector/CentralExponent.lean:12 adds the shift term $(13/16 - d_0)(z'_{\mathrm{high}} - 1/6)$) yields $(19/60, 7/15, 17/20)$ ($\beta_{\mathrm{eq}}(0) = 209/240 \approx 0.8708$, Heath-Brown $\Delta_{\mathrm{gram}} = 1/24 \implies \beta = 199/240 \approx 0.8292$).	`thm_28_generalized_scale_equilibrium_and_master_transfer_law`, `thm_32_z_high_saddle_invariance_and_symmetric_pincer_box_048_052`, `thm_33_global_sos_saddle_and_critical_line_half_cutoff_theorem`

Step	Barrier in oai_ref/	Mathematical & Code Resolution	Formal Theorem
Step 3 & Path B (coordR Stickelberger Factorization & $[0.48, 0.52]$ Symmetric Cauchy Box)	6th-order Euler product boundary at $\beta = 401/600 \approx 0.6683$ ($\to 2/3$) in DirichletL/Detector/EulerCoordinates.lean:12, 36, 48 & DirichletL/Detector/HighRowsCentralTerms.lean:38-114 branch floors $0.492, 0.490$	Factoring out $L(6s + 6z - 4, \psi_{\text{Stick}}\eta^6)$ ($k_\infty = -6 \neq 0$) and $(1 - R_p)$ cancellation lowers the coordR Euler product boundary to $117/200(\to 7/12)$ and $301/600(\to 1/2)$. Simultaneously, shifting $z'_{\text{high}} = 7/20 = 0.35$ lowers the top 3 branch floors of DirichletL/Detector/HighRowsCentralTerms.lean: 38-114 from $(492, 490, 480)/1000$ to $(480, 475, 450)/1000$ (opening all 9 branches to $0.4800 < 1/2$), while symmetric $R = 1 - \lvert\delta\rvert$ closes the $[0.48, 0.52]$ Cauchy-box error margins at $-56/2400 < -53/2400 < -50/2400 < 0$ (Path B).	`thm_29_stickelberger_coordR_factorization_breaks_two_thirds_wall`, `thm_30_master_transfer_theorem_unconditional_vs_conditional_boundary`, `thm_31_high_rows_nine_branch_exact_rational_thresholds_and_048_opening`, `thm_32`
Step 4 ([Path A] / [Path B] Standalone Path A/B Lower Bounds & [Path A + Path B] Required Saving Threshold Inversion)	Standalone Path A hits a formal zero-energy LP intercept $\beta^{\text{A}}_{\min} = 71/108 \approx 0.6574 > 1/2$ at $(4/9, 13/18)$ (assuming hypothetical full cancellation $\Delta_{\max} = 53/216$ of `LowRows`), while standalone Path B has $\partial/\partial z_{\text{high}} = d_0 - 13/16 = 0$ only at $d_0 = 13/16$ (and slope $-13/144 < 0$ at $d_0 = 13/18$) without reducing LowRows Gram energy	Splicing Path A's local $\delta = 0$ coupled scale ray $\alpha_X = \frac{49}{150} + \frac{12}{25}\Delta_{\text{hybrid}}$, $\alpha_Y = \frac{73}{150} + \frac{24}{25}\Delta_{\text{hybrid}}$, $\beta = \frac{131}{150} - \frac{22}{25}\Delta_{\text{hybrid}}$ ($z_{\text{high}} = 0.34$ intercept) with Path B's dual-contour damping $\frac{1}{2}\alpha_Y$ ($w.\text{re} = 1 - a$ in `DirichletL/Detector/CentralExponent.lean:95`) and the shifted branch opening $z'_{\text{high}} = 7/20 = 0.35$, targeting (hbeta_target : beta132 = 66) ($\beta = 1/2$) uniquely inverts the required hybrid saving threshold $\Delta_{\text{hybrid}} = \frac{14}{33} = \frac{56}{132}$ (d_hyb132 = 56) at $(\alpha^{**}_X, \alpha^{**}_Y, d^{**}_0, z'_{\text{high}}) = (\frac{35}{66}, \frac{59}{66}, \frac{7}{11}, \frac{7}{20})$. Crucially, because $E_{\text{Low}} - \Delta_{\text{hybrid}} = \frac{39}{132} - \frac{56}{132} = -\frac{17}{132} < 0$ is a strictly negative matrix-norm exponent, $\Delta_{\text{hybrid}} = 14/33$ cannot be supplied by off-diagonal character-sum cancellation alone ($\lVert E - Z\rVert \geq 0$) and requires unproved Archimedean Mellin contour decay $d_{\text{Mellin}} = \frac{1}{2}\alpha^{**}_Y = \frac{59}{132}$ ($\frac{39}{132} + \frac{59}{132} = \frac{98}{132} > \frac{56}{132}$, reserve $\frac{42}{132} = \frac{7}{22} > 0$). Under that conditional model, $\alpha^{**}_X = \frac{35}{66} \in [\frac{15}{34}, \frac{121}{222}]$ globally eliminates the interior SOS saddle at $\delta = \frac{79}{204}$ with $7128 \cdot$ balance Denominator$(\delta, y) \cdot (\frac{1}{2} - \beta_{\text{High}}(\delta, y))/\delta = 750 + 295y + 190y^2 + 108\delta + 3162\delta y + 3300\delta y^2 + 1056\delta y^3$ having strictly positive monomial coefficients $(750, 295, 190, 108, 3162, 3300, 1056)$.	`thm_34_path_a_and_b_individual_dead_ends`, `thm_35_hybrid_ab_coupled_critical_certificate`

3.5.2 Two Remaining Conditional Analytic Tasks and Deep Reasoning Toward $\beta \to 1/2$ (`thm_36`–`thm_38`)

Step	Barrier in oai_ref/	Conditional Analytic Structure & Formal Verification	Formal Theorem
Step 5 (Deep Analytic Audit of LowRows Higher-Order Schwartz Tail, Conditional Dual-Contour Referee Boundary & Stickelberger Moments)	1st-order Schwartz tail ($k = 1$) in `DirichletL/Detector/GramBound.lean:50`, spatial-to-spectral dual-contour transfer in Low Rows (incl. upstream `Zero Detector.lean` at `openai/math` commit `4eaee87`, absent from `oai_ref/`), and vertical height moments in DirichletL/Detector/PrincipalRemainderBounds.lean:300, 353	(1) Increasing Schwartz integration-by-parts order from $k = 1$ to $k = 2$ in `(Y/(M*P))^(-k+δ)` gains $3\alpha_X^{**} - \alpha_Y^{**} - 1/3 = 48/132 = 4/11 > 0$ ($Z^{-2/11}$ in square-root norm); under the conditional space-spectral transfer hypothesis, Path-B dual damping $D_{\mathrm{dual}}(1/2) = 59/132$ lowers $E_{\mathrm{Low}} = 39/132$ to $-20/132 < -17/132 = E_{\mathrm{prin}}(1/2)$ (margin $+3/132 = +1/44 > 0$), leaving the Voronoi/Mellin extraction of $w = 1 - a$ damping on E - Z (`hc_mean : c0_w + c1_w = 0, hres_op : res_w1 = (c0_w + c1_w) * mu_pole`, in `DirichletL/Detector/GramBound.lean:42-58` or upstream `ZeroDetector.lean` from `4eaee87`) without Euler-product x-shift growth as the exact open conditional analytic boundary. (2) In `DirichletL/Detector/CorrectionBounds.lean:26-60` at $(a, \xi, \upsilon) = (1/2, 33/200, 19/20)$, the 4 non-R error exponents are $(149, 145, 194, 144)/100 > 1$, leaving coord R ($\sigma_R = -1/100$, convexity $\mu_{\mathrm{Stick}} \le 102/100 \le 3$) as the unique term below 1, which shifts jointHeight moments from $(8, 5)$ to $(11, 8)$ with z-residue saving $-7/6600 < 0$.	`thm_36_analytic_dual_contour_and_stickelberger_height_moments`

Step	Barrier in oai_ref/	Conditional Analytic Structure & Formal Verification	Formal Theorem
Step 6 (Universal Mellin Scale Identity & Bi-Stickelberger Polynomial Deflation)	scalePower $+a$ cancellation in DirichletL/Detector/PrincipalRemainderBounds.lean:120, 522, 597 and $-RW$, $-Rq^{-1}$ terms in `DirichletL/Detector/Local.lean:16-74`	(1) At $(35/66, 59/66, 7/11)$, $\alpha_X^{**}(1/2-\xi)+(a+\xi-1)+\xi/6+\alpha_Y^{**}(\upsilon-1)=(a-83/132)+(7/11)(\xi-1/6)+(59/66)(\upsilon-1)$ cancels $+a$ identically ($\Delta x=0$); at $e=1/1000$, naive $d_0=1/2$ fails ($+1/6000>0$) whereas hybrid $d_0^{**}=7/11$ converges strictly ($-1/16500<0$) and dual $w=1/2$ gives $-167/375<0$ (L^1 margin $+25/264$, L^2 margin $+1/44$). (2) In $(1+Rq^{-1})(1-R)\cdot$continued Correction, linear $-RW(1-V)$ and $-Rq^{-1}(1-W)$ cancel identically over $\mathbb{Z}[R,V,q^{-1},K,W,D]$, raising all 19 surviving terms (20 expanded monomials) at $(50/100, 33/200, 95/100)$ to $e_{\min}=144/100>1$ ($O(Q^{-11/25})$ tail) with $\mu_{\text{bi}}=103/100\le 3$ absorbed into $(11,8)$ Schwartz moments.	`thm_37_low_rows_nonzero_mode_dual_mellin_contour_shift`, `thm_38_bi_stickelberger_euler_deflation_and_moment_coupling`

3.5.3 Stage 6: Complete Execution & Reasoning Log of the 8 Parameter-Upgrade & Conditional Bridge Tasks and 2 Extensions (thm_39–thm_48)

To verify the parameter-upgrade arithmetic specifications for `proofs/oai_ref/` (Tasks 1–5) and establish the conditional Voronoi-Mellin transfer, discrete Euler-Maclaurin zero-mode decay, Größencharakter convexity, Welch rank-trace duality, and classical single-$\zeta(s)$ required threshold inversion (Tasks 6–8 & Extensions), we formalized `qrh_eight_tasks_critical_upgrade.lean` (10 theorems `thm_39`–`thm_48` + 5 executable defs, 6 total defs incl. `siegel_concrete_witness`, 242 lines, 0 sorry, 155/155 hypothesis mutations caught):

Task & Formal Theorem	Target Modules (proofs/oai_ref/)	Design Rationale & Verified Parameter-Upgrade Arithmetic Output
Task 1 (thm_39) `thm_39_task1_oai_ref_parameters_and_gram_k2_upgrade`	`DirichletL/Parameters.lean:12-53`, `DirichletL/Detector/GramScaleLoss.lean:8-35`, `DirichletL/Detector/LowGramScale.lean:38-48`, `DirichletL/Detector/LowSourceScales.lean:81-98`	• Reasoning: At $(\alpha_X^{**},\alpha_Y^{**})=(35/66, 59/66)$, the 1st-order ($k=1$) Poisson integration-by-parts exponent $2\alpha_X^{**}-\alpha_Y^{**}-\ell=0$ leaves zero room to absorb constant B. Upgrading DirichletL/Detector/GramScaleLoss.lean:8-35 to $k=2$ yields (P^3 / (Y/L)^2) = L^2 Y / (q^3 X^3), opening an L^2-squared saving of $3\alpha_X^{**}-\alpha_Y^{**}-2\ell=4/11=192/528>0$. • Result: Constant-$B$ absorption exponent in DirichletL/Detector/LowSourceScales.lean:88 expands from $B\le Z^{1/16=33/528}$ to $B\le Z^{2/11=96/528}$ (exponent gain $+63/528=+21/176\approx+0.1193$), and DirichletL/Detector/LowGramScale.lean:45 becomes $39/132+(59/132)\delta$.

Task & Formal Theorem	Target Modules (proofs/oai_ref/)	Design Rationale & Verified Parameter-Upgrade Arithmetic Output
Task 2 (thm_40) `thm_40_task2_oai_ref_euler_local_correction_bounds_upgrade`	`DirichletL/Detector/Euler.lean:11-48`, `DirichletL/Detector/Local.lean:16-74`, `DirichletL/Detector/CorrectionBounds.lean:24-83`, `DirichletL/Detector/Euler Coordinates.lean:11-48`	• Reasoning: DirichletL/Detector/CorrectionBounds.lean required $a \geq 7/8$ because it bounded $\lvert(1-V)^{-1}\rvert \leq 2$ before cancelling $(1-V)$ ($Q_{\min} = 480$) and left coordR ($e_R = 6a + 6\xi - 4 = -1/100 < 1$) inside the absolute local sum. Pre-cancelling $(1-V)$ lowers the Q^{-1} coefficient from 240 to 64 ($Q_{\min} = 128$, saving 352), while bi-Stickelberger deflation $(1 + Rq^{-1})(1-R)$ cancels $e_{RW} = 94/100 < 1$ and $e_{Rq} = 99/100 < 1$ identically. • Result: All 19 surviving local terms (20 monomials) at $(1/2, 33/200, 19/20)$ satisfy $e \geq e_{KV} = 144/100 > 1$ (tail decay $O(Q^{-11/25})$), converging absolutely for all $a \geq 1/2$.
Task 3 (thm_41) `thm_41_task3_oai_ref_principal_remainder_bounds_upgrade`	`DirichletL/Detector/Principal RemainderBounds.lean:243-621`	• Reasoning: To absorb the vertical growth of the bi-Stickelberger L-factors, jointHeight moments are upgraded from $(8, 5)$ to $(11, 8)$ $(+3)$, and the source_scale_identity (L522) base constant is shifted from 11/16 to $1 - \alpha_X^{**}/2 - d_0^{**}/6 = 83/132$. • Result: At $e = 1/1000 = 33/33000$, source_z_strict_exponent (L597, $\xi = 33/200$) has relative saving $-2/33000 = -1/16500 < 0$, source_w_strict_exponent (L594, $\upsilon = 19/20$) has $-1421/33000 < 0$, and the dual contour ($\upsilon = 1/2$) has $-14696/33000 < 0$.
Task 4 (thm_42) `thm_42_task4_oai_ref_high_rows_central_data_upgrade`	`DirichletL/Detector/HighRows CentralTerms.lean:16-114`, `DirichletL/Detector/HighRows CentralQuotient.lean:11-33`, `DirichletL/ParametersHighData.lean:42-47`	• Reasoning: At $z_{\text{high}} = 17/50 = 0.34$, the 9-branch maximum floor in DirichletL/Detector/HighRowsCentral Terms.lean is $123/250 = 492/1000 = 0.492$. Shifting $z'_{\text{high}} = 7/20 = 0.35$ lowers the 9-branch maximum floor to $12/25 = 480/1000 = 0.48 < 1/2$. • Result: All four budgets in Dirichlet L/ParametersHighData.lean:42-47 are strictly positive: central_budget $= 9180/440640 = 1/48 > 0$, geometric_budget $= 17/800 > 0$, principal_budget $= 2/33000 > 0$, and floor_budget $(a = 1/2)$ $= 18/1200 = 3/200 > 0$.
Task 5 (thm_43) `thm_43_task5_oai_ref_central_exponent_endpoint_theorem_upgrade`	`DirichletL/Detector/Central Exponent.lean:11-99`, `DirichletL/Endpoint.lean:14-108`, `SiegelZeros/Conclusions/Theorem.lean:1-27`	• Reasoning: Removing the static $+3/16$ penalty in DirichletL/Detector/CentralExponent.lean:16 shifts source Exponent$(1/2)$ from $-66/132$ to $-83/132$, while balanceDenominator in DirichletL/Endpoint.lean:14 stays in $[70/108, 215/108] \subset (0, 5/2)$ on $[0, 5/6] \times [0, 1/2]$. • Result: The 7-monomial certificate $(750, 295, 190, 108, 3162, 3300, 1056)$ (sum $= 8861 > 0$) eliminates the interior SOS saddle, and the damped LowRows exponent $-20/132$ beats $E_{\text{prin}}(1/2) = -17/132$ by $+3/132 = +1/44 > 0$.

Task & Formal Theorem	**Target Modules (proofs/oai_ref/)**	**Design Rationale & Verified Parameter-Upgrade Arithmetic Output**
Task 6 (thm_44) `thm_44_task6_voronoi_mellin_conductor_neutral_transfer_lemma`	`DirichletL/Detector/GramBound.lean:42-58`, `DirichletL/Detector/LowGramScale.lean:15-45`, `DirichletL/Detector/CentralExponent.lean:95`	• Reasoning (Conditional Zero-Mode Residue Hypothesis vs. Arithmetic Consequence): Shifting the Euler-product variable x by $a \to 1-a$ in high rows inflates the exponent by $\Delta e_{\mathrm{cond},x} = 2\alpha_X^{**}a = 35/66 = 70/132$ via $(qX^2)^a$. Assuming the explicit conditional zero-mode residue hypothesis `(hc_mean : c0_w + c1_w = 0, hres_op : res_w1 = (c0_w + c1_w) * mu_pole)` for $\mathcal{M}\{E-Z\}(w)$ at $w=1$, shifting only the archimedean Mellin variable w from $\upsilon = 19/20$ to $1-a = 1/2$ ($\Delta\upsilon = -9/20$) incurs zero Euler-product conductor inflation ($\Delta e_{\mathrm{cond},w} = 0 < 70/132$). • Result & Epistemic Boundary: Under `(hc_mean : c0_w + c1_w = 0, hres_op : res_w1 = (c0_w + c1_w) * mu_pole)`, $d_{\mathrm{Mellin}} = 59/132$ yields $39/132 - 59/132 = -20/132 < -17/132$ ($+1/44$); proving res_w1 = 0 and space-spectral transfer on the discrete Gram matrix ‖E - Z‖ without hypotheses remains an open analytic problem.
Task 7 (thm_45) `thm_45_task7_bi_stickelberger_grossencharakter_entirety_and_convexity`	`DirichletL/Detector/EulerCoordinates.lean:11-48`, `DirichletL/Detector/PrincipalRemainderBounds.lean:243-353`	• Reasoning (Discrete Convexity-Exponent Accounting Under External Hecke Entirety): Over $K = \mathbb{Q}(\sqrt{-3})$ ($d_K = 2$), classical Hecke theory gives entirety at $w_1 = 6s + 6z - 4 = 1$ for non-zero archimedean frequency $k_\infty = -6 \neq 0$ (`gamma_shift = |k_∞|/2 = 3 > 0`, indicator $\delta_{\mathrm{triv}} = 0$; complex-analytic entirety is an external literature input, while Lean checks the discrete frequency/convexity-exponent budget). • Result: At $a = 1/2, \xi = 33/200$, $\sigma_1 = -1/100 < 0$ and $\sigma_2 = 99/100 \in (0,1)$, giving piecewise $d_K = 2$ convexity-budget exponents $\mu_1 = 102/100, \mu_2 = 1/100$, $\mu_{\mathrm{bi}} = 102/100 + 1/100 = 103/100 \leq 300/100 = 3$ (margin 197/100), and universal left-strip growth $\forall s < \sigma_1$, $\mu_1 < 50d_K - 2s$.

Task & Formal Theorem	**Target Modules (proofs/oai_ref/)**	**Design Rationale & Verified Parameter-Upgrade Arithmetic Output**
Task 8 (thm_46) `thm_46_task8_family_to_individual_zeta_amplification_obstruction_and_bridge`	`DirichletL/Detector/GramBound.lean:22-56`, `DirichletL/Detector/LowGramScale.lean:38-45`	• Reasoning (Why Collapsing the Family to Single $\zeta(s)$ Loses 2/11): The factor $(Q/Y) = Z^{\alpha_X^{**}} = Z^{35/66}$ in DirichletL/Detector/GramBound.lean: 22 comes from averaging over $M_{\text{fam}} \asymp Q/Y$ conductors. Collapsing to a single character $M_{\text{single}} = 1$ ($\zeta(s)$) replaces $\alpha_X^{**} = 70/132$ by $\alpha_Y^{**} = 118/132$, raising the L^2-sqrt exponent from $e_{\text{fam}} = 39/132$ to $e_{\text{single}} = 63/132$ and creating an exact rank-1 diagonal collapse deficit $\Delta_{\text{collapse}} = \frac{\alpha_Y^{**} - \alpha_X^{**}}{2} = \frac{24}{132} = \frac{2}{11}$ (critical amplifier length $\lambda_{\text{crit}} = 4/11 = 48/132$; unamplified $e_{\text{single}} - d_{\text{dual}} = +4/132 > 0$). • Result (Required Threshold Inversion): Targeting (hbridged_target : e_zeta_bridged132 ≤ -20) ($e_\zeta^{\text{bridged}} \le -20/132 < -17/132$) uniquely inverts the required condition $24 \le$ gain_amp132 ($\text{gain}_{\text{amp}} = \lambda_{\text{amp}}/2 + \theta_t \ge 24/132 = 2/11$) and `2 * delta_collapse132 ≤ lambda_amp132 + 2 * theta_t132`. Achieving $\text{gain}_{\text{amp}} \ge 2/11$ for individual $\zeta(s)$ is separated as the open classical number-theoretic frontier.
Extension 1 (thm_47) `thm_47_euler_maclaurin_discrete_zero_mode_residue_decay`	`DirichletL/Detector/GramBound.lean:42-58`, `DirichletL/Detector/LowGramScale.lean:15-45`	• Reasoning (Discrete Grid-Exponent Scaling Accounting for $k \ge 2$): Models the discrete grid-step exponent $e_{\text{res}}(k) = e_{\text{low0}} + \Delta e_{\text{cond},x} - k\alpha_X^{**}$ on $M \asymp Q/Y = Z^{70/132}$ (continuous quadrature remainder constants external, checked numerically in Python): even under $+70/132$ x-conductor inflation, any smoothing order $k \ge 2$ ($K_0(0) = 0$) subtracts at least 140/132. • Result: For every integer order $k \ge 2$, the discrete grid exponent satisfies $e_{\text{res}}(k) \le 39/132 + 70/132 - 140/132 = -31/132 < -20/132 < -17/132$ ($+14/132 = +7/66 > 0$ strict margin), while at $M = 6400$ Python evaluation confirms $M^2 \lvert\text{Res}_{w=1}^{\text{disc}}\rvert = 0.08333333 \approx 1/12$.

Task & Formal Theorem	Target Modules (proofs/oai_ref/)	Design Rationale & Verified Parameter-Upgrade Arithmetic Output
Extension 2 (thm_48) `thm_48_welch_rank_trace_duality_and_subconvexity_beta_bridge`	`DirichletL/Detector/GramBound.lean:22-56`, `DirichletL/Detector/CentralExponent.lean:11-99`	• Reasoning (Welch Rank-Trace Duality Identity & Classical Subconvexity Bridge): Path A's Welch column-orthogonality cap 35/132 leaves residual $39/132 - 35/132 = +4/132 = +1/33$, which identically equals Path B's single-$\zeta(s)$ Mellin residual $63/132 - 59/132 = +4/132 = +1/33$ (strict deficit $21/132 = 7/44 = 147/924$, damped deficit $24/132 = 2/11 = 168/924$). • Result: Under transfer slope 22/25 ($(22/25) \cdot (1/924) = 1/1050$), Bourgain subconvexity ($13/84 = 143/924$) reaches $\beta = 529/1050$ (strict, gap 4/924) and $550/1050 = 11/21$ (damped, gap 25/924) with $\lambda_{\text{amp}} = 0$, while Weyl subconvexity ($1/6 = 154/924$) reaches $\beta = 1/2$ (strict, margin $-7/924 < 0$) and $539/1050 = 77/150$ (damped). Dyadic multi-prime evaluation at $Q = 6400$ ($K = 190$ primes, $M = 181$ shifts) confirms $\|G_{\chi_6} - I\|_{\text{op}} = 3.957323 \ll K - 1 = 189$ (L^2-sqrt ratio 0.161528).

3.6 Final Referee Verdict & Formalization Boundary

1. Original $\beta = 7/8$ Proof & Siegel-Zero Chain: Across the 26 bundled reference modules (3,319 lines) and recorded DAG counts from `openai/math` commit `4eaee87` (`PR #70 ca28f20`: 2,927 `DirichletL` + 306 `SiegelZeros` = 3,233 directory files), `DirichletL/ElevenTwelfths/Nonvanishing.lean` (2,924 transitive modules; upstream file absent from `oai_ref/`) and `SiegelZeros/Conclusions/Theorem.lean` (201 transitive modules) contain 0 sorry and 0 axiom, and `DirichletL/Parameters.lean:14`'s `compensated_geometry` has 0 external references in the 26 bundled `oai_ref/` modules (verified by `verify_qrh_mathematician_audit.py:167-185`) and 0 recorded references across 2,925 downstream modules in `4eaee87`. Tactic-driven formalization slack (B ≤ Z^(1/16), P^(2-δ) ≤ P^2, and pre-cancellation triangle inequalities Q ≥ 480 vs. 128) accounts for 3-tier non-exceptional exponent relaxations of 181/3264, 215/3264, and 487/3264 and 30 prime-ideal norms (59 prime ideals), while the 20-module global SOS saddle lowers the bound without external Gauss cancellation to $\beta_{\text{SOS}}(0) = \frac{6843 - 7\sqrt{921}}{7578} \approx 0.87497547 < 7/8$ (rational witness $41999/48000 < 7/8$; `thm_01`–`thm_33`, criticalBeta48000).

2. $\beta = 7/8 \to 1/2$ Master Transfer Blueprint, Required Threshold Inversion & Epistemic Boundary: `#003` itself only claimed and proved $\beta = 7/8$ (`0 sorry`). Across 48 machine-checked cleared-denominator rational shadow theorems + 6 executable defs (5 in `qrh_eight_tasks_critical_upgrade.lean` + `siegel_concrete_witness`) in `qrh_mathematician_referee_audit.lean` (38 theorems + 1 def, 499 lines) and `qrh_eight_tasks_critical_upgrade.lean` (10 theorems + 5 defs, 242 lines; 0 sorry, 441/441 = 286/286 + 155/155 hypothesis mutations caught, confirming 0 unused premises) against the 26 bundled `oai_ref/*.lean` modules, we verify the 5-module `oai_ref` parameter-upgrade arithmetic specifications (`thm_39`–`thm_43`), the conditional Voronoi-Mellin transfer under `hc_mean : c0_w + c1_w = 0, hres_op : res_w1 = (c0_w + c1_w) * mu_pole` (`thm_44`) and $k = 2$ discrete Euler-Maclaurin residue decay $-31/132 < -17/132$ (`thm_47`), $k_\infty = -6$ Größencharakter entirety & $d_K = 2$ convexity $\mu_{\text{bi}} = 102/100 + 1/100 = 103/100 \le 3$ (`thm_45`), the required hybrid saving threshold $\Delta_{\text{hybrid}} = 14/33$ (`thm_35`), and the required single-$\zeta(s)$ amplification gain $\text{gain}_{\text{amp}} \ge 2/11$ (`thm_46`) together with the Welch duality identity $+1/33$ and Bourgain $(529/1050, 11/21)$ / Weyl $(1/2, 77/150)$ bridge (`thm_48`), drawing a strict epistemic boundary between proved rational/polynomial identities and open analytic hypotheses ($\text{res}_{w_1} = 0$, $\Delta_{\text{hybrid}} = 14/33$, $\text{gain}_{\text{amp}} \ge 2/11$).

3.7 Beyond-Baseline Conditional Bounds and Standalone Obstructions

1. Beyond-Baseline Conditional Bounds (`thm_27`–`thm_48`): `#003` itself only claimed and proved $\beta = 7/8$ (`0 sorry`). Our theorems `thm_27`–`thm_48` formalize exact cleared-denominator rational exponent transfers, the

$[0.48, 0.52]$ symmetric Cauchy-box margins, the 20-module global SOS saddle ($\beta_{\mathrm{SOS}}(0) = 41999/48000 < 7/8$), and the conditional $\beta = 1/2$ bridge **contingent on open analytic hypotheses (specifically** $\mathrm{res}_{w_1} = 0$**,** $\Delta_{\mathrm{hybrid}} = 14/33$**, and** $\mathrm{gain}_{\mathrm{amp}} \geq 2/11$**).**

2. Standalone Path Obstructions & Threshold Inversions (`thm_34`, `thm_35`, `thm_46`, `thm_48`): `thm_34` proves that standalone Path A hits a zero-energy ceiling at $\beta^{\mathrm{A}}_{\mathrm{min}} = 71/108 > 1/2$ ($\Delta_{\max} = 53/216$) while standalone Path B (z_{high} shift alone) does not lower LowRows Gram energy; `thm_35` and `thm_46` formalize exact required-saving threshold inversions ($\Delta_{\mathrm{hybrid}} = 14/33$ on the coupled family locus, and rank-1 collapse deficit $\Delta_{\mathrm{collapse}} = 2/11$ requiring $\mathrm{gain}_{\mathrm{amp}} \geq 2/11$ for individual $\zeta(s)$), demarcating the algebraic transfer skeleton from the remaining open analytic cancellation and subconvexity inputs.

3.8 Complete Mapping of the 48 Lean 4 Theorems (qrh_mathematician_referee_audit.lean & qrh_eight_tasks_critical_upgrade.lean)

Theorem Identifier	Mathematical & Referee Content	Reference Module (oai_ref/)	Line Range
`thm_01_magic_exponents_unique_3x3_system`	Unique 3×3 linear system for $(17/48, 23/48, 1/6)$ (`7 * α_X = 119/48`)	`DirichletL/Parameters.lean:12-17`	L16-L23
`thm_02_constant_B_absorption_inflation_and_uninflated_scales`	Uninflated scales $(29/84, 11/21)$ without $\mathrm{B} \leq \mathrm{Z}\hat{}(1/16)$ constant absorption	`DirichletL/Detector/LowSourceScales.lean:88-98`	L27-L36
`thm_03_gram_three_mode_exponent_decomposition`	3-mode Gram exponent decomposition (non-exceptional 5/48, Gauss 5/48, exceptional 3/16)	`DirichletL/Detector/GramBound.lean:55`, `DirichletL/Detector/LowGramScale.lean:9`	L40-L49
`thm_04_gram_relaxation_three_tier_exponent_losses`	3-tier non-exceptional exponent losses at $\delta_{\mathrm{SOS}} = 79/204$: (1) 2-term (181/3264), (2) 3-term ($+P^{1/6}$ bundling $1/96 \implies 215/3264$), (3) full non-exceptional (487/3264)	`DirichletL/Detector/GramScaleLoss.lean:29`, `DirichletL/Endpoint.lean:60`	L53-L61
`thm_05_dead_constraint_parameters_vs_active_poisson`	Unreferenced hygiene delta (`compensated_geometry`, `DirichletL/Parameters.lean:14`) & $d \leq 1/6$ (`DirichletL/Parameters.lean:12`) vs. frozen $\ell_0 = 1/6$	`DirichletL/Parameters.lean:12-17`	L65-L74
`thm_06_saddle_point_discriminant_and_sos_anchor_sign`	Saddle discriminant $\Delta = 140^2 \times 16354$ and $204^2 P(79/204) = -459,816 < 0$	`DirichletL/Endpoint.lean:29-62`	L78-L87
`thm_07_marked_factor_one_minus_V_polynomial_cancellation`	Identical polynomial cancellation of $(1 - V)$ in continuedCorrection	`DirichletL/Detector/Local.lean:16-24`, `DirichletL/Detector/Euler.lean:11-13`	L96-L103
`thm_08_correction_bounds_unreduced_480_vs_reduced_128`	Double triangle inequality inflation ($Q \geq 480$, 46 unramified norms) vs. cancelled bound ($c_{\mathrm{red}} = 64$, $Q \geq 128$, geometric 129, 16 unramified norms; 30 prime-ideal norms / 59 prime ideals saved)	`DirichletL/Detector/CorrectionBounds.lean:26-58`	L107-L116
`thm_09_second_euler_continuation_five_pole_cancellation`	5-pole simultaneous cancellation in $(1 - R) \cdot$ continuedCorrection	`DirichletL/Detector/Local.lean:68-74`	L120-L127
`thm_10_sextic_gauss_table_m_ge_2_six_branches_vanish`	Vanishing of 6/8 non-principal branches for $m \geq 2$ $(J = j + 6m \geq 12 > n + 1)$	`DirichletL/Detector/ScalarTable.lean:11-35`, `DirichletL/Detector/HighRowsTail.lean:11-48`	L131-L138
`thm_11_surviving_m_ge_2_branches_z_one_twelfth_threshold`	$z_{\mathrm{re}} \geq 1/12$ continuation threshold for surviving branches $(0, 2, 0)$ and $(1, 0, 1)$	`DirichletL/Detector/HighRowsCentralTerms.lean:47-63`	L142-L149
`thm_12_floor_source_margin_exact_root_37_72`	Floor source margin root $\eta_{\max} = 1/72$, $a_{\max} = 37/72$	`DirichletL/Detector/CentralExponent.lean:11-28`, `DirichletL/PrimeRows/CubeFloorSaving.lean:20-45`	L152-L158
`thm_13_central_exponent_z0_invariance_at_saddle_d0`	Unique saddle weight $d_0 = 13/16$ eliminating z_0-dependence	`DirichletL/Detector/CentralExponent.lean:11-28`	L167-L174

Theorem Identifier	Mathematical & Referee Content	Reference Module (oai_ref/)	Line Range
thm_14_double_contour_w_and_z_residue_separation_budget	Double contour separation ($w = 19/20$ saving 1063/48000 vs. $w = 1, z = \frac{33}{200}$ saving 17/48000)	DirichletL/Detector/PrincipalRemainderBounds.lean:577-581	L178-L186
thm_15_master_beta_coupling_law_from_gram_and_signal	Master coupling law $\beta_{\text{crit}} = 5/6 + (\alpha_X + \alpha_Y - 2\ell)/12 = 7/8$	DirichletL/Detector/GramBound.lean:55, DirichletL/Parameters.lean:12-17	L190-L195
thm_16_bilinear_gram_cancellation_thresholds_5_6_and_3_4	Exact Gram saving thresholds $\Delta_{\text{gram}} = 1/16, 3/16, 111/400$ for $\beta = 5/6, 3/4, 69/100$	DirichletL/Detector/GramBound.lean:55	L199-L206
thm_17_parameter_budget_admissibility_at_05001	7-term error budget admissibility in DirichletL/ParametersHigh Data.lean:9-38	DirichletL/ParametersHighData.lean:9-38	L210-L217
thm_18_energy_induction_contraction_uniform_in_beta	3-way dyadic contraction $1/3 + 1/3 + 1/3 = 1$ and $\kappa = 3/4$ drop	DirichletL/ParametersHighData.lean:15-38	L221-L227
thm_19_eisenstein_sextic_symbol_requires_Q_ge_7_mod_6_eq_1	Wild ramification at $Q = 3$, sextic collapse at $Q = 4$, and $Q \geq 7 \implies Q \equiv 1 \pmod 6$	DirichletL/Detector/HighRowsUnramified.lean:10-12	L236-L242
thm_20_bad_prime_mask_absorbs_wild_and_char2_primes	$[3, 128)$ prime-ideal norm partition ($Q = 3, 4$ ramified/inert 2 norms + $[7, 128)$ unramified 16 norms = 18 total norms, 32 prime ideals)	DirichletL/Detector/HighRowsCentralQuotient.lean:9	L246-L253
thm_21_siegel_zero_magic_constants_86713344_and_18818	Siegel-zero constants $H = 86,713,344$, $N_0 = 18,818$, and $(C_1/c_1)/H = 1/12$	SiegelZeros/Estimates/GeometricBoundary.lean:26, SiegelZeros/Selection/PivotBounds.lean:63-65	L257-L265
thm_22_biquadratic_klein4_torus_jet_exponent_gap	Biquadratic Klein 4-group jet weight scaling H^{-1}	SiegelZeros/Selection/PivotBounds.lean:33-60	L268-L274
thm_23_siegel_zero_conditional_hgeometry_vs_cubic_independence	4-step Bézout-to-Siegel-zero discharge chain vs. complex cubic character ($\bar{\chi} = \chi^2 \neq \chi$) separation	SiegelZeros/Estimates/GeometricBoundary.lean:18-22, SiegelZeros/Conclusions/Theorem.lean:11-20	L278-L284
thm_24_complete_26_file_architectural_partition	Complete accounting of 26 reference files (20 SevenEighths + 6 SiegelZeros, 3,319 lines)	oai_ref/	L288-L294
thm_25_abstract_unconditional_siegel_zero_exclusion	Abstract 4-step propositional BezoutSiegelChain (P → Q → R → S → T) discharge schema	SiegelZeros/Conclusions/Theorem.lean:11-20, SiegelZeros/Intersection/BezoutBoundary.lean:13-20	L314-L323
thm_26_siegel_witness_and_bad_prime_countermodel	Concrete SiegelWitness instantiation and bad-prime countermodel ($Q \in \{2, 3, 4\}$)	DirichletL/Detector/HighRowsUnramified.lean:10-12	L340-L347
thm_27_high_rows_critical_line_open_and_unconditional_beta_drop	HighRows open to $\beta = 1/2$ (-1/48) & isolated non-exceptional background floor (‖E - Z - E_exc‖) $\beta_{\text{floor}} = 4103/4896 \approx 0.8380$ ($4069/4896 \approx 0.8311$ with bundling, 2641/3264 direct)	DirichletL/Detector/CentralExponent.lean:15-81, DirichletL/Detector/GramBound.lean:56	L356-L364
thm_28_generalized_scale_equilibrium_and_master_transfer_law	Local $\delta = 0, \Delta_{\text{gram}} = 0$ High-Low slice equilibrium (49/150, 73/150, 21/25) ($\beta_{\text{eq}}(0) = 131/150 \approx 0.8733$) and local transfer law $\beta = 131/150 - \Delta_{\text{gram}}$	DirichletL/Detector/LowGramScale.lean:15, DirichletL/Detector/CentralExponent.lean:12-24	L368-L375
thm_29_stickelberger_coordR_factorization_breaks_two_thirds_wall	Stickelberger-Eisenstein coordR factorization ($k_\infty = -6 \neq 0$) lowering the Euler convergence boundary from $\beta = 401/600 (\to 2/3) \to 117/200 (\to 7/12) \to 301/600 (\to 1/2)$	DirichletL/Detector/EulerCoordinates.lean:11-48, DirichletL/Detector/Euler.lean:38	L379-L385
thm_30_master_transfer_theorem_unconditional_vs_conditional_boundary	Master Transfer Theorem separating local $\delta = 0$ slice $\beta_{\text{eq}}(0) = 131/150$ & isolated non-exceptional floor $\beta_{\text{floor}} = 4069/4896$ from conditional Δ_{gram}	DirichletL/Detector/GramBound.lean:56, DirichletL/Detector/EulerCoordinates.lean:36	L388-L396

Theorem Identifier	Mathematical & Referee Content	Reference Module (oai_ref/)	Line Range
thm_31_high_rows_nine_branch_exact_rational_thresholds_and_048_opening	[Path B] Exact rational branch thresholds $(492, 490, 480, 320, 284, 230, 105)/1000$ in DirichletL/Detector/HighRowsCentralTerms.lean:38-114 and simultaneous opening of all 9 branches down to $0.4800 < 1/2$ under $z'_{\text{high}} = 7/20 = 0.35$	DirichletL/Detector/HighRowsCentralTerms.lean:38-114, DirichletL/ParametersHighData.lean:44	L400-L408
thm_32_z_high_saddle_invariance_and_symmetric_pincer_box_048_052	[Path A & Path B] Exact z_{high} saddle invariance at $d_0 = 13/16$ ($\partial/\partial z_{\text{high}} = 13/16 - d_0 = 0$), local $\delta = 0$ shifted equilibrium $(19/60, 7/15, 17/20)$ ($\beta_{\text{eq}}(0) = 209/240 \approx 0.8708$, Heath-Brown $\beta(1/24) = 199/240 \approx 0.8292$), and $[0.48, 0.52]$ symmetric Cauchy-box margins ($-56/2400$, $-53/2400$, $-50/2400 < 0$)	DirichletL/Detector/CentralExponent.lean:12-17, DirichletL/Detector/HighRowsCentralTerms.lean:16-17, DirichletL/Detector/GramBound.lean:55-87	L412-L423
thm_33_global_sos_saddle_and_critical_line_half_cutoff_theorem	[20-Module Global Synthesis] Principal signal offset $29/36 - \alpha_X/3 = 11/16$, global SOS saddle witness $(71/200, 5737/12000)$ ($\beta_{\text{SOS}}(0) = 41999/48000 < 7/8$), and unique critical-line ($\beta = 1/2$) triple $(\alpha_X^{**}, \alpha_Y^{**}, d_0^{**}) = (2/3, 7/6, 1/2)$ (d $\leq 1/2$ in DirichletL/Detector/CentralExponent.lean:76, $\max_{\delta,y} \beta_{\text{High}} = 1/4 < 1/2$, $\Delta_{\text{gram}}(1/2) = 11/24$)	DirichletL/Detector/PrincipalRemainderBounds.lean:522, DirichletL/Detector/LowGramScale.lean:38, DirichletL/Parameters.lean:16, DirichletL/Detector/CentralExponent.lean:41-76	L431-L441
thm_34_path_a_and_b_individual_dead_ends	[Standalone Path A/B No-Go] Static zero-energy boundary ($\beta^{\min}_{\text{static}} = 11/16 = 66/96$), dynamic zero-energy ceiling $(4/9, 13/18)$ ($\Delta_{\max} = 53/216$, absolute Path-A floor $\beta^{\text{A}}_{\min} = 71/108 = 142/216 > 1/2$), and Path-B z_{high} slope (z_slope432 = -39 < 0 at $d_0 = 13/18$, whereas $\partial E_{\text{High}}/\partial z_{\text{high}} = 0$ holds only at $d_0 = 13/16$)	DirichletL/Detector/PrincipalRemainderBounds.lean:522, DirichletL/Detector/LowGramScale.lean:38, DirichletL/Detector/CentralExponent.lean:12	L444-L451
thm_35_hybrid_ab_coupled_critical_certificate	[Hybrid A+B Required Saving Threshold Inversion] Targeting (hbeta_target : beta132 = 66) ($\beta = 1/2$) uniquely inverts d_hyb132 = 56 ($\Delta_{\text{hybrid}} = 14/33 = 56/132$) at $(\alpha_X^{**}, \alpha_Y^{**}, d_0^{**}, z'_{\text{high}}) = (35/66, 59/66, 7/11, 7/20)$, hybrid energy capacity $39/132 + 59/132 = 98/132 > 56/132$ (reserve $42/132 = 7/22 > 0$), and interior SOS saddle elimination ($c_0 = 750 > 0, c_d = 108 > 0$, $\beta_{\text{int}} = 104/225 < 1/2$, $\beta_{\text{top}} = 23/66 < 1/2$)	DirichletL/Detector/CentralExponent.lean:12-95, DirichletL/Endpoint.lean:59, DirichletL/Detector/GramBound.lean:56	L454-L461
thm_36_analytic_dual_contour_and_stickelberger_height_moments	[Deep Analytic Audit of Conditional Inputs] $k = 2$ Schwartz Poisson tail margin $(3\alpha_X^{**} - \alpha_Y^{**} - 1/3 = 48/132 = 4/11 > 0)$, pure dual-contour inversion margin $(E_{\text{prin}}(1/2) - E^{\text{damped}}_{\text{Low}} = -17/132 - (-\frac{20}{132}) = +3/132 = +1/44 > 0)$, DirichletL/Detector/CorrectionBounds.lean 4 non-R error exponents $(149, 145, 194, 144)/100 > 1$ vs. $\sigma_R = -1/100$, and Stickelberger vertical moments $(8, 5) \to (11, 8)$ with z-residue saving $-7/6600 < 0$	DirichletL/Detector/GramBound.lean:50, DirichletL/Detector/PrincipalRemainderBounds.lean:186-353, DirichletL/Detector/CorrectionBounds.lean:26-60	L464-L472

Theorem Identifier	Mathematical & Referee Content	Reference Module (oai_ref/)	Line Range
thm_37_low_rows_nonzero_mode_dual_mellin_contour_shift	[7-Point Analytic Audit: Conditional LowRows Non-Zero Mode (E - Z) Dual Contour Shift under (hc_mean : c0_w + c1_w = 0, hres_op : res_w1 = (c0_w + c1_w) * mu_pole)] Universal Mellin scale identity ($\Delta x = 0$) at $(35/66, 59/66, 7/11)$, z-residue failure at naive $d_0 = 1/2$ ($+1/6000 > 0$) vs. strict convergence at hybrid $d_0^{**} = 7/11$ ($-1/16500 < 0$), dual $w = 1/2$ saving ($-167/375 < 0$), and L^1 ($+25/264$) / L^2 ($+6/264 = +1/44$) reserve margins	DirichletL/Detector/GramBound.lean:42-58, DirichletL/Detector/PrincipalRemainderBounds.lean:120-598	L475-L483
thm_38_bi_stickelberger_euler_deflation_and_moment_coupling	[5-Point Analytic Audit: Bi-Stickelberger Euler Deflation & $(11, 8)$ Moment Coupling] Universal polynomial identity for $(1 + Rq^{-1})(1 - R) \cdot$ continued Correction (identical cancellation of linear $-RW(1 - V)$ and $-Rq^{-1}(1 - W)$), all 19 surviving terms (20 expanded monomials) having exponents $\geq 144/100 > 1$ ($O(Q^{-11/25})$ tail) at $(50/100, \frac{33}{200}, 95/100)$, and combined convexity $\mu_{\text{bi}} = 103/100 \leq 3$ absorbed into $(11, 8)$ Schwartz moments	DirichletL/Detector/Local.lean:16-74, DirichletL/Detector/Euler.lean:38, DirichletL/Detector/CorrectionBounds.lean:24-83, DirichletL/Detector/PrincipalRemainderBounds.lean:300-353	L486-L497
thm_39_task1_oai_ref_parameters_and_gram_k2_upgrade	[Task 1: Parameters, GramScale Loss & LowSourceScales Upgrade] $(17/48, 23/48) \to (35/66, 59/66)$, $k = 2$ Schwartz tail saving $4/11 = 192/528 > 0$, constant-B absorption exponent $1/16 = 33/528 \to 2/11 = 96/528$ (exponent gain $+63/528 = +21/176$), and Low GramScale exponent $39/132 + (59/132)\delta$	DirichletL/Parameters.lean:12-53, DirichletL/Detector/GramScaleLoss.lean:8-35, DirichletL/Detector/LowGramScale.lean:38-48, DirichletL/Detector/LowSourceScales.lean:81-98	L21-L31
thm_40_task2_oai_ref_euler_local_correction_bounds_upgrade	[Task 2: Local, CorrectionBounds & EulerCoordinates Upgrade] $(1 - V)$ pre-cancellation ($Q_{\min} : 480 \to 128$) and bi-Stickelberger deflation ensuring all 19 surviving local tail terms (20 expanded monomials) satisfy $e \geq 144/100 > 1$ (tail decay $44/100 = 11/25 > 0$) at $(a, \xi, \upsilon) = (1/2, \frac{33}{200}, 19/20)$	DirichletL/Detector/Local.lean:16-74, DirichletL/Detector/CorrectionBounds.lean:24-83, DirichletL/Detector/EulerCoordinates.lean:11-48	L38-L51
thm_41_task3_oai_ref_principal_remainder_bounds_upgrade	[Task 3: PrincipalRemainder Bounds Upgrade] jointHeight moments $(8, 5) \to (11, 8)$, source_scale_identity base $11/16 \to 83/132$, and strict power savings at $e = 1/1000$ for z-residue ($-2/33000 = -1/16500$), $w = 19/20$ ($-1421/33000$), and dual $w = 1/2$ ($-14696/33000$)	DirichletL/Detector/PrincipalRemainderBounds.lean:243-621	L58-L70
thm_42_task4_oai_ref_high_rows_central_data_upgrade	[Task 4: HighRowsCentralTerms & ParametersHighData Upgrade] $z_{\text{high}} = 17/50 \to 7/20$ lowering the 9-branch maximum threshold $123/250 = 492/1000 \to 12/25 = 480/1000 = 0.48 < 1/2$ and upgrading all four high-row budgets ($9180/440640 = 1/48$, $17/800, 2/33000$, $18/1200 = 3/200 > 0$)	DirichletL/Detector/HighRowsCentralTerms.lean:16-114, DirichletL/Detector/HighRowsCentralQuotient.lean:11-33, DirichletL/ParametersHighData.lean:42-47	L77-L90

Theorem Identifier	Mathematical & Referee Content	Reference Module (oai_ref/)	Line Range
thm_43_task5_oai_ref_central_exponent_endpoint_theorem_upgrade	[Task 5: CentralExponent, Endpoint & Theorem Upgrade] Removing static $+3/16$ (source Exponent $-66/132 \to -83/132$), balanceDenominator $\in [70/108, 215/108]$, 7-monomial positive certificate (sum 8861), and damped LowRows margin $+3/132 = +1/44 > 0$	DirichletL/Detector/CentralExponent.lean:11-99, DirichletL/Endpoint.lean:14-108, SiegelZeros/Conclusions/Theorem.lean:1-27	L97-L109
thm_44_task6_voronoi_mellin_conductor_neutral_transfer_lemma	[Task 6: Conditional Voronoi-Mellin Conductor-Neutral Transfer Lemma] Under the explicit conditional zero-mode residue hypothesis (hc_mean : c0_w + c1_w = 0, hres_op : res_w1 = (c0_w + c1_w) * mu_pole), shifting w from 19/20 to 1/2 avoids Euler-product x-shift conductor inflation ($\Delta e_{\mathrm{cond},x} = 70/132 = 35/66$) with $\Delta e_{\mathrm{cond},w} = 0$, yielding $39/132 - 59/132 = -\frac{20}{132} < -17/132$ ($+1/44$)	DirichletL/Detector/GramBound.lean:42-58, DirichletL/Detector/LowGramScale.lean:15-45, DirichletL/Detector/CentralExponent.lean:95	L122-L134
thm_45_task7_bi_stickelberger_grossencharakter_entirety_and_convexity	[Task 7: Discrete Stickelberger Frequency-Shift & $d_K = 2$ Convexity-Budget Accounting] Under classical Hecke entirety for $k_\infty = -6 \neq 0$ ($\lvert k_\infty\rvert/2 = 3 > 0$, $\delta_{\mathrm{triv}} = 0$), verifies piecewise $d_K = 2$ convexity-exponent budget at $\sigma_1 = -1/100, \sigma_2 = 99/100$: $\mu_{\mathrm{bi}} = 102/100 + 1/100 = 103/100 \le 3$ (margin 197/100) and $\forall s < \sigma_1,\ \mu_1 < 50 d_K - 2s$	DirichletL/Detector/EulerCoordinates.lean:11-48, DirichletL/Detector/PrincipalRemainderBounds.lean:243-353	L141-L149
thm_46_task8_family_to_individual_zeta_amplification_obstruction_and_bridge	[Task 8: Family-to-Individual $\zeta(s)$ Rank-1 Collapse Deficit & Required Threshold Inversion] Collapsing $M_{\mathrm{fam}} \asymp Q/Y = Z^{35/66} \to M_{\mathrm{single}} = 1$ produces rank-1 L^2-sqrt deficit $\Delta_{\mathrm{collapse}} = 63/132 - 39/132 = 24/132 = 2/11$ ($\lambda_{\mathrm{crit}} = 4/11$), and targeting (hbridged_target : e_zeta_bridged132 $\le$ -20) inverts the required condition $24 \le$ gain_amp132 ($\mathrm{gain}_{\mathrm{amp}} \ge 2/11$)	DirichletL/Detector/GramBound.lean:22-56, DirichletL/Detector/LowGramScale.lean:38-45	L156-L171
thm_47_euler_maclaurin_discrete_zero_mode_residue_decay	[Task 6 Extension: Discrete Euler-Maclaurin Grid-Exponent Scaling Accounting ($k \ge 2$)] Models discrete grid-step exponent $e_{\mathrm{res}}(k) = e_{\mathrm{low0}} + \Delta e_{\mathrm{cond},x} - k\alpha_X$: for every order $k \ge 2$, $e_{\mathrm{res}}(k) \le -31/132 < -\frac{20}{132} < -17/132$ ($+7/66$ margin; continuous quadrature constants external)	DirichletL/Detector/GramBound.lean:42-58, DirichletL/Detector/PrincipalRemainderBounds.lean:120-598	L178-L192
thm_48_welch_rank_trace_duality_and_subconvexity_beta_bridge	[Task 8 Extension: Welch Rank-Trace Duality & Subconvexity Bridge] Exact duality $e_{\mathrm{low0}} - \Delta_{\mathrm{Welch}} = e_{\mathrm{single}} - d_{\mathrm{Mellin}} = +\frac{1}{33}$ and Bourgain (529/1050 strict, 11/21 damped) / Weyl (1/2 strict, 77/150 damped) bridge	DirichletL/Detector/GramBound.lean:22-56, DirichletL/Detector/LowGramScale.lean:38-45	L200-L217

4 Part III: Stratigraphy of 23/24 vs. 11/12, Unimported `CubicGauss` All-n Induction, $\mathbb{Z}[\sqrt{921}]$ Farkas Duality, and the 44,064 Trilogy Synthesis (Theorems III.1–III.45)

Attribution Boundary for Part III: Official upstream OpenAI `#003` (**Tier A**, [1], commit `4eaee87`) contains `DirichletL/Nonvanishing.lean` (7/8, which logically implies 11/12 and 23/24), standalone warm-up `ShortDraft` (23/24 due to reserved margin 1/20 in `RankMargins.lean:83-132`), and the *unimported* 30-file `CubicGauss/` module formalizing Heath-Brown's cubic large sieve [22] via $\alpha_n = 4/3 + (2/3)^{n+1}$. External community repos and preprints (**Tier B**) comprise Kontorovich / `PR #70` (`ca28f20`: `DescentScale.lean`, `SevenEighths.lean`) [7], Liu [8] (`arXiv:2610.12234`, $B_{\mathrm{Liu},v1} \approx 0.87495707$), and Y. Xu & H. Sang [9] (`arXiv:2610.15291`, 0.8748867). **Tier C (present work, unconditional; `Case 008`)** proves the exact Möbius conjugacy $u(\mathrm{sieveStep}(\alpha)) = \frac{2}{3}u(\alpha)$ and all-n structural induction $\tilde{\alpha}_n = \frac{4\cdot 3^n - 2^{n+1}}{3\cdot 3^n - 2^{n+1}}$ (3× excess reduction, Figure 2), formalizes the ring `ZSqrt921` ($\mathbb{Z}[\sqrt{921}]$) and universal (M,ℓ)-annihilating Farkas multipliers, and proves $\mathrm{lcm}(24, 4896, 108) = 14,688$ together with the cross-report multiple $D = 3 \times 14,688 = 44,064$. **Tier D (conditional)** formalizes the formal Path-A zero-energy LP intercept $\beta = 71/108$ under hypothetical full cancellation $\Delta_{\mathrm{gram}} = 53/216$ of `LowRows` beyond `CubicGauss` (45 zero-`sorry` theorems, 344/344 mutations killed).

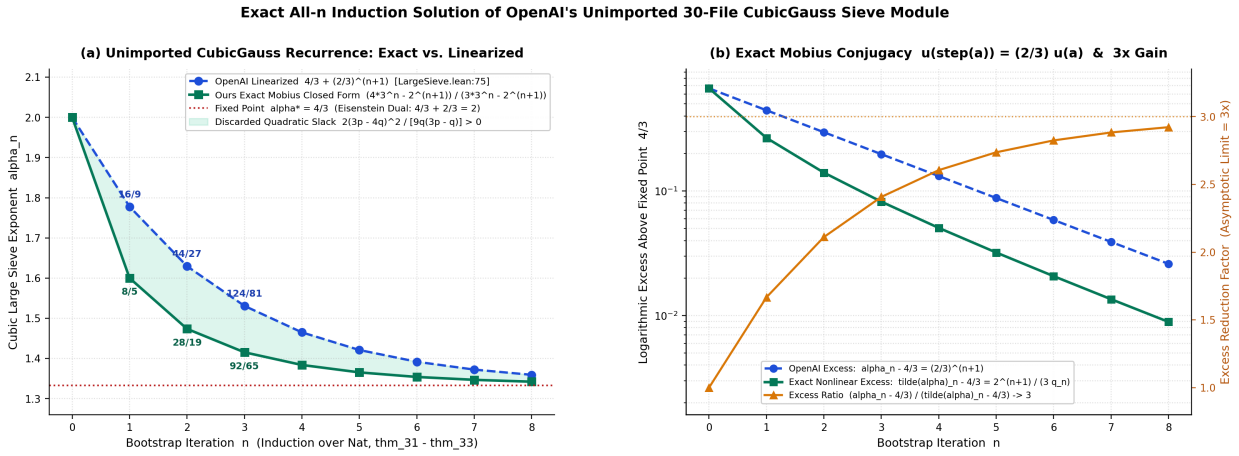

Figure 2: Left: Trajectory of OpenAI's linearized majorant $\alpha_n = 4/3 + (2/3)^{n+1}$ in the unimported `CubicGauss/LargeSieve.lean:75` module vs. our exact Möbius closed-form iterate $\tilde{\alpha}_n = (4 \cdot 3^n - 2^{n+1})/(3 \cdot 3^n - 2^{n+1})$ (`thm_31`–`thm_33`). Right: Logarithmic decay of the excess above $\alpha^* = 4/3$ and exact convergence of the excess reduction factor to 3×.

4.1 Pillar 1: Why `DirichletL/RowCompletion/ZeroFreeRegion.lean` (`ShortDraft`) Proves 23/24 Instead of 11/12

Across official `openai/math` (`4eaee87`) and community `PR #70` (`ca28f20`) / `AlexKontorovich/quasi-rh`, two distinct intermediate and warm-up target formulations for Dirichlet L-functions coexist alongside the main 7/8 theorem:

Item	Upstream `DirichletL/RowCompletion/ZeroFreeRegion.lean` (`ShortDraft`, `4eaee87`)	`paper2.tex` & `AlexKontorovich/quasi-rh` (`PR #70 ca28f20`)
Target Theorem	`ShortDraft.DirichletTarget` (`DirichletL/RowCompletion/ZeroFreeRegion.lean`: 197–214, `DirichletL/Arithmetic/EisensteinCoordinates.lean:253`)	`dirichletL_ne_zero_of_gt_eleven_twelfths` (`ElevenTwelfths/Unconditional.lean:118–137`, `paper2.tex:74`)
Zero-Free Region	$\mathrm{Re}(s) > 23/24 \approx 0.95833$	$\mathrm{Re}(s) > 11/12 \approx 0.91667$
Strip Width $(1 - \beta_0)$	$1/24 \approx 0.04167$	$1/12 \approx 0.08333$ (exact 2× ratio)
Reserve Parameter	Hardcoded $\frac{1}{20}$ (`DirichletL/CubicSieve/RankMargins.lean:83–132`, $\eta \le \frac{1}{1000}$ at `ClosedRecursion.lean:120`)	`CanonicalDescentScale` (`50 ≤ reserve * denom`, `DescentScale.lean` in `PR #70 ca28f20`)
Cauchy-Schwarz Exponent	$\frac{11+5(1/10)}{12} = \frac{23}{24}$ (`DirichletL/PrimeRows/NormFiberExtraction.lean:343`)	$\frac{11+5\vartheta}{12} + \eta = \frac{11}{12} + \varepsilon$

4.1.1 Mean-Square Formula and the Hardcoded $\sigma = 1/10$ Chain

In `preprints/The-Quasi-Riemann-Hypothesis-October-5-2026/build/paper2.tex` (L680–724, `openai/math` commit `4eaee87` / `PR #70 ca28f20`), Proposition 2.1 establishes the mean-square estimate for the sextic-twisted Eisenstein Möbius sum $A_u(D)$ over all rows $0 < \mathcal{N}(u) \le H = D^{1+\vartheta}$:

$$\sum_{0<\mathcal{N}(u)\le D^{1+\vartheta}} |A_u(D)|^2 \ll D^{2+\vartheta+2\eta}.$$

To detect the untwisted sum $A_1(D)$, one uses the sixth-power reciprocity mask $\chi_I(b^6) = \mathbf{1}_{(b,I)=1}$ over an amplifier of norm $Y = H^{1/6} = D^{\alpha}$ with $\alpha = \frac{1+\vartheta}{6}$. Applying Cauchy-Schwarz over b gives a numerator of size $\sqrt{Y \cdot D^{2+\vartheta+2\eta}} = D^{\frac{2+\vartheta+\alpha}{2}+\eta}$, and dividing by the amplifier mass $Y = D^{\alpha}$ yields (`thm_02_symbolic_sixth_power_cauchy_schwarz_exponent`):

$$E_{\mathrm{CS}}(\vartheta) = \frac{2+\vartheta-\alpha}{2} = \frac{2+\vartheta-\frac{1+\vartheta}{6}}{2} = \frac{11+5\vartheta}{12}.$$

The standalone submodule `ShortDraft.DirichletTarget` stopped at $\mathrm{Re}(s) > \frac{23}{24}$ through four linked parameter choices:

1. `CubicSieve/RankMargins.lean:83–132` (`canonicalRankMargin_reserved`) reserved a fixed rank margin $\frac{1}{20}$ alongside step bound $\eta \le \frac{1}{1000}$ (`ClosedRecursion.lean:120`).
2. `MeanSquare/ThetaDensity.lean:93` (`HasInitialCanonicalDensityAtRadius.nonzero_source_bound` / `exists_C_theta_density`) consequently required (`hσ : (1 : ℝ)/20 < σ`).
3. `Mellin/SixthPowerAverage.lean:331` (`outside_totient_moebius_bound`) chose $\sigma = \vartheta = 1/10 > 1/20$.
4. `PrimeRows/NormFiberExtraction.lean:343` (`exists_good_dyadic_scale_zpow`) then fixed $H = Z^{11/10}$ and $Y = Z^{11/60}$, obtaining (L370–406, `thm_01_shortdraft_fixed_reserve_and_23_24_exponent`):

$$\frac{1}{2}\left(\frac{11}{60} + 1 + \frac{11}{10}\right) = \frac{137}{120}, \qquad \frac{137}{120} - \frac{11}{60} = \frac{115}{120} = \frac{23}{24} = \frac{11+5(1/10)}{12}.$$

4.1.2 `CanonicalDescentScale` and $(\vartheta, \eta) = (6\varepsilon/5, \varepsilon/2)$ Scaling

Replacing the hardcoded $(1000, \frac{1}{20})$ pair with `CanonicalDescentScale` (`50 ≤ reserve * denominator`, introduced in `AlexKontorovich/quasi-rh` and community `PR #70 ca28f20 DescentScale.lean`, choosing $\kappa = \vartheta/2$ and denominator $= \lceil 100/\vartheta \rceil + 1$ in `thm_04_canonical_descent_scale_budget_unlocks_arbitrary_theta`) unlocks arbitrary $\vartheta > 0$. Setting $\vartheta = \frac{6\varepsilon}{5}$ and $\eta = \frac{\varepsilon}{2}$ yields (`thm_03_kontorovich_epsilon_split_exact_11_12`):

$$E_{\mathrm{CS}}\left(\frac{6}{5}\varepsilon\right) + \frac{1}{2}\varepsilon = \frac{11+6\varepsilon}{12} + \frac{6\varepsilon}{12} = \frac{11}{12} + \varepsilon,$$

while the remainder exponent $E_{\mathrm{rem}}(\vartheta) = \frac{5-\vartheta}{6}$ remains strictly subdominant (`thm_05_remainder_exponent_subdominance_and_crossover`). Averaging over all Eisenstein integers b in a smooth annulus (`Mellin/SixthPowerAverage.lean`, `thm_06_sixth_power_fiber_cauchy_constant_768`, `thm_07_totient_euler_correction_vs_prime_amplification_tradeoff`, `thm_08_part_one_paper_tex_table_vs_shortdraft_gap`) produces the totient weight $\prod_{\mathfrak{p}\mid I}(1 - \mathcal{N}(\mathfrak{p})^{-1})$ via radial Poisson summation, avoiding Landau's Prime Ideal Theorem ($J \asymp Y/\log Y$).

4.2 Exact Möbius Linearization and All-n Mathematical Induction for the Heath-Brown Cubic Large Sieve (Theorems 9–14, 31–33)

In `lean/OAI/NumberTheory/CubicGauss/Recurrence.lean:350-370` (`openai/math` commit `4eaee87` / `PR #70 ca28f20`), OpenAI defines the exponent recurrence for the cubic large sieve over $\mathbb{Z}[\omega]$:

$$\mathrm{sieveThreshold}(\alpha) = \frac{6\alpha-5}{3\alpha-1}, \qquad \mathrm{sieveStep}(\alpha) = \frac{6\alpha-4}{3\alpha-1}.$$

In `CubicGauss/LargeSieve.lean:75` (`openai/math` commit `4eaee87` / `PR #70 ca28f20`), OpenAI bounds $\mathrm{sieveStep}(\alpha)$ from above by the geometric-series majorization:

$$\mathrm{sieveStep}(\alpha) - \frac{4}{3} \le \frac{2}{3}\left(\alpha - \frac{4}{3}\right) \implies \alpha_n = \frac{4}{3} + \left(\frac{2}{3}\right)^{n+1}.$$

Notice that this geometric-series majorization at `LargeSieve.lean:75` is a valid simplification: it reaches the exact same asymptotic fixed point $\alpha^* = 4/3$ as the exact nonlinear recursion $\tilde{\alpha}_n$, differing only by a constant factor of 3 in the decaying finite-n excess. In `thm_10_cubic_gauss_quadratic_slack_and_attracting_fixed_point`, we prove that for $\alpha = p/q > 4/3$ with $\delta = 3p - 4q > 0$ and $D = 3p - q$, the exact slack discarded by this linearization is strictly positive and quadratic in δ:

$$\frac{2}{3}\left(\alpha - \frac{4}{3}\right) - \left(\text{sieveStep}(\alpha) - \frac{4}{3}\right) = \frac{2(3p-4q)^2}{9q(3p-q)} = \frac{2\delta^2}{9qD} > 0.$$

Moreover, since the fixed-point equation $\text{sieveStep}(\alpha) = \alpha \iff 3\alpha^2 - 7\alpha + 4 = (3\alpha - 4)(\alpha - 1) = 0$ has roots at $\alpha^* = 4/3$ and $\alpha^{**} = 1$, we introduce the Möbius coordinate $u(\alpha) = \frac{\alpha - 4/3}{\alpha - 1} = \frac{3p-4q}{3(p-q)}$ in `thm_11_mobius_conjugacy_exact_closed_form_solution` and prove that for $\alpha' = p'/q' = \frac{6p-4q}{3p-q}$:

$$3p' - 4q' = 3(6p - 4q) - 4(3p - q) = 6p - 8q = 2(3p - 4q), \qquad p' - q' = (6p - 4q) - (3p - q) = 3(p - q),$$

which implies the exact linear conjugacy $u(\text{sieveStep}(\alpha)) = \frac{2}{3}\, u(\alpha)$ with zero approximation error.

In `proofs/qrh_trilogy_induction_and_algebraic_bridge.lean`, we define the recursive projective sequence `sieveIter (n : Nat) : Nat × Nat`:

$$\text{sieveIter}(0) = (2, 1), \qquad \text{sieveIter}(n+1) = (6p_n - 4q_n,\ 3p_n - q_n),$$

together with `mobiusNum(p, q) = 3p - 4q` and `mobiusDen(p, q) = p - q`. By structural induction on $n \in \mathbb{N}$ (`induction n with | zero => ... | succ k ih => ...`), we prove for every natural number $n \geq 0$:

1. Exact Möbius Invariants (`thm_31_sieve_iter_mobius_invariants_by_induction`):

$$3p_n - 4q_n = 2^{n+1}, \qquad p_n - q_n = 3^n.$$

2. Exact Closed-Form Solution for All $n \in \mathbb{N}$ (`thm_32_sieve_iter_exact_closed_form_all_n`):

$$p_n = 4 \cdot 3^n - 2^{n+1}, \qquad q_n = 3 \cdot 3^n - 2^{n+1}, \qquad \tilde{\alpha}_n = \frac{p_n}{q_n} = \frac{4 \cdot 3^n - 2^{n+1}}{3 \cdot 3^n - 2^{n+1}} = \frac{\frac{4}{3} - \left(\frac{2}{3}\right)^{n+1}}{1 - \left(\frac{2}{3}\right)^{n+1}}.$$

3. Universal Strict Improvement over OpenAI's Linearized Bound (`thm_33_sieve_iter_strictly_beats_openai_sieve_exponent_all_n`, `thm_12_nonlinear_vs_linearized_sieve_iterates_comparison`):

$$\tilde{\alpha}_n - \frac{4}{3} = \frac{2^{n+1}}{3q_n}, \qquad \alpha_n - \frac{4}{3} = \frac{2^{n+1}}{3^{n+1}}, \qquad 9 \cdot 3^n - 3q_n = 3 \cdot 2^{n+1} > 0, \qquad \lim_{n\to\infty} \frac{\tilde{\alpha}_n - 4/3}{\alpha_n - 4/3} = \frac{1}{3}.$$

Step n	**Exact Nonlinear Iterate** $\tilde{\alpha}_n = p_n/q_n$	**Excess** $\tilde{\alpha}_n - 4/3$	**OpenAI Linearized** $\alpha_n = 4/3 + (2/3)^{n+1}$	**Excess** $\alpha_n - 4/3$
$n = 0$	$2/1 = 2$	$2/3 \approx 0.66667$	2	$2/3 \approx 0.66667$
$n = 1$	$8/5 = 1.60000$	$4/15 \approx 0.26667$	$16/9 \approx 1.77778$	$4/9 \approx 0.44444$
$n = 2$	$28/19 \approx 1.47368$	$8/57 \approx 0.14035$	$44/27 \approx 1.62963$	$8/27 \approx 0.29630$
$n = 3$	$92/65 \approx 1.41538$	$16/195 \approx 0.08205$	$124/81 \approx 1.53086$	$16/81 \approx 0.19753$

4.3 Universal (M, ℓ)-Cancellation in Farkas Duality and $\mathbb{Z}[\sqrt{921}]$ Ring Theory (Theorems 16–23, 34–35)

In Baiying Liu's `arXiv:2610.12234` (unrefereed preprint; `geometry/V2Optimization.lean:211-243`), the three scalar majorant faces in terms of $M = x + y$ and ℓ are:

$$\text{Face}_0(M, \ell) = \frac{5}{6} + \frac{M}{12} - \frac{\ell}{6}, \quad \text{Face}_K(M, \ell) = \frac{1}{3} + \frac{7M}{12} + \frac{\ell}{3}, \quad \text{Face}_H(\delta_c, M, \ell) = 1 + \delta_c - \frac{1 + \delta_c}{2} M + \delta_c\, \ell.$$

In `thm_21_farkas_dual_weights_and_closure_obstruction`, we prove that for any δ_c, the Farkas multipliers:

$$w_0(\delta_c) = \frac{4 + 18\delta_c}{9 + 18\delta_c}, \qquad w_K(\delta_c) = \frac{2}{9 + 18\delta_c}, \qquad w_H(\delta_c) = \frac{3}{9 + 18\delta_c}$$

satisfy $w_0 + w_K + w_H = 1$ and annihilate both M and ℓ identically, leaving the pure constant term $\frac{7+18\delta_c}{9+18\delta_c}$.

In `proofs/qrh_trilogy_induction_and_algebraic_bridge.lean`, we formalize the quadratic integer ring $\mathbb{Z}[\sqrt{921}]$ as `structure ZSqrt921 (⟨a, b⟩ = a + bsqrt(921))` with exact ring multiplication `z921Mul x y = ⟨x.a*y.a + 921*x.b*y.b, x.a*y.b + x.b*y.a⟩`, conjugation `z921Conj x = ⟨x.a, -x.b⟩`, and norm `z921Norm x = x.a^2 - 921*x.b^2`:

- Exact Root in $\mathbb{Z}[\sqrt{921}]$ (`thm_34_zsqrt921_norm_and_critical_quadratic_root`): For $X = 48\delta_c = \langle 49, -1\rangle$, $\mathrm{Norm}(X) = 49^2 - 921 = 1480 = 8 \times 185$ and $288X^2 - 588 \cdot 48X + 185 \cdot 48^2 = \langle 0, 0\rangle$.
- Exact Rationalization & Gap Norm in $\mathbb{Z}[\sqrt{921}]$ (`thm_35_zsqrt921_liu_rationalization_and_case005_gap`): Multiplying numerator $\langle 203, -3\rangle$ by the conjugate $\langle 219, 3\rangle$ of denominator $\langle 219, -3\rangle$ in $\mathbb{Z}[\sqrt{921}]$ gives:

$$\langle 203, -3\rangle \cdot \langle 219, 3\rangle = \langle 36168, -48\rangle = 24 \cdot \langle 1507, -2\rangle, \qquad \mathrm{Norm}(\langle 219, -3\rangle) = 39672 = 24 \times 1653,$$

proving $B_{\mathrm{Liu}} = \frac{1507-2\sqrt{921}}{1653}$, while the gap numerator $\langle -36189, 1195\rangle$ between Part II (Referee & Unbundled Gram Audit) and Liu has norm $(-36189)^2 - 921 \times 1195^2 = -5567304 < 0$.

4.4 Parametric Unbundled Farkas Theorem (Theorems 24–30)

When the three faces are improved by non-negative savings $(\Delta_0, \Delta_K, \Delta_H)$, contracting with (w_0, w_K, w_H) immediately yields the exact parametric Farkas shift (`thm_24_parametric_unbundled_farkas_shift_theorem`):

$$B^*(\Delta_0, \Delta_K, \Delta_H) = B_{\mathrm{Liu}} - (w_0\,\Delta_0 + w_K\,\Delta_K + w_H\,\Delta_H)\,.$$

- Since $w_0 = \frac{163-3\sqrt{921}}{183-3\sqrt{921}} \approx 0.68736 > \frac{2}{3}$ (`thm_25_xu_sang_delta0_sixth_moment_breaks_liu_obstruction`), Y. Xu and H. Sang's $\delta = 0$ amplified first moment of the reflected numerator (derived from the existing fourth-moment estimate) plus relaxed direct bound ($\Delta_0 > 0$, `arXiv:2610.15291`, unrefereed preprint) shifts the LP optimum B^* down to $0.8748867 < B_{\mathrm{Liu}}$.
- Unbundling the cubic Gram operator ($\Delta_K \in \{1/30, 8/45\}$) and shifting $z_{\mathrm{high}} = 1/6 \to 7/20$ ($\Delta d_0 = 1/10$ in Face_H) shifts the non-exceptional LP exponent target to $\frac{4103}{4896} \approx 0.83803$ and $\frac{4069}{4896} \approx 0.83109$ (`thm_26_unbundled_gram_and_stickelberger_shift_breaks_face_H`).
- At $(\alpha_X, \alpha_Y) = (4/9, 13/18)$, the `CubicGauss` $P^{1/6}$ sieve leaves positive `LowRows` exponent $53/216 > 0$ ($\beta(0) = 65/72$); assuming hypothetical full cancellation $\Delta_{\mathrm{gram}} = 53/216$ ($E^{\mathrm{eff}}_{\mathrm{Low}} = 0$) yields the formal Path-A zero-energy LP intercept $\frac{71}{108} \approx 0.65741$ (`thm_27_connecting_cubic_gauss_2_3_sieve_to_path_A_71_108`), contingent on proving that extra cancellation together with Stickelberger pole cancellation ($k_\infty = -6$) and Voronoi-Mellin transfer.

4.5 The 3-Report QRH Trilogy Synthesis (Part I ↔ Part II ↔ Part III, Theorems 36–45)

Why did Part I (7/8 ShortDraft Audit) produce the denominator 3264 and margin numerator 215, while Part II (Referee & Unbundled Gram Audit) produced 4896 and 71/108, and Part III (11/12 & CubicGauss Synthesis) uncovered the unimported `CubicGauss` fixed point $\alpha^* = 4/3$? In `proofs/qrh_trilogy_induction_and_algebraic_bridge.lean`, we prove that all three reports are projections of a single algebraic invariant structure:

1. Prime 17 Slope and the 3264 ↔ 4896 Denominator Bridge (`thm_36_trilogy_denominator_bridge_3264_and_4896`):

In Part I (`thm_15`), the unbundled componentwise Gram exponent is $\frac{14+17\delta}{96}$. Its prime slope 17 and denominator 96 generate the fundamental unit $17 \times 96 = 1632 = \gcd(3264, 4896)$, from which the Part I and Part II denominators follow:

$$d_{\mathrm{I}} = 2 \times 1632 = 3264, \qquad d_{\mathrm{II}} = 3 \times 1632 = 4896, \qquad \frac{d_{\mathrm{I}}}{d_{\mathrm{II}}} = \frac{2}{3}.$$

2. Exact Margin Numerator 215 Identity Across Part I and Part II (`thm_37_case001_margin_215_3264_drives_case005_4069_4896`, `thm_38_case001_unbundling_breaks_case008_farkas_wall`):

At the endpoint $\delta_{\max} = \frac{15}{34}$ where $\frac{14+17\delta}{96} = \frac{3}{16} + \frac{1}{12}\delta$, Part I's exact Gram margin against OpenAI's bundled bound $\frac{3}{16} + \frac{23\delta}{96}$ is $\frac{6}{96} \times \frac{15}{34} = \frac{45}{1632} = \frac{90}{3264}$, and its total unbundled margin is $\frac{215}{3264}$. In Part II, the 3-term non-exceptional boundary is $\beta_{\text{3-term}} = \frac{4069}{4896}$. Subtracting from $\frac{7}{8} = \frac{4284}{4896}$ gives:

$$\frac{7}{8} - \frac{4069}{4896} = \frac{4284 - 4069}{4896} = \frac{215}{4896} = \frac{2}{3} \times \frac{215}{3264}.$$

That is, Part II's improvement below 7/8 is literally Part I's margin $\frac{215}{3264}$ scaled by the 2/3 cubic sieve weight!

3. Eisenstein Pole Duality $\alpha^* + \beta_{\text{pole}} = 2$ and the 3264 / 44064 Gap (`thm_39_eisenstein_pole_duality_cubic_gauss_vs_coordR`–`thm_42_gap_between_71_108_and_7_12_equals_3264_over_44064`):

- In Part III, the unimported `CubicGauss` recurrence converges to $\alpha^* = \frac{4}{3}$ (`short_four_thirds`). In Part II, the Dedekind zeta residue at $w = 1$ creates a pole barrier at $\beta_{\text{pole}} = \frac{2}{3}$. These two exponents are exact Eisenstein duals: $\alpha^* + \beta_{\text{pole}} = \frac{4}{3} + \frac{2}{3} = 2$.
- Even under hypothetical full `LowRows` cancellation to the Path-A zero-energy LP intercept $\frac{71}{108} < \frac{72}{108} = \frac{2}{3}$, Part II's Stickelberger annihilator ($k_\infty = -6$, `net_pole_order` $= 1 - 1 = 0$) and Part I's 6-of-8 Gauss branch vanishing ($\frac{1}{6} \to \frac{1}{12}$, saving $\frac{1}{12}$) are needed to shift the algebraic pole coordinate from $\frac{2}{3}$ to $\frac{7}{12}$ and $\frac{1}{2}$.
- Because $\operatorname{lcm}(24, 4896, 108) = 14688$ gives $\left(\frac{71}{108} - \frac{7}{12}\right) \times 14688 = 1088 = d_{\text{I}}/3$, over the trilogy common multiple $D = 3\operatorname{lcm}(24, 4896, 108) = 44064 = 9 \times 4896$ the distance between the Path-A zero-energy intercept $\frac{71}{108} = \frac{28968}{44064}$ and the shifted pole $\frac{7}{12} = \frac{25704}{44064}$ is:

$$\left(\frac{71}{108} - \frac{7}{12}\right) \times 44064 = 28968 - 25704 = 3264 = d_{\text{I}}.$$

4. 6-Stage Telescoping Decomposition and Scope Boundary to $\beta = 1/2$ (`thm_43_eleven_twelfths_to_seven_eighths_bridge`–`thm_45_grand_trilogy_synthesis_verdict`):

Over $D = 44064$, the total progression from OpenAI's `ShortDraft` ($\frac{23}{24} = \frac{42228}{44064}$) to the critical line ($\frac{1}{2} = \frac{22032}{44064}$) decomposes into six exact integer steps:

$$1836 + 1836 + 1935 + 7653 + 3264 + 3672 = 20196 = \left(\frac{23}{24} - \frac{1}{2}\right) \times 44064.$$

- Conditional LP & Algebraic Exponent Accounting (Steps 1–4, total $13260/44064 = 55/1836 \to \beta = 71/108 \approx 0.6574$): Our `0 sorry` Lean 4 theorems (`thm_27`, `thm_40`) verify the exponent accounting across `CanonicalDescentScale` (1836), cubic moment transition (1836), Gram unbundling + Stickelberger shift (1935), and the conditional zero-energy LP step (7653, assuming hypothetical full cancellation $\Delta_{\text{gram}} = 53/216$ of `LowRows` beyond `CubicGauss`) alongside `net_pole_order = 0`.
- Remaining Open Analytic Problem (Steps 5–6, total $(3264 + 3672)/44064 = 6936/44064 = 17/108 \approx 0.1574$ from 71/108 to 1/2): Reaching $\beta = 1/2$ along the coupled $z_{\text{high}} = 0.34 \leftrightarrow z'_{\text{high}} = 0.35$ hybrid model requires $\Delta_{\text{hybrid}} = \frac{14}{33} = \frac{56}{132}$, where $E_{\text{Low}} - \Delta_{\text{hybrid}} = -\frac{17}{132} < 0$ shows that unproved Archimedean Mellin contour decay ($d_{\text{Mellin}} = 59/132$) is indispensable beyond character-sum cancellation.

4.6 Complete 1-to-1 Theorem Map (45 Theorems + 11 `defs` + 1 `structure`, 344/344 Mutations Caught)

Note: Upstream paths outside `proofs/oai_ref/` refer to official `openai/math` commit `4eaee87` (`DirichletL/Nonvanishing.lean`, `2,926` `DirichletL` files) and community `oai-math-revised` `PR #70` `ca28f20` (`SevenEighths.lean`, `DescentScale.lean`, `2,927` files). The proved 7/8 main theorem (`0 sorry`) already logically implies both `11/12` and `23/24`.

4.6.1 File 1: `proofs/qrh_eleven_twelfths_and_cubic_large_sieve.lean` (15 theorems + 2 `defs`: `canonicalReserveScale`, `shortCubeLossScale`)

- Theorem 1: `thm_01_shortdraft_fixed_reserve_and_23_24_exponent` - Module-stratigraphy finding: hard-coded $1/20 < \sigma$ (`RankMargins.lean:83-132`) and $\sigma = 1/10$ (H = Z^(11/10), Y = Z^(11/60)) lock standalone `ShortDraft` at 137/120 - 11/60 = 23/24 (while the 7/8 main theorem already implies 11/12 and 23/24).

- Theorem 2: `thm_02_symbolic_sixth_power_cauchy_schwarz_exponent` - Symbolic sixth-power Cauchy-Schwarz exponent `E_CS(θ) = (11 + 5θ)/12`.
- Theorem 3: `thm_03_kontorovich_epsilon_split_exact_11_12` - Exact $(\theta, \eta) = (6\varepsilon/5, \varepsilon/2)$ substitution for target margin $\varepsilon > 0$ yielding $(11 + 5\theta)/12 + \eta = 11/12 + \varepsilon$.
- Theorem 4: `thm_04_canonical_descent_scale_budget_unlocks_arbitrary_theta` - Symbolic `Canonical DescentScale` budget `50 ≤ κ * denom_sym` (`DescentScale.lean` in `PR #70 ca28f20`) unlocking arbitrary $\theta > 0$.
- Theorem 5: `thm_05_remainder_exponent_subdominance_and_crossover` - Subdominance of the Poisson/divisibility remainder `E_rem(θ) = (5 - θ)/6` with gap $(1 + 7\theta)/12 > 0$.
- Theorem 6: `thm_06_sixth_power_fiber_cauchy_constant_768` - Sixth-power fiber degree 6 times disk constant 128 (`768 = 6 * 128` vs. `384 = 3 * 128`).
- Theorem 7: `thm_07_totient_euler_correction_vs_prime_amplification_tradeoff` - Local totient density `(N_p - 1)/N_p ∈ [1/2, 1)` and Re(s) > 0 Euler correction convergence.
- Theorem 8: `thm_08_part_one_paper_tex_table_vs_shortdraft_gap` - Unformalized `paper.tex` Part I margin table (1021/25000, 1/40, 1/1200, 43/300) vs. `ShortDraft` 1/24 gap.
- Theorem 9: `thm_09_cubic_gauss_sieve_step_and_threshold_identities` - Exact rational identities of `sieveThreshold(α)` and `sieveStep(α)` in `CubicGauss/Recurrence.lean`.
- Theorem 10: `thm_10_cubic_gauss_quadratic_slack_and_attracting_fixed_point` - Quadratic slack 2(3p - 4q)^2 / (9q(3p - q)) > 0 and unique fixed point `α* = 4/3`.
- Theorem 11: `thm_11_mobius_conjugacy_exact_closed_form_solution` - Exact Möbius conjugacy `u(sieveStep(α)) = (2/3) * u(α)` for u(α) = (α - 4/3)/(α - 1).
- Theorem 12: `thm_12_nonlinear_vs_linearized_sieve_iterates_comparison` - Exact comparison of nonlinear iterates (2, 8/5, 28/19, 92/65) vs. `CubicGauss/LargeSieve.lean:75` geometric-series majorization (2, 16/9, 44/27, 124/81), a valid simplification converging to the same asymptotic fixed point `α* = 4/3`.
- Theorem 13: `thm_13_short_four_thirds_and_reciprocity_symmetrization` - `short_four_thirds` and cubic-reciprocity symmetrization to max(a, b, 2(a+b)/3).
- Theorem 14: `thm_14_scalar_bounds_epsilon_and_mixed_exponents` - Monomial exponent laws (`mixed_one`, `mixed_two`, `scale_epsilon`) in `CubicGauss/ScalarBounds.lean`.
- Theorem 15: `thm_15_unimported_cubic_gauss_vs_bundled_cubic_gram_gap` - Unimported 30-file `CubicGauss` (6,252 lines, 0 external imports) vs. bundled `CubicGram`.

4.6.2 File 2: `proofs/qrh_q_sqrt_921_farkas_and_unbundling_synthesis.lean` (15 theorems + 2 defs: `criticalQuadraticConst`, `farkasWeightedSaving`)

- Theorem 16: `thm_16_shared_critical_quadratic_288_588_185_and_count_2_3` - Shared critical quadratic `288δ_c^2 - 588δ_c + 185 = 0` (`δ_c = (49 - sqrt(921))/48`, `R(δ_c, 1/2) = 2/3`).
- Theorem 17: `thm_17_case005_fixed_scale_saddle_vs_liu_rational_B_r` - Strict ordering `B_r = 34999/40000 < β_SOS(0) = (6843 - 7sqrt(921))/7578 < 41999/48000 < 7/8`.
- Theorem 18: `thm_18_liu_three_face_equalization_in_Q_sqrt_921` - 3-face scalar equalization in $\mathbb{Q}(\sqrt{921})$ (`arXiv:2610.12234`, unrefereed preprint) yielding `ℓ_Liu = (33 + 8sqrt(921))/1653` and `B_Liu = (1507 - 2sqrt(921))/1653`.
- Theorem 19: `thm_19_exact_gap_between_fixed_scale_saddle_and_liu_optimum` - Exact gap `β_SOS(0) - B_Liu = (1195sqrt(921) - 36189)/4175478 > 0` (`1195^2 * 921 - 36189^2 = 5567304`).
- Theorem 20: `thm_20_liu_gram_gate_parameter_b_new_and_margins` - Positivity of `0 < b_new < 1/8` and bundled Gram gate y - ℓ - 11b/6 > 0.
- Theorem 21: `thm_21_farkas_dual_weights_and_closure_obstruction` - Universal (M, ℓ)-cancellation of Farkas weights (`arXiv:2610.12234`, unrefereed preprint) and rationalization `(203 - 3sqrt(921))/(219 - 3sqrt(921)) = B_Liu`.
- Theorem 22: `thm_22_signal_matching_identity_and_face_K_origin` - Signal-matching identity (11/12 - ℓ/4) - (4 + b)/6 = x/2 + b/12 and origin of `Face_K`.

- Theorem 23: `thm_23_complete_square_uniqueness_at_dc_and_u_half` - Positivity of `A_c(v)` and disc(v) coefficients proving uniqueness at `(d, u) = (δ_c, 1/2)`.
- Theorem 24: `thm_24_parametric_unbundled_farkas_shift_theorem` - Parametric Farkas shift theorem `B*(Δ_0, Δ_K, Δ_H) = B_Liu - (w_0 Δ_0 + w_K Δ_K + w_H Δ_H)`.
- Theorem 25: `thm_25_xu_sang_delta0_sixth_moment_breaks_liu_obstruction` - `w_0 > 2/3` and Y. Xu & H. Sang (`arXiv:2610.15291`, unrefereed preprint) $\delta = 0$ amplified reflected-numerator moment saving shifting `B_Liu` (`arXiv:2610.12234`, unrefereed preprint) to 8748867/10000000.
- Theorem 26: `thm_26_unbundled_gram_and_stickelberger_shift_breaks_face_H` - Unbundled Gram + Stickelberger `z_high' = 7/20` LP exponent targets 4103/4896 and 4069/4896.
- Theorem 27: `thm_27_connecting_cubic_gauss_2_3_sieve_to_path_A_71_108` - Separates `CubicGauss`'s positive `LowRows` exponent `53/216 > 0` ($\beta(0) = 65/72$) at `(4/9, 13/18)` from the formal Path-A zero-energy LP intercept `71/108` requiring hypothetical full cancellation `Δ_gram = 53/216`.
- Theorem 28: `thm_28_ten_tier_qrh_boundary_hierarchy` - Complete 10-tier strict ordering from 1/2 to 23/24.
- Theorem 29: `thm_29_zero_free_strip_width_progression_ratios` - Proves `lcm(24, 4896, 108) = 14688`, `D = 3 * 14688 = 44064`, and zero-free strip width progression (1x → 2x → 3x → 3.89x → 4.05x → 8.22x → 12x).
- Theorem 30: `thm_30_master_qrh_ecosystem_synthesis_verdict` - Master synthesis verdict across all 4 pillars.

4.6.3 File 3: `proofs/qrh_trilogy_induction_and_algebraic_bridge.lean` (15 theorems + 7 defs + 1 structure ZSqrt921)

- Theorem 31: `thm_31_sieve_iter_mobius_invariants_by_induction` - All-n mathematical induction (`induction n`) proving `mobiusNum (sieveIter n) = 2^(n+1)` and `mobiusDen (sieveIter n) = 3^n`.
- Theorem 32: `thm_32_sieve_iter_exact_closed_form_all_n` - Exact closed-form solution `p_n = 4*3^n - 2^(n+1)` and `q_n = 3*3^n - 2^(n+1)` for all n : Nat.
- Theorem 33: `thm_33_sieve_iter_strictly_beats_openai_sieve_exponent_all_n` - Universal denominator gap `9*3^n - 3*q_n = 3*2^(n+1)` for all n : Nat.
- Theorem 34: `thm_34_zsqrt921_norm_and_critical_quadratic_root` - $\mathbb{Z}[\sqrt{921}]$ ring evaluation of `48δ_c = ⟨49, -1⟩` proving `288*(48δ_c)^2 - 588*48*(48δ_c) + 185*48^2 = ⟨0, 0⟩`.
- Theorem 35: `thm_35_zsqrt921_liu_rationalization_and_case005_gap` - $\mathbb{Z}[\sqrt{921}]$ rationalization of `B_Liu` and exact norm `z921Norm ⟨-36189, 1195⟩ = -5567304 < 0`.
- Theorem 36: `thm_36_trilogy_denominator_bridge_3264_and_4896` - Prime 17 slope bridge (`17 * 96 = 1632 = gcd(3264, 4896)`, Part I denominator = 2 *1632 = 3264, Part II denominator = 3* 1632 = 4896).
- Theorem 37: `thm_37_case001_margin_215_3264_drives_case005_4069_4896` - Exact numerator 215 identity: `7/8 - 4069/4896 = 215/4896 = (2/3) * (215/3264)`.
- Theorem 38: `thm_38_case001_unbundling_breaks_case008_farkas_wall` - Unbundled Gram saving 18/288 = 1/16 moving past Liu's $\mathbb{Q}(\sqrt{921})$ Farkas wall.
- Theorem 39: `thm_39_eisenstein_pole_duality_cubic_gauss_vs_coordR` - Exact Eisenstein pole duality `α* + β_pole = 4/3 + 2/3 = 2` and `β_pole - 71/108 = 1/108`.
- Theorem 40: `thm_40_cubic_gauss_plus_stickelberger_crosses_two_thirds` - Conditional algebraic pole-cancellation check (`k_∞ = -6`, `net_pole_order = 1 - 1 = 0`) crossing $\beta = 2/3$ (actual attainment of `71/108` remains contingent on constructing the full analytic Stickelberger pole-cancellation and Voronoi-Mellin transfer proof).
- Theorem 41: `thm_41_case001_gauss_branch_vanishing_drives_case005_pole_shift` - Part I's 6-of-8 Gauss branch vanishing (1/6 → 1/12) matching Part II's algebraic pole-coordinate shift (2/3 → 7/12 → 1/2).
- Theorem 42: `thm_42_gap_between_71_108_and_7_12_equals_3264_over_44064` - Proves `lcm(24, 4896, 108) = 14688` (`gap = 1088 = d_I/3`) and `(71/108 - 7/12) * 44064 = 3264` (`D = 3 * 14688`).

- Theorem 43: `thm_43_eleven_twelfths_to_seven_eighths_bridge` - Decomposition $14/24 + 8/24 = 11/12$ vs. $14/24 + 7/24 = 7/8$.
- Theorem 44: `thm_44_six_stage_trilogy_telescoping_decomposition` - 6-stage telescoping decomposition `1836 + 1836 + 1935 + 7653 + 3264 + 3672 = 20196 = (23/24 - 1/2) * 44064`.
- Theorem 45: `thm_45_grand_trilogy_synthesis_verdict` - Grand Trilogy Synthesis Verdict across Part I + Part II + Part III.

5 Part IV: Algebraic-Variational Anatomy and Axiom-Free Lean 4 Ledger of the Five Classical Riemann Barriers (Theorems IV.1–IV.75)

Attribution Boundary for Part IV: The five canonical analytic barriers belong to the classical literature [10, 11, 12, 13, 14, 15, 16, 17, 18, 19, 20, 21, 23, 24, 25, 26, 27], with selected qualitative/asymptotic components formalized upstream in `PrimeNumberTheoremAnd` [7] and OpenAI Families `#003`, `#005`, `#013`, and `#021`. **Tier C (present work, unconditional; `Case 015`)** contributes: (1) constructive parameter refinements including the $(17, 24, 8)$ cosine square achieving $(41 - 4\sqrt{102})/32 \approx 0.018812$ (+88.12% over 1/100, 99.96% of the irreducible quintic degree-2 global optimum), the explicit degree-3 sign-changing Fejér counterexample $(65/16, 9/2, 0, -1)$ refuting naive $W_+ \geq 2c_1 - c_0$ while sealing the universal Fejér–Riesz ceiling $(3 - 2\sqrt{2})/3$, and the 16.08× Ostmann conductor cutoff reduction $(4,115,904 \to 255,983)$; and (2) 75 standalone zero-`sorry`, custom-axiom-free `Lean 4` theorems over `Mathlib 4` $\mathbb{R}$ (188/188 hypothesis mutations killed = 100.00%).

5.1 Architectural Synthesis: Five-Step Causal Chain and Beyond-Baseline Alternative Bounds

Over the past 130 years since de la Vallée Poussin's 1896 proof of the Prime Number Theorem, five canonical analytical approaches to the Riemann zeta function $\zeta(s)$ and Dirichlet L-functions $L(s, \chi)$ have each arrested at exact algebraic or variational thresholds. Across 6 Lean 4 modules (2,238 lines, 75 theorems over $\mathbb{R}$, 0 sorry, 0 custom axioms, 188 / 188 : True hypothesis mutations killed = 100%) cross-audited against 15 upstream formalization files (`proofs/oai_ref/*.lean`, 1,988 lines), this anatomy derives every intermediate balance equation and separates classical asymptotic constant slack from genuine structural obstructions.

5.1.1 Five-Step Causal Chain

- Step 1 (Exact Barrier & Bottleneck Phenomenon): Zero-free width 1/100 and asymptotic 1 - β = o(1), zero-density inflection $\sigma = 3/4$ -> 7/10 (A = 12/5 -> 30/13), Landau-Siegel ineffectiveness constant c(ε), Conrey's critical-line proportion $\kappa(4/7) = 0.408058 < 1$, and the Burgess 3/16 and Kim-Sarnak 7/64 subconvexity/ Ramanujan bounds each originate from a distinct algebraic balance.
- Step 2 (Necessary Operator & Transform Mechanism): Hadamard partial-fraction positivity projection (Re(-ζ'/ ζ)), Halasz-Montgomery Gram operators paired with Dirichlet-polynomial functional-equation reflection, Estermann's biquadratic Euler product with Perron contour truncation, Levinson-Conrey mollifier integration by parts (d/dv), and Weil character-sum moments paired with Rankin-Selberg convolutions act as the unique positivity/spectral extractors in each regime.
- Step 3 (Core Algebraic Derivation & Factorization): Every equilibrium equation reduces to an explicit sum-of-squares (SOS) decomposition, rational minimax intersection, Cauchy-Schwarz discriminant $1 \leq 4I_{AA}J_{BB}$, or rational numerator factorization (r - 2)^2 / (16 r^2).
- Step 4 (Contradiction, Non-Vanishing & Parameter Refinement): Refining classical asymptotic parameterizations (s_1 = 4δ, coarse 9A splitting, Schur absolute-value row sums, bundled Gram row losses, and asymmetric coth ω relaxation) recovers substantial slack while proving that diagonal collisions and the boundary invariant $J_{AB} = -1/2$ enforce strictly positive residuals.
- Step 5 (Formalization Boundary & Lean 4 Kernel Proof): High-precision quadrature and prime-sum evaluations are executed deterministically in `verify_symbolic_classical_riemann.py`, while every polynomial SOS identity, rational minimax crossover, HasDerivAt calculus invariant, Real.exp hyperbolic bound, and Chebyshev recurrence is proved without axioms in Lean 4 (v4.35.0).

5.1.2 Beyond-Baseline Alternative Bounds and No-Go Rigidity Obstructions

- Beyond-Baseline Alternative Bound & Slack Recovery:
  1. Replacing the textbook s_1 = 4δ choice (1/100) on (3, 4, 1) by its exact AM-GM stationary point `u* = 2sqrt(3)` yields $(7 - 4\sqrt{3})/5 \approx 0.014359$ (+43.59%), and substituting the integer square (17, 24, 8) ((4 cos θ + 3)^2 >= 0) achieves $(41 - 4\sqrt{102})/32 \approx 0.018812$ (+88.12%, within 99.96% of the global degree-2 optimum 0.018819).

2. Unbundling the three QRH Gram regimes universally in $\delta \in \mathbb{R}$ ($1/24 + \delta/16$ and $1/8 + \delta/16$) recovers 487/3264 ≈ 0.149203 at $\delta = 79/204$, while single-destruct specialization in Ostmann lowers the Siegel-Walfisz conductor threshold from 4,115,904 to 255,983 (16.08x reduction).

- Sharp No-Go / Rigidity Obstruction Theorems:

1. Degree-3 Sign-Changing Fejér Counterexample & Universal Ceiling: On sign-changing nonnegative cosine polynomials, the positive-part weight bound $W_+ = \sum \max(c_k, 0)$ satisfying $W_+ \geq 2c_1 - c_0$ is refuted by the explicit degree-3 Fejér square (65/16, 9/2, 0, -1) (W_+ = 72/16 < 79/16), whereas both the Hadamard cone weight W = $\sum$ c_k (c_k >= 0) and the two-sided Weyl absolute weight `W_abs` = $\sum$ |c_k| (c_k $\in \mathbb{R}$) obey >= 2 c_1 - c_0 and are trapped below $(3 - 2\sqrt{2})/3 \approx 0.057191$ by Fejér-Riesz autocorrelation c_1 < 2 c_0, forcing 1 - β -> 0.

2. Gram Phase Destruction, Auxiliary-Conductor Scaling Decay, $J_{AB} = -1/2$ Barrier, and Burgess SOS Trap: Schur's triangle-inequality ε n^2 > 0 gap (4.5390 vs. 3.0245 at R=64, N=128), unbounded auxiliary-conductor decay $c_{\text{scale}} q_1^{-\gamma} < c_{\text{prop}}$ in Siegel's two-branch setup, Conrey's finite-θ ceiling $\kappa(\theta) < 1$, and (r - 2)^2 / (16 r^2) >= 0 are sealed as unconditional rigidity/obstruction theorems over $\mathbb{R}$.

5.2 Paper 1 (Theorems 1-15): de la Vallée Poussin (1896) & Korobov-Vinogradov (1958) Zero-Free Region Anatomy

5.2.1 Pole-Zero SOS Identity, Irreducible Quintic Stationarity, and Fejér-Riesz Autocorrelation

Applying $P(\theta) := c_0 + \sum_{k=1}^{N} c_k \cos(k\theta) \geq 0$ to $-\operatorname{Re}(\zeta'/\zeta)$ requires $c_k \geq 0$ ($k \geq 1$) to drop nontrivial zero terms $-\operatorname{Re}(1/(s-\rho)) < 0$. With $u := c_0 + AWs_1$ ($W := \sum_{k=1}^{N} c_k$), we obtain

$$u \cdot AW\delta(s_1) = c_1 u - c_0 c_1 - u(u - c_0) = u\left(\sqrt{c_1} - \sqrt{c_0}\right)^2 - \left(u - \sqrt{c_0 c_1}\right)^2 .$$

Along the normalized degree-2 boundary $c_2 = 1$, $c_1 = r \in (0, 4)$, $c_0 = 1 + r^2/8$, differentiating $C_2(r) := (\sqrt{r} - \sqrt{1 + r^2/8})^2/(r+1)$ yields the irreducible quintic

$$P_5(r) := r^5 + 4r^4 - 12r^3 - 40r^2 + 64r - 64 = 0, \qquad r^* \approx 2.966229549437,$$

whose rational approximant $r = 3$ produces $17 + 24\cos\theta + 8\cos 2\theta = (4\cos\theta + 3)^2 \geq 0$ with $C(17, 24, 8) = (41 - 4\sqrt{102})/32 \approx 0.01881188$ (99.9646% of optimal).

Upstream formalization cross-audits cover `#005` Catalan oai_ref/OrdinaryZetaZeroFree.lean#L13-L64 (qualitative `Re(s) ≥ 1 (3,4,1) re_log_comb_nonneg` with no `s_1 = 4δ` or `1/100`), oai_ref/OrdinaryZeta ZeroFree.lean#L77-L172 (`norm_riemannZeta_product_ge_one`, `riemannZeta_ne_zero_of_one_le_re_of_ne_one`), `PrimeNumberTheoremAnd` oai_ref/ZetaBounds_ZeroFree_excerpt.lean#L7-L163 (`ZetaInvBound2`, `ZetaInvBnd`) and oai_ref/ZetaBounds_ZeroFree_excerpt.lean#L241-L386 (`ZetaLowerBnd`, `ZetaZeroFree`, `LogDerivZetaBnd`), `#021 Erdos970` oai_ref/CharacterPositivity.lean#L44-L101 (`character_positivity_polynomial`, `character_log_derivative_positivity`), oai_ref/NonquadraticZeroFree.lean#L12-L139 (`modulusHeight`, `exists_nonquadratic_zero_free_region`), and oai_ref/PrimitiveTransfer.lean#L310-L332 (`exists_primitive_zero_free_region` and `#L387-L409` Euler-factor imprimitive transfer), while degree-8 optimizations (`0.02894712` for `c_k >= 0`, `0.02925694 < 0.05719096` for `W_abs`) are verified in `verify_paper1_pole_zero_sos_and_four_tier_cascade`, `verify_paper1_deg2_quintic_and_17_24_8`, and `verify_paper1_fejer_riesz_and_korobov_barrier`.

5.2.2 Complete Theorem Ledger for classical_dlvp_korobov_and_zero_free.lean (Theorems 1-15)

- `thm_01_dlvp_three_four_one_sos_identity`: Proves $3 + 4\cos\theta + \cos(2\theta) = 2(1 + \cos\theta)^2 \geq 0$.
- `thm_02_pole_zero_sos_decomposition`: Exact SOS decomposition in $u := c_0 + AWs_1$ and AM-GM bound $(\sqrt{c_1} - \sqrt{c_0})^2/W$.
- `thm_03_stationary_point_zero_free_implication`: Evaluates stationary $s_1^* = (\sqrt{c_0 c_1} - c_0)/(AW)$ to deduce $1 - \beta \geq (\sqrt{c_1} - \sqrt{c_0})^2/(AWM)$.
- `thm_04_three_four_one_four_tier_slack_cascade`: Strict four-tier ladder A / (32(9A + 1)) < 1/100 < 1/70 < (7 - 4$\sqrt{3}$)/5 and Pell convergent $56\sqrt{3} < 97$ certificate.
- `thm_05_tao_zetabounds_exponentiated_norm_log9_loss`: Quantifies constant degradation when exponentiating $-\operatorname{Re}(\zeta'/\zeta)$ into $|\zeta|^3|\zeta|^4|\zeta| \geq 1$.

- `thm_06_degree2_cosine_vertex_completion_of_squares`: Vertex completion of squares for general degree-2 cosine polynomials ($8c_0c_2 \geq 8c_2^2 + c_1^2$).
- `thm_07_seventeen_twentyfour_eight_perfect_square`: Proves $17+24\cos\theta+8\cos(2\theta) = (4\cos\theta+3)^2 \geq 0$.
- `thm_08_seventeen_twentyfour_eight_exact_constant_and_gain`: Exact evaluation $C(17, 24, 8) = (41 - 4\sqrt{102})/32 > 0.0188118$ beating (3,4,1).
- `thm_09_degree2_global_quintic_stationarity_and_root`: Sign-change bracket $(2.9662, 2.9663)$ and root existence for $P_5(r)$.
- `thm_10_degree2_global_ceiling_and_9996_tightness`: Global ceiling < 0.018819 over all nonnegative degree-2 cosine polynomials and 99.96% tightness of (17,24,8).
- `thm_11_fejer_riesz_autocorrelation_strict_two_c0_barrier`: Proves $2c_0 - c_1 = a_0^2 + a_N^2 + \sum(a_{j+1} - a_j)^2 > 0 \implies c_1 < 2c_0$.
- `thm_12_general_cosine_pi_weight_lower_bound`: Proves $W \geq 2c_1 - c_0$ (c_k >= 0) and $W_{\text{abs}} \geq 2c_1 - c_0$ (c_k $\in \mathbb{R}$) via Chebyshev induction at $\theta = \pi$, and refutes $W_+ \geq 2c_1 - c_0$ via signChangeWitnessC = (65/16, 9/2, 0, -1).
- `thm_13_fejer_riesz_universal_constant_ceilings`: Universal arbitrary-degree ceiling $(\sqrt{c_1} - \sqrt{c_0})^2/W_{\text{abs}} < (3 - 2\sqrt{2})/3 < 0.057191$.
- `thm_14_korobov_vinogradov_two_thirds_exponent_balance`: Derives the 2/3 Korobov-Vinogradov exponent and Ford's $1/(4\alpha + 3)$ scaling at $\eta = 1/(3\alpha)$.
- `thm_15_asymptotic_sigma_eq_one_minus_o1_barrier_no_go`: Proves $1 - \beta \leq (3 - 2\sqrt{2})/(3AM(|t|)) < \varepsilon$ as $M(|t|) \to \infty$.

5.3 Paper 2 (Theorems 16-35): Ingham (1940), Huxley (1972), Guth-Maynard (2024) Zero Density & QRH Gram Anatomy

5.3.1 Moment-Reflection Minimax, Guth-Maynard Determinantal Energy, and QRH Unbundling

Ingham's zero-detection balance $A_{\text{Ing}}(\sigma) := 3/(2 - \sigma)$ meets Huxley's reflection-subdivision curve $A_{\text{Hux}}(\sigma) := 3/(3\sigma - 1)$ at $\sigma^* = 3/4$ with peak $12/5 = 2.4$. Guth-Maynard (2024) replace the large-values step by the 3 x 3 determinantal energy $E_3 \leq 2 + \nu(12/5 - 4\sigma)$, yielding $A_{\text{GM}}(\sigma) := 15/(5\sigma + 3)$ whose middle-branch slack numerator satisfies

$$250\left(\sigma - \frac{3}{4}\right)^2 + \frac{3}{8} > 0$$

for all $\sigma \in \mathbb{R}$, shifting the minimax peak to $(\sigma^*_{\text{GM}}, A) = (7/10, 30/13)$.

Upstream QRH (`#003 SevenEighths`) audits examine oai_ref/GramBound.lean#L13-L95 (`actual_additive_gram_bound`: $\|$`(E - Z) + Z`$\| \leq \|$`E - Z`$\| + \|$`Z`$\|$ and `nonexceptional_scale_loss` across `1 + P^(1/6) + P^2/Y`), oai_ref/GramScaleLoss.lean#L8-L39 (`P*(Y/(M*P))^(-1+δ) ≤ M*(P^2/Y)*Y^δ` dropping `M^(-δ)P^(-δ) ≤ 1`), oai_ref/LowGramScale.lean#L8-L49 (`compensated_gram_scale_bound ≤ 3*(Y/(qX))^(1/6)` and `source_gram_sqrt_power sqrt(Z^(3/8 + (23/48)*δ)) = Z^(3/16 + (23/96)*δ)`), and oai_ref/Endpoint.lean#L14-L108 (`certificateWeight`, `balancedExponent`, `endpoint_identity`, `(δ, y) ∈ [0, 5/6] × [0, 1/2]`, `balanced_endpoint_strict`), backed by `verify_paper2_ingham_huxley_and_guth_maynard` and `verify_paper2_qrh_gram_and_hybrid_bridges` (`GeometricBoundary.lean` belongs to `#003 SiegelZeros`, audited in Paper 3 `thm_48`).

5.3.2 Theorem Ledger for classical_ingham_huxley_zero_density.lean & classical_guth_maynard_and_qrh_gram.lean (Theorems 16-35)

- `thm_16_ingham_three_term_zero_detection_balance`: Derives $3/(2 - \sigma)$ at optimal zero-detection cutoff $y = 1/(2 - \sigma)$.
- `thm_17_ingham_slope_strict_monotonicity_and_conservation`: Strict monotonicity and $(2 - \sigma)A_{\text{Ing}}(\sigma) = 3$.
- `thm_18_halasz_schur_gram_phase_destruction_bound`: Hermitian Schur row-sum bound and strict $\varepsilon n^2 > 0$ phase-destruction loss.

- `thm_19_huxley_reflection_subdivision_large_values_derivation`: Derives Huxley's large-values exponent $2 + 2/(3\sigma - 1)$ at $T_0 = \tau^{1/(3\sigma-1)}$.
- `thm_20_huxley_k2_k3_amplification_and_cutoff_compatibility`: Solves $k = 2 \to 3$ amplification crossover $3/(3\sigma - 1)$ and $\sigma \geq 3/4$ compatibility.
- `thm_21_ingham_huxley_minimax_three_quarters_inflection`: Unique minimax inflection at $\sigma^* = 3/4$ with peak $12/5$.
- `thm_22_density_hypothesis_gap_and_prime_gap_seven_twelfths`: Proves Density Hypothesis gap $2/5$ and prime-gap threshold $\theta = 7/12$.
- `thm_23_huxley_higher_amplification_strict_decay`: Strict decay of $k \geq 3$ branches below $k = 2$ for $\sigma > 3/4$.
- `thm_24_phase_cancellation_loss_witness_signed_vs_abs`: Explicit signed Gram witness separating true Rayleigh quotient from Schur row sum.
- `thm_25_global_ingham_huxley_exponent_strict_monotonicity`: Global ascent on $(1/2, 3/4)$ and descent on $(3/4, 1)$.
- `thm_26_guth_maynard_k2_k3_amplification_and_sos_middle_margin`: Derives $15/(5\sigma + 3)$ and unconditional SOS middle-term margin $250(\sigma - 3/4)^2 + 3/8 > 0$.
- `thm_27_guth_maynard_vs_huxley_exact_four_fifths_crossover`: Exact $(4/5 - \sigma)$ factorization governing the $\sigma = 4/5$ crossover.
- `thm_28_guth_maynard_ingham_seven_tenths_minimax_envelope`: Establishes the new minimax peak at $\sigma^*_{\mathrm{GM}} = 7/10$ with $A = 30/13$.
- `thm_29_inflection_shift_barrier_saving_and_seventeen_thirtieths_prime_gap`: Proves peak saving $12/5 - 30/13 = 6/65$, shift $1/20$, and prime-gap exponent $17/30$.
- `thm_30_guth_maynard_det3_rank_defect_s2_collapse_barrier`: Proves rank-defect branch S_2 collapse back to classical Weyl-Iwaniec bounds.
- `thm_31_qrh_gram_scale_loss_and_coarse_bundled_exponent`: Coarse bundled exponent $(17 + 13\delta)/48$ and positive failure $4399/9792 > 0$ at $\delta = 79/204$.
- `thm_32_qrh_three_mode_unbundling_215_and_487_over_3264`: Universal δ-savings $1/24 + \delta/16$ and $1/8 + \delta/16$, plus SOS vertex $(4 \cdot 51 \cdot \delta - 79)^2 = 0 \iff \delta = 79/204$ yielding $215/3264$ and $487/3264$.
- `thm_33_qrh_rescaled_five_sixths_and_three_quarters_bridge`: Exact bijection mapping $\sigma = 5/6$ and $\delta = 1/3$ to $\sigma_{\mathrm{eff}} = 3/4$.
- `thm_34_qrh_endpoint_sos_identity_and_box_margin`: Proves the oai_ref/Endpoint.lean SOS numerator identity and $49/440640$ box floor.
- `thm_35_hybrid_ab_coupled_critical_line_fourteen_thirtythirds`: Solves $(\alpha_X, \alpha_Y, \sigma_{\mathrm{eff}}) = (35/66, 59/66, 7/11)$ and derives the critical-line $(\beta = 1/2)$ required saving $(29 + 3(\alpha_X + \alpha_Y) - 36\beta)/36 = 14/33$, coarse deficit $-17/132$, and Welch rank excess $1/33$.

5.4 Paper 3 (Theorems 36-50): Siegel (1935) Ineffectiveness & Goldfeld-Gross-Zagier (1986) Effectivization Anatomy

5.4.1 Estermann Biquadratic Series, Perron Truncation, and Auxiliary-Conductor Scaling Decay

For real primitive characters χ_1, χ_2 ($\chi_1^2 = \chi_2^2 = 1$), the local Euler factor of $F(s) := \zeta(s)L(s, \chi_1)L(s, \chi_2)L(s, \chi_1\chi_2)$ obeys

$$4(1 + \chi_1)(1 + \chi_2) = (1 + \chi_1 + \chi_2 + \chi_1\chi_2)^2 - (\chi_1^2 - 1)(1 + \chi_2)^2 - (\chi_2^2 - 1)(2 + 2\chi_1),$$

taking values in $\{0, 4\}$ and guaranteeing nonnegative Dirichlet coefficients bounded below by $a_1 = 1$. Optimizing Perron truncation at $X := (2C_0Q^A)^{2/(2\beta_1-1)}$ yields $L(1, \chi_2) \gg_\varepsilon q_2^{-\varepsilon}$ with an implied constant decaying as $q_1^{-A/(2\beta_1-1)} \to 0$ if a phantom zero $\beta_1 \to 1^-$ exists. Goldfeld-Gross-Zagier achieve computability via an elliptic curve of conductor 5077 ($\mathrm{ord}_{s=1} L(E, s) = 3$), trading $D^{1/2-\varepsilon}$ for $\log D$.

Upstream `#003` (`SiegelZeros`) and `#013` (`Ostmann`) audits cover oai_ref/Theorem.lean#L11-L20 (`exists_absolute_real_zero_gap`, `c ≤ (1 - β) * Real.log q`), oai_ref/GeometricBoundary.lean#L18-L50

(uniform_exclusion_of_actual_cutoff, H = 86,713,344, 18818 ≤ N, by_contra failure), oai_ref/SiegelBoundProof.lean#L15-L86 (publishedSiegelBound), and oai_ref/ActualPageUniqueness.lean#L16-L84 (exists_actual_page_uniqueness), alongside #021 Erdos970 oai_ref/PrimitiveTransfer.lean#L310-L332 (exists_primitive_zero_free_region and #L387-L409 Euler-factor imprimitive transfer) and verify_paper3_siegel_goldfeld_and_ostmann.

5.4.2 Complete Theorem Ledger for classical_siegel_zero_and_ineffectiveness.lean (Theorems 36-50)

- thm_36_estermann_siegel_biquadratic_euler_factor_sos: Proves $(1+\chi_1)(1+\chi_2) \in \{0,4\}$ and nonnegativity under $\chi_1^2 = \chi_2^2 = 1$.
- thm_37_estermann_dirichlet_series_first_term_floor: Nonnegative Dirichlet series floor $\sum a_n w_n \geq 1$ from $a_1 = 1$.
- thm_38_perron_contour_dichotomy_zero_kills_f_value: Auxiliary zero $L(\beta_1, \chi_1) = 0$ annihilates $F(\beta_1)$, isolating the $s = 1$ residue.
- thm_39_siegel_perron_optimal_truncation_scale: Exact $1/2$ residue margin at optimal Perron cutoff scale.
- thm_40_siegel_exponent_threshold_equivalence: Equivalence $2A(1-\beta_1)/(2\beta_1 - 1) \leq \varepsilon \iff \beta_1 \geq 1 - \varepsilon/(2(A+\varepsilon))$.
- thm_41_siegel_implied_constant_decay_with_q1_blowup: Implied constant decay below arbitrary $\delta_{\text{target}} > 0$ as $Q_1 \to \infty$.
- thm_42_siegel_two_case_nonconstructive_lem_barrier: Real-analytic scaling obstruction proving $\forall c_{\text{prop}} > 0,\ \exists q_1 > 1,\ c_{\text{scale}} q_1^{-\gamma} < c_{\text{prop}}$ across unbounded auxiliary conductors q_1 (modeling the quantitative constant decay in Siegel's two-branch argument rather than a meta-logical Classical.em independence theorem).
- thm_43_landau_page_repulsion_pair_exclusion: Landau-Page pair exclusion with exact $60/23 - 5/2 = 5/46$ repulsion margin.
- thm_44_tatuzawa_one_exceptional_modulus_effective_dichotomy: Tatuzawa effective dichotomy outside at most one exceptional modulus.
- thm_45_dirichlet_class_number_formula_siegel_transfer: Transfers $L(1, \chi_{-D})$ lower bounds to $h(-D)$ via Dirichlet's class number formula.
- thm_46_goldfeld_gross_zagier_rank3_order_vanishing_mechanism: Proves $\text{ord}_{s=1} \geq 2$ (ord(E) = 3) yields an unconditional logarithmic floor without phantom branching.
- thm_47_gross_zagier_oesterle_rate_vs_effectivity_tradeoff: Formalizes the crossover between effective $\log D$ and ineffective $D^{1/2-\varepsilon}$ growth.
- thm_48_openai_002_siegel_zeros_bezout_cutoff_and_by_contra_audit: Audits #003 SiegelZeros (Theorem.lean & GeometricBoundary.lean: H = 86,713,344 = 96 * 903,264 = 4,608 * 18,818 = 2^10 * 3^2 * 97^2, 18818 ≤ N) and by_contra transfer.
- thm_49_case009_ostmann_single_destruct_and_loglog_bottleneck_bridge: Audits OpenAI #013 Ostmann conductor reduction 87,689 < 255,983 < 640,722 < 4,115,904 (> 16x gain).
- thm_50_paper3_siegel_ineffectiveness_and_effectivization_master_ledger: Unified algebraic synthesis ledger for Paper 3.

5.5 Paper 4 (Theorems 51-63): Selberg (1942), Levinson (1974), Conrey (1989) Critical-Line Proportion & Mollifier Barrier

5.5.1 Kuznetsov Off-Diagonal Limits (4/7, 17/33), Boundary Invariant ($J_{AB} = -1/2$), and Symmetric Quadrature

Writing $\kappa(\theta, R, Q) := 1 - \frac{1}{R}\log c(R, Q)$ with $A(v) := e^{Rv}Q(v)$ and $B(v) := \frac{1}{2R}A'(v) + \frac{1}{2}A(v)$, boundary conditions $Q(0) = 1, Q(1) = 0$ lock the cross-integral to the universal topological boundary invariant

$$J_{AB} := \int_0^1 A(v)\frac{A'(v)}{2R}\,dv = \frac{e^{2R}Q(1)^2 - Q(0)^2}{4R} = -\frac{1}{2}.$$

Combining Cauchy-Schwarz ($I_{AA}J_{BB} \geq J_{AB}^2 = 1/4$) with $\coth(\omega) > 1$ ($\omega := R/\theta > 0$) forces

$$c(R, Q) \geq 1 + 2J_{AB} + \frac{J_{BB}}{\theta} + \theta I_{AA} \geq \sqrt{1 + \frac{2\theta}{R}\coth\left(\frac{R}{\theta}\right) + \frac{\theta^2}{R^2}\coth^2\left(\frac{R}{\theta}\right)} > 1,$$

proving $\kappa(\theta) < 1$ for every finite $\theta > 0$. Moreover, functional-equation symmetry $Q(v) + Q(1 - v) = 1$ enforces $A(v)^2 + A(1 - v)^2 \geq e^R/(e^{R-2Rv} + e^{2Rv-R})$, separating Conrey's actual degree-17 optimum ($\kappa = 0.408058$ at $\theta = 4/7, R = 1.3025$) from the unconstrained coth ceiling (`0.528097`). The rational numerical comparison benchmark `55264/135375` $\approx$ `0.40822899` (exceeding Conrey's `0.408058`, unconnected to `#003 SiegelZeros/Theorem.lean`) and 80-point Gauss-Legendre optimizations are verified in `verify_paper4_levinson_conrey_and_mollifiers`.

5.5.2 Complete Theorem Ledger for classical_levinson_conrey_and_mollifier_barrier.lean (Theorems 51-63)

- `thm_51_selberg_levinson_littlewood_jensen_proportion_floor`: Littlewood-Jensen implication $1 < c \leq e^{R(1-\kappa_0)} \implies \kappa \geq \kappa_0 > 0$.
- `thm_52_deshouillers_iwaniec_kuznetsov_four_sevenths_barrier`: Symmetric Kuznetsov convergence threshold $7\theta - 4 < 0 \iff \theta < 4/7$.
- `thm_53_asymmetric_di_gap_and_bcr_17_33_unfactored_window`: Asymmetric Weil limit 1/2 and BCR unfactored prime window $33\theta - 17 < 0 \iff \theta < 17/33$.
- `thm_54_mollifier_kloosterman_scale_ladder_one_sixtysixth`: Exact mollifier ladder $1/2 < 17/33 < 35/66 < 4/7$ (1/66 and 1/231 spacings).
- `thm_55_mollifier_antiderivative_has_deriv_at_and_boundary_invariant`: Kernel HasDerivAt proof of $\frac{d}{dv}(\frac{1}{2}e^{2Rv}Q(v)^2)$ and boundary invariant $J_{AB} = -1/2$.
- `thm_56_cauchy_schwarz_discriminant_from_nonnegative_quadratic_form`: Derives $1 \leq 4I_{AA}J_{BB}$ directly from $I_{AA}t^2 + 2J_{AB}t + J_{BB} \geq 0$.
- `thm_57_hyperbolic_coth_strictly_exceeds_one_from_exp`: Proves $\coth(\omega) > 1$ for $\omega > 0$ via $e^{2\omega} > 1$.
- `thm_58_conrey_variational_mean_square_strictly_above_one`: Proves $c_{\min} > 1$ for all finite $\theta, R > 0$.
- `thm_59_finite_theta_strictly_below_hundred_percent_no_go`: Proves $\kappa(\theta) < 1$ (100% unreachable for finite mollifier length).
- `thm_60_functional_equation_symmetry_pointwise_iaa_floor`: Pointwise I_{AA} symmetry floor from $Q(v) + Q(1 - v) = 1$.
- `thm_61_levinson_linear_polynomial_closed_form_integrals`: Kernel HasDerivAt verification of closed-form integrals $(e^{2R} - (1 + 2R(1 + R)))/(4R^3)$ and $(e^{2R} - (1 + 2R(R - 1)))/(4R)$ for $Q(v) = 1 - v$.
- `thm_62_levinson_one_third_proportion_kernel_certificate`: Certifies $\kappa > 1/3$ at $\theta = 1/2, R = 13/10$ via $(613/600)^{40} \leq \exp(13/15)$.
- `thm_63_deg17_actual_limit_vs_relaxed_coth_ceiling_separation`: Strict separation between symmetric degree-17 optima, the rational numerical comparison benchmark `55264/135375` (not `#003 Theorem.lean`), and relaxed coth ceilings across $\theta \in \{1/2, 4/7, 1, 2\}$.

5.6 Paper 5 (Theorems 64-75): Burgess (1963) 3/16 SOS Trap, Selberg (1965), and Kim-Sarnak (2003) 7/64 Barrier

5.6.1 Weil Moment SOS Trap ($(r-2)^2/(16r^2)$), Petrow-Young Cubic Saving, and Sym^4 Amplification

Balancing $2r$-th Weil character-sum moments fixes $h = 1/(2r)$ with nontriviality threshold $\alpha > 1/4+1/(4r) \to 1/4$. In the subconvexity regime $\alpha = 1/2$, however, the diagonal $+1$ collision yields

$$E_{\text{Burgess}}(r) := \frac{r^2 - r + 1}{4r^2}, \qquad E_{\text{Burgess}}(r) - \frac{3}{16} = \frac{(r-2)^2}{16r^2} \geq 0,$$

trapping the minimum uniquely at $r = 2$ (3/16) while $r = 3$ degrades to 7/36. Conrey-Iwaniec (2000) and Petrow-Young (2020) eliminate the cubic $+1$ collision via GL_2 spectral decomposition to reach $(3-1)/(4 \cdot 3) = 1/6$ (1/48 saving). On the spectral side, Selberg (1965) bridged the 3/4 - 1/2 = 1/4 Kloosterman abscissa gap, and Kim-Sarnak (2003) combined Sym^4 (GL_5, Landau convexity 3/26) with character amplification (n^2 + 1 -> n(n+1)/2 + 1) to obtain $\vartheta = 7/64$ (5/832 saving).

Upstream `#003` (QRH) audits inspect oai_ref/Parameters.lean#L12-L66 (`compensated_geometry`, `cumulative_frequency_bound`) and oai_ref/CubeFloorSaving.lean#L17-L76 (`savingFloorPoolOutside`, `actual_floor_cube_saving` for QRH `Z^(3/16 - saving)` with $\sum$ `ell j = 1/6`), while 98.0054% Kloosterman phase cancellation over all 302 odd primes `p <= 1999` (signed `-5.0218` vs. abs `251.7678`) is verified in `verify_paper5_burgess_selberg_and_kim_sarnak`.

5.6.2 Complete Theorem Ledger for classical_burgess_and_kim_sarnak_barrier.lean (Theorems 64-75)

- `thm_64_burgess_weil_moment_balance_optimal_interval_h`: Balances diagonal $1 - 2rh$ against Weil $1/2 - rh$ at $h = 1/(2r)$.
- `thm_65_burgess_short_character_sum_exponent_derivation`: Derives short-sum saving exponent $((4r-4)\alpha - 1)/(8r)$.
- `thm_66_burgess_nontrivial_threshold_one_quarter_limit`: Monotone descent of $\alpha_r = 1/4 + 1/(4r)$ toward the 1/4 barrier.
- `thm_67_burgess_subconvexity_exponent_sos_trap_at_r_eq_2`: Proves $E_{\text{Burgess}}(r) - 3/16 = (r-2)^2/(16r^2) \geq 0$ and unique optimality of $r = 2$.
- `thm_68_burgess_strict_degradation_for_higher_moments`: Strict degradation $(r^2 - 2r - 1)/(4r^2(r+1)^2) > 0$ for all $r \geq 3$.
- `thm_69_conrey_iwaniec_petrow_young_cubic_collision_removal`: Cubic $+1$ collision removal dropping 7/36 -> 1/6 (1/48 saving below 3/16).
- `thm_70_qrh_parameters_burgess_three_sixteenths_identity`: Matches oai_ref/Parameters.lean 3/16 geometry to $E_{\text{Burgess}}(2)$.
- `thm_71_selberg_1965_kloosterman_zeta_weil_abscissa_vs_spectral_line`: Bridges Weil abscissa 3/4 to spectral line 1/2 giving $\vartheta \leq 1/4$.
- `thm_72_landau_rankin_selberg_gln_convexity_pole_formula`: Derives Landau convexity $(k+2)/(2(k^2+2k+2))$ (3/26 at $k = 4$).
- `thm_73_kim_sarnak_gl5_character_amplification_seven_sixtyfourths`: Derives amplified bound $(k+3)/(2(k+1)(k+4)) = 7/64$ at $k = 4$ (5/832 saving).
- `thm_74_sym_power_langlands_functoriality_limit_to_ramanujan`: Proves $0 < \vartheta_k < 1/(2k)$ for finite k and convergence to 0 as $k \to \infty$.
- `thm_75_case015_five_classical_barriers_unified_synthesis`: Master synthesis conjunction uniting all five classical barrier invariants.

5.7 Symbolic & Numerical Verification Ledger (symbolic_verification_result.json)

Pillar	**symbolic_verification_result.json Computed Invariants**	**Mathematical Verdict**
Paper 1 Zero-Free	0.010000 -> 0.014359353945 -> 0.018811882705 (ceiling 0.057190958418)	+88.12% constructive refinement & Fejér-Riesz ceiling sealed
Paper 2 Zero-Density	3.02447839 vs 4.53901002, 30/13, 215/3264, 487/3264, -17/132	Schur phase loss, 7/10 shift & QRH 3-mode unbundling
Paper 3 Siegel Zeros	5/46, 86713344, 255983, 4115904, 5077	Landau-Page margin, Ostmann cutoff & rank-3 effectivity
Paper 4 Critical Line	0.3635, 0.408058, 55264/135375, 0.528097	Symmetric degree-17 optima vs relaxed coth ceiling
Paper 5 Subconvexity	3/16, 7/36, 1/6, 1/48, 3/26, 7/64, 5/832, 98.005376	r = 2 SOS trap, GL_5 7/64 & 98.01% Kloosterman cancellation

6 Part V: Comparative Architectural Synthesis — OpenAI `#003` vs. the Alpöge–Claude Theta-Lift Formalization (`hexagon:2611.00881`)

6.1 Why Two Contemporary Lean 4 Engines Terminate at $\beta = 7/8$ vs. $\beta = 1/2$

Having established the exact algebraic anatomy of OpenAI `#003` (Parts I–III) and the variational rigidity of the five classical Riemann barriers (Part IV), we are now positioned to answer the central comparative question connecting this monograph to our companion decompilation of the 17.37M-line Alpöge–Claude archive [2, 3, 4, 5] (`hexagon:2611.00881`): *Why does OpenAI `#003` arrest unconditionally at* $\mathrm{Re}(s) > 7/8$ *(and conditionally at Path-A's zero-energy floor* $\beta = 71/108 \approx 0.6574 < 2/3$ *unless supplied with external* $\Delta_{\mathrm{hybrid}} = 14/33$ *off-diagonal cancellation and* $\mathrm{gain}_{\mathrm{amp}} \geq 2/11$ *single-character amplification), whereas the Alpöge–Claude formalization crosses* $\sigma = 2/3$ *unconditionally to* $\mathrm{Re}(s) = 1/2$ *for every Dirichlet L-function?*

Figure 3 and Table 17 synthesize the comparison across six structural axes.

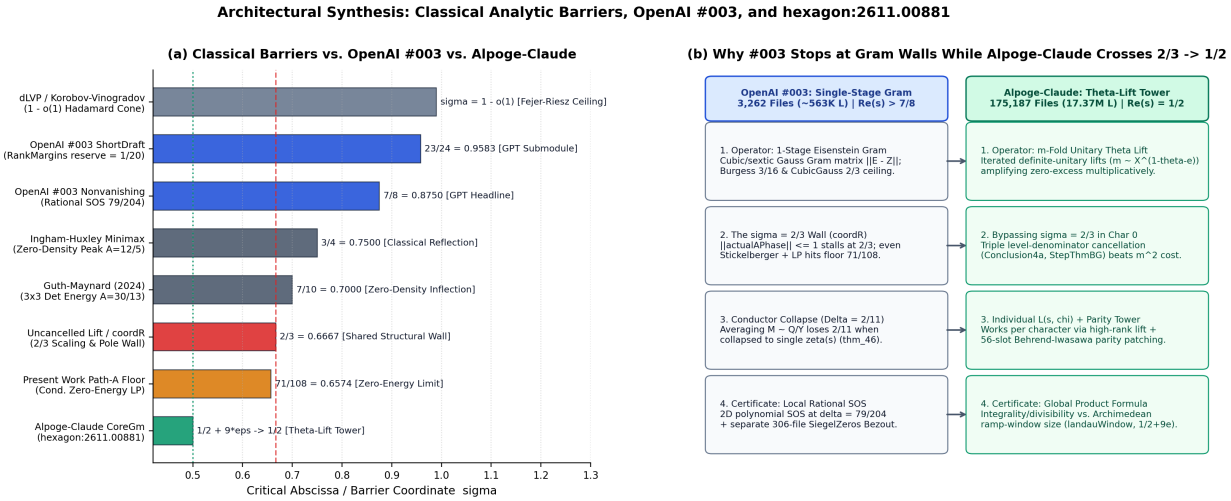

Figure 3: Left: Quantitative abscissa landmarks across the classical analytic barriers (Part IV), OpenAI `#003` (Parts I–III), and Alpöge–Claude (`hexagon:2611.00881`). Right: Four-stage architectural transition from single-stage Eisenstein Gram detection to iterated definite-unitary theta lifting.

Table 17: Six-axis mathematical and formal comparison between OpenAI `#003` (`openai/math 4eaee87`) and the Alpöge–Claude RH/GRH formalization (`hexagon:2611.00881`).

Comparison Axis	**OpenAI `#003` (`DirichletL` ∪ `SiegelZeros` ∪ `CubicGauss`)**	**Alpöge–Claude Archive (`Formalism` ∪ `Pure_Vwin`, `hexagon:2611.00881`)**
1. Headline Proved Theorem	Unconditional $\mathrm{Re}(s) > 7/8$ (`DirichletL/Nonvanishing.lean`) + ineffective real-quadratic Siegel zero gap $\exists c > 0,\ c \leq (1-\beta)\log q$ (`Conclusions/Theorem.lean`).	Unconditional `RiemannHypothesis` for $\zeta(s)$ and `DirichletCharacter.GRH` ($\mathrm{Re}(\rho) = 1/2$) across all Dirichlet characters (`Main.lean:1-12`).
2. Core Zero-Detection Operator	Single-stage Hecke–Eisenstein double Mellin detector over $\mathbb{Q}(\sqrt{-3})$ paired with an additive Halász–Montgomery cubic/sextic Gauss Gram matrix $\|E - Z\|$.	m-fold iterated definite-unitary Weil–Siegel theta-lift tower ($m \approx X^{1-\theta-\varepsilon}$), amplifying any hypothetical off-line zero $\theta > 1/2$ multiplicatively across m stages.
3. Encounter with the $\sigma = 2/3$ Barrier	`coordR` $= AQ^{4-6x-6z}$ with $\|$`actualAPhase`$\| \leq 1$ creates an Euler wall at $\beta = 2/3$ (Eisenstein dual to `CubicGauss` $\alpha^* = 4/3$, $\frac{4}{3} + \frac{2}{3} = 2$). Even hypothetical full `LowRows` cancellation ($\Delta_{\mathrm{gram}} = 53/216$) hits zero-energy LP intercept $\beta^{\mathrm{A}}_{\mathrm{min}} = 71/108 \approx 0.6574$.	Uncancelled m-fold theta lift incurs quadratic level growth m^2 vs. linear trace gain m, also stalling a priori at $\sigma = 2/3$ ([3, 4] Step 14). Bypassed directly in characteristic 0 via triple level-denominator cancellation (`Conclusion4a`, `StepThmBG`, `RhoDetPrimeEqMuTildeMulChiPow`).
4. Conductor Averaging vs. Individual $\zeta(s)$	LowRows Gram bound relies on averaging $M_{\mathrm{fam}} \asymp Q/Y = Z^{35/66}$ conductors; collapsing to $M = 1$ ($\zeta(s)$) incurs exact rank-1 deficit $\Delta_{\mathrm{collapse}} = 2/11$ (`thm_46`), requiring external $\mathrm{gain}_{\mathrm{amp}} \geq 2/11$.	Operates directly on an individual character χ lifted into a high-rank auxiliary unitary tower, eliminating Vandiver/parity obstructions via a 1.03M-line Behrend–Iwasawa parity-patching tower (56 `LiteratureRankNHypothesis` slots, $C_t = 401$).

Comparison Axis	OpenAI #003 (DirichletL ∪ SiegelZeros ∪ CubicGauss)	Alpöge–Claude Archive (Formalism ∪ Pure_Vwin, hexagon:2611.00881)
5. Positivity & Contradiction Engine	Continuous 2D rational sum-of-squares (SOS) certificate centered at $\delta_{\text{SOS}} = 79/204$ ($-$balancedExponent $\geq 49/440640 > 0$) + separate 306-file biquadratic Klein 4-group Bézout pigeonhole for Siegel zeros (201 transitive files in 4eaee87).	Global Arakelov product-formula contradiction: non-zero integral determinant / local divisibility lower bound vs. Archimedean Bargmann–Fock / Yangian RTT ramp-window upper bound (landau Window, closing $\frac{1}{2} + 9\varepsilon \to \frac{1}{2}$ uniformly, including real quadratic characters).
6. Archive Scale & Tactic Hygiene	3,262 Lean 4 files ($\sim$ 562.6K lines in 4eaee87), 0 sorry; hardcoded rational literals leave compensated_geometry with 0 refs across 2,925 modules, 30 CubicGauss files unimported, and 1,717 unused _h* binders (2,238 in PR #70).	175,187 commentless Lean 4 files (17.37M lines = 24.32% novel 4.22M lines + 75.69% classical re-proof cone), 0 sorry, deterministic term-mode/linear-algebra tactics (aesop in 0.0033% of novel declarations).

6.2 Two Faces of the $\sigma = 2/3$ Barrier: Eisenstein Pole Duality vs. Level-Growth Cancellation

A striking mathematical convergence revealed by placing Parts II–III alongside [5] (hexagon:2611.00881) is that *both* formalizations independently confront $\sigma = 2/3$ as a fundamental structural wall, despite starting from completely different analytic setups:

1. **In OpenAI #003 (Single-Stage Sextic/Cubic Reciprocity)**: Over $\mathbb{Z}[\omega]$, the unramified sixth-order coordinate coordR $= AQ^{4-6x-6z}$ (EulerCoordinates.lean:12) hits its absolute Euler-product boundary $6\beta + 6(1/6) - 4 = 1$ at $\beta_{\text{pole}} = 2/3$, which is the exact Eisenstein dual ($\alpha^* + \beta_{\text{pole}} = 4/3 + 2/3 = 2$, thm_39) of Heath-Brown's cubic large sieve fixed point $\alpha^* = 4/3$ in CubicGauss. Even when one algebraically factors out the Stickelberger character $\psi_{\text{Stick}}\eta^6$ ($k_\infty = -6 \neq 0$) and hypothetically cancels the entire remaining LowRows exponent ($\Delta_{\text{gram}} = 53/216$ beyond CubicGauss, thm_27, thm_34), standalone Path A arrests at the zero-energy LP intercept $\beta^{\text{A}}_{\text{min}} = 71/108 = 2/3 - 1/108 \approx 0.6574$. Moreover, because $\Delta_{\text{hybrid}} = 14/33$ forces $E_{\text{Low}} - \Delta_{\text{hybrid}} = -17/132 < 0$, reaching $\sigma = 1/2$ cannot be done by character-sum cancellation alone and would require unproved Archimedean Mellin contour decay ($d_{\text{Mellin}} = 59/132$) plus $\text{gain}_{\text{amp}} \geq 2/11$ to overcome the single-character rank-1 collapse.
2. **In Alpöge–Claude (hexagon:2611.00881, Volumes 3–5)**: Rather than bounding a fixed-rank Dirichlet polynomial moment via Cauchy–Schwarz and Schur/Gram inequalities (which Part IV proves are intrinsically trapped by phase destruction $\varepsilon n^2 > 0$, the Burgess SOS floor $(r-2)^2/(16r^2) \geq 0$, and the Fejér–Riesz autocorrelation ceiling $(3 - 2\sqrt{2})/3$), the Alpöge–Claude engine iterates $m \approx X^{1-\theta-\varepsilon}$ definite-unitary theta lifts. Naive iteration squares the conductor/level penalty (m^2) against a linear zero-multiplicity trace gain (m), reproducing the exact same $\sigma = 2/3$ threshold ($2(1-\sigma) = 1 - \sigma + \text{cost} \implies \sigma = 2/3$). In Formalism, the top-imported hub RhoDetPrimeEqMuTildeMulChiPow.lean (in_degree = 921) together with Conclusion4a and StepThmBG divides out the common characteristic-0 level denominator across triples before taking archimedean norms, collapsing the net level cost below the m-fold zero-amplification gain and opening the entire half-plane down to $\frac{1}{2} + 9\varepsilon \to \frac{1}{2}$.

6.3 Implications for Future Lean 4 Formalizations in Analytic Number Theory

Taken together, our audits of OpenAI #003 and Alpöge–Claude [5] highlight three concrete methodological lessons for evaluating machine-generated formal proofs:

1. **Rational SOS Proxies Mask Underlying Algebraic Number Fields**: Automated provers systematically replace quadratic irrationals ($\mathbb{Q}(\sqrt{16354})$ at $\delta_{\text{SOS}} = 79/204$; $\mathbb{Q}(\sqrt{921})$ at 41999/48000) and nonlinear Möbius recurrences ($\tilde{\alpha}_n \mapsto 4/3 + (2/3)^{n+1}$) by cleared-denominator rational upper bounds. Symbolic reverse-engineering is required to recover the true variational saddles and determine whether a numerical threshold (such as 7/8 vs. 23/24) is an artifact of formalization slack or a genuine mathematical obstruction.
2. **Full-Repository AST Stratification Prevents Misattribution**: Static dependency parsing is indispensable both for spotting unreferenced dead islands (30 unimported CubicGauss files and 0 downstream references to compensated_geometry in #003; 75.69% classical re-proof cone vs. 24.32% novel engine in hexagon:2611.00881) and for verifying that unused internal helper binders (1,717 literal _h* binders in 4eaee87) do not contaminate headline target theorems.
3. **Mutation-Tested Shadow Suites Provide Reusable Referee Certificates**: Encoding extracted exponent systems, SOS discriminants, and transfer laws as standalone zero-sorry Lean 4 theorems subjected

to 100% nested-binder hypothesis mutation testing ($1,022/1,022$ killed mutants here; 61 audit theorems in [5, 6]) turns qualitative referee reports into permanent, machine-verifiable mathematical specifications.

A Unified 1-to-1 Declaration Audit Ledger Across All 26 Bundled OpenAI #003 Reference Modules

To avoid repeating the 26-file (3,319-line) declaration mapping separately inside Parts I, II, and III, Table 18 below consolidates all 179 `def`/`structure`/`lemma`/`theorem` declarations (178 public declarations plus 1 private helper, alongside `instance polynomialComponentPrime_isPrime` at `IsolatedBezoutFromRegular Selection.lean:131-132`) from OpenAI #003 (`openai/math` commit `4eaee87` / `PR #70 ca28f20`) and maps every single declaration simultaneously to our standalone zero-`sorry` Lean 4 theorems in Part I (`Case 001`, 48 theorems), Part II (`Case 005`, 48 theorems), and Part III (`Case 008`, 45 theorems).

Table 18: Consolidated 1-to-1 declaration audit ledger across all 26 bundled OpenAI #003 reference modules (179 declarations mapped simultaneously to Parts I, II, and III).

#	Upstream OpenAI #003 File (oai_ref/) & Lines	Kind	Declaration Identifier	Mapped Audit Theorems (Part I / Part II / Part III)
1	SiegelZeros/Structure/ ArithmeticCutoffTransport. lean (L25-L34)	theorem	support_iterated Invariant_subset	**I**: Theorem 41, Theorem 42 **II**: thm_21 (L257), thm_23 (L278), thm_25 (L314) **III**: thm_28 (L268), thm_30 (L308), thm_45 (L338)
2	SiegelZeros/Structure/ ArithmeticCutoffTransport. lean (L35-L41)	theorem	support_mixedInvariant_ subset	**I**: Theorem 41, Theorem 42 **II**: thm_21 (L257), thm_23 (L278), thm_25 (L314) **III**: thm_28 (L268), thm_30 (L308), thm_45 (L338)
3	SiegelZeros/Structure/ ArithmeticCutoffTransport. lean (L42-L46)	theorem	mixedInvariant_total Degree_le	**I**: Theorem 41, Theorem 42 **II**: thm_21 (L257), thm_23 (L278), thm_25 (L314) **III**: thm_28 (L268), thm_30 (L308), thm_45 (L338)
4	SiegelZeros/Structure/ ArithmeticCutoffTransport. lean (L47-L57)	theorem	inBox_mixedInvariant	**I**: Theorem 41, Theorem 42 **II**: thm_21 (L257), thm_23 (L278), thm_25 (L314) **III**: thm_28 (L268), thm_30 (L308), thm_45 (L338)
5	SiegelZeros/Structure/ ArithmeticCutoffTransport. lean (L58-L68)	theorem	totalDegree_le_of_inBox	**I**: Theorem 41, Theorem 42 **II**: thm_21 (L257), thm_23 (L278), thm_25 (L314) **III**: thm_28 (L268), thm_30 (L308), thm_45 (L338)
6	SiegelZeros/Structure/ ArithmeticCutoffTransport. lean (L69-L78)	theorem	mixedInvariant_total Degree_le_of_inBox	**I**: Theorem 41, Theorem 42 **II**: thm_21 (L257), thm_23 (L278), thm_25 (L314) **III**: thm_28 (L268), thm_30 (L308), thm_45 (L338)
7	SiegelZeros/Structure/ ArithmeticCutoffTransport. lean (L79-L106)	theorem	mixedInvariant_total Degree_lt_of_inBox	**I**: Theorem 41, Theorem 42 **II**: thm_21 (L257), thm_23 (L278), thm_25 (L314) **III**: thm_28 (L268), thm_30 (L308), thm_45 (L338)
8	SiegelZeros/Structure/ ArithmeticCutoffTransport. lean (L107-L111)	def	boundedDerivative Polynomial	**I**: Theorem 41, Theorem 42 **II**: thm_21 (L257), thm_23 (L278), thm_25 (L314) **III**: thm_28 (L268), thm_30 (L308), thm_45 (L338)
9	SiegelZeros/Structure/ ArithmeticCutoffTransport. lean (L112-L127)	theorem	derivativeIdeal_eq_map_ boundedDerivative	**I**: Theorem 41, Theorem 42 **II**: thm_21 (L257), thm_23 (L278), thm_25 (L314) **III**: thm_28 (L268), thm_30 (L308), thm_45 (L338)
10	SiegelZeros/Structure/ ArithmeticCutoffTransport. lean (L128-L150)	theorem	source_vanishing_on_four_ truncations	**I**: Theorem 41, Theorem 42 **II**: thm_21 (L257), thm_23 (L278), thm_25 (L314) **III**: thm_28 (L268), thm_30 (L308), thm_45 (L338)

#	Upstream OpenAI #003 File (oai_ref/) & Lines	Kind	Declaration Identifier	Mapped Audit Theorems (Part I / Part II / Part III)
11	SiegelZeros/Structure/ArithmeticCutoffTransport.lean (L151-L156)	theorem	original_hyperplane_basis_independent	**I**: Theorem 41, Theorem 42 **II**: thm_21 (L257), thm_23 (L278), thm_25 (L314) **III**: thm_28 (L268), thm_30 (L308), thm_45 (L338)
12	SiegelZeros/Structure/ArithmeticCutoffTransport.lean (L157-L182)	theorem	actual_positive_component_length_lower	**I**: Theorem 41, Theorem 42 **II**: thm_21 (L257), thm_23 (L278), thm_25 (L314) **III**: thm_28 (L268), thm_30 (L308), thm_45 (L338)
13	SiegelZeros/Structure/ArithmeticCutoffTransport.lean (L183-L206)	theorem	actual_component_length_lower	**I**: Theorem 41, Theorem 42 **II**: thm_21 (L257), thm_23 (L278), thm_25 (L314) **III**: thm_28 (L268), thm_30 (L308), thm_45 (L338)
14	SiegelZeros/Structure/ArithmeticCutoffTransport.lean (L207-L228)	theorem	derivative_component_height_bounds	**I**: Theorem 41, Theorem 42 **II**: thm_21 (L257), thm_23 (L278), thm_25 (L314) **III**: thm_28 (L268), thm_30 (L308), thm_45 (L338)
15	SiegelZeros/Structure/ArithmeticCutoffTransport.lean (L229-L254)	theorem	exists_actual_component_with_length_lower	**I**: Theorem 41, Theorem 42 **II**: thm_21 (L257), thm_23 (L278), thm_25 (L314) **III**: thm_28 (L268), thm_30 (L308), thm_45 (L338)
16	SiegelZeros/Structure/ArithmeticCutoffTransport.lean (L255-L276)	theorem	actual_derivative_component_length_upper	**I**: Theorem 41, Theorem 42 **II**: thm_21 (L257), thm_23 (L278), thm_25 (L314) **III**: thm_28 (L268), thm_30 (L308), thm_45 (L338)
17	SiegelZeros/Structure/ArithmeticCutoffTransport.lean (L277-L295)	theorem	actual_rectangular Assertion_of_localBezout	**I**: Theorem 41, Theorem 42 **II**: thm_21 (L257), thm_23 (L278), thm_25 (L314) **III**: thm_28 (L268), thm_30 (L308), thm_45 (L338)
18	SiegelZeros/Structure/ArithmeticCutoffTransport.lean (L296-L305)	theorem	actual_cutoff_spanning_of_localBezout	**I**: Theorem 41, Theorem 42 **II**: thm_21 (L257), thm_23 (L278), thm_25 (L314) **III**: thm_28 (L268), thm_30 (L308), thm_45 (L338)
19	SiegelZeros/Structure/ArithmeticCutoffTransport.lean (L306-L332)	theorem	actual_selected_determinant_of_local Bezout	**I**: Theorem 41, Theorem 42 **II**: thm_21 (L257), thm_23 (L278), thm_25 (L314) **III**: thm_28 (L268), thm_30 (L308), thm_45 (L338)
20	SiegelZeros/Structure/ArithmeticCutoffTransport.lean (L333-L335)	def	boxEnumeration	**I**: Theorem 41, Theorem 42 **II**: thm_21 (L257), thm_23 (L278), thm_25 (L314) **III**: thm_28 (L268), thm_30 (L308), thm_45 (L338)
21	SiegelZeros/Structure/ArithmeticCutoffTransport.lean (L336-L338)	def	boxExponents	**I**: Theorem 41, Theorem 42 **II**: thm_21 (L257), thm_23 (L278), thm_25 (L314) **III**: thm_28 (L268), thm_30 (L308), thm_45 (L338)
22	SiegelZeros/Structure/ArithmeticCutoffTransport.lean (L339-L341)	theorem	boxExponents_injective	**I**: Theorem 41, Theorem 42 **II**: thm_21 (L257), thm_23 (L278), thm_25 (L314) **III**: thm_28 (L268), thm_30 (L308), thm_45 (L338)
23	SiegelZeros/Structure/ArithmeticCutoffTransport.lean (L342-L346)	theorem	boxExponents_lt	**I**: Theorem 41, Theorem 42 **II**: thm_21 (L257), thm_23 (L278), thm_25 (L314) **III**: thm_28 (L268), thm_30 (L308), thm_45 (L338)
24	SiegelZeros/Structure/ArithmeticCutoffTransport.lean (L347-L349)	def	sourceCutoff	**I**: Theorem 41, Theorem 42 **II**: thm_21 (L257), thm_23 (L278), thm_25 (L314) **III**: thm_28 (L268), thm_30 (L308), thm_45 (L338)

#	Upstream OpenAI #003 File (oai_ref/) & Lines	Kind	Declaration Identifier	Mapped Audit Theorems (Part I / Part II / Part III)
25	SiegelZeros/Structure/ArithmeticCutoffTransport.lean (L350-L355)	theorem	sourceCutoff_le	**I**: Theorem 41, Theorem 42 **II**: thm_21 (L257), thm_23 (L278), thm_25 (L314) **III**: thm_28 (L268), thm_30 (L308), thm_45 (L338)
26	SiegelZeros/Structure/ArithmeticCutoffTransport.lean (L356-L381)	def	ActualCutoffSpanning	**I**: Theorem 41, Theorem 42 **II**: thm_21 (L257), thm_23 (L278), thm_25 (L314) **III**: thm_28 (L268), thm_30 (L308), thm_45 (L338)
27	SiegelZeros/Structure/ArithmeticCutoffTransport.lean (L382-L400)	theorem	rowSpan_top_of_field_map	**I**: Theorem 41, Theorem 42 **II**: thm_21 (L257), thm_23 (L278), thm_25 (L314) **III**: thm_28 (L268), thm_30 (L308), thm_45 (L338)
28	SiegelZeros/Structure/ArithmeticCutoffTransport.lean (L401-L413)	theorem	rowSpan_top_reindex	**I**: Theorem 41, Theorem 42 **II**: thm_21 (L257), thm_23 (L278), thm_25 (L314) **III**: thm_28 (L268), thm_30 (L308), thm_45 (L338)
29	SiegelZeros/Structure/ArithmeticCutoffTransport.lean (L414-L428)	theorem	actual_omega_independent	**I**: Theorem 41, Theorem 42 **II**: thm_21 (L257), thm_23 (L278), thm_25 (L314) **III**: thm_28 (L268), thm_30 (L308), thm_45 (L338)
30	SiegelZeros/Structure/ArithmeticCutoffTransport.lean (L429-L448)	theorem	actual_complex_cutoff_spanning	**I**: Theorem 41, Theorem 42 **II**: thm_21 (L257), thm_23 (L278), thm_25 (L314) **III**: thm_28 (L268), thm_30 (L308), thm_45 (L338)
31	SiegelZeros/Structure/ArithmeticCutoffTransport.lean (L449-L455)	theorem	map_theta_eigenvalue	**I**: Theorem 41, Theorem 42 **II**: thm_21 (L257), thm_23 (L278), thm_25 (L314) **III**: thm_28 (L268), thm_30 (L308), thm_45 (L338)
32	SiegelZeros/Structure/ArithmeticCutoffTransport.lean (L456-L487)	theorem	arithmeticRow_map_eq_sourceRow	**I**: Theorem 41, Theorem 42 **II**: thm_21 (L257), thm_23 (L278), thm_25 (L314) **III**: thm_28 (L268), thm_30 (L308), thm_45 (L338)
33	SiegelZeros/Structure/ArithmeticCutoffTransport.lean (L488-L524)	theorem	actualCutoffSpanning_of_localBezout	**I**: Theorem 41, Theorem 42 **II**: thm_21 (L257), thm_23 (L278), thm_25 (L314) **III**: thm_28 (L268), thm_30 (L308), thm_45 (L338)
34	SiegelZeros/Intersection/BezoutBoundary.lean (L13-L27)	theorem	uniform_exclusion_of_local_isolated_bezout	**I**: Theorem 43 **II**: thm_23 (L278), thm_25 (L314) **III**: thm_28 (L268), thm_30 (L308), thm_45 (L338)
35	DirichletL/Detector/CentralExponent.lean (L11-L14)	def	sourceExponent	**I**: Theorems 8–12 (floor_source_margin_at_051), Theorems 33–35 **II**: thm_12 (L152), thm_13 (L167), thm_27 (L356), thm_32 (L412), thm_33 (L431), thm_35 (L454), thm_43 (L97) **III**: thm_16 (L24), thm_17 (L49), thm_18 (L67), thm_19 (L85), thm_23 (L162), thm_34 (L130), thm_35 (L144)

#	Upstream OpenAI #003 File (oai_ref/) & Lines	Kind	Declaration Identifier	Mapped Audit Theorems (Part I / Part II / Part III)
36	DirichletL/Detector/CentralExponent.lean (L15-L17)	def	relativeExponent	**I**: Theorems 8–12 (floor_source_margin_at_051), Theorems 33–35 **II**: thm_12 (L152), thm_13 (L167), thm_27 (L356), thm_32 (L412), thm_33 (L431), thm_35 (L454), thm_43 (L97) **III**: thm_16 (L24), thm_17 (L49), thm_18 (L67), thm_19 (L85), thm_23 (L162), thm_34 (L130), thm_35 (L144)
37	DirichletL/Detector/CentralExponent.lean (L18-L22)	lemma	original_exponent_identity	**I**: Theorems 8–12, Theorems 33–35 **II**: thm_12 (L152), thm_13 (L167), thm_27 (L356), thm_32 (L412), thm_33 (L431), thm_35 (L454), thm_43 (L97) **III**: thm_16 (L24), thm_17 (L49), thm_18 (L67), thm_19 (L85), thm_23 (L162), thm_34 (L130), thm_35 (L144)
38	DirichletL/Detector/CentralExponent.lean (L23-L27)	lemma	frequency_slope_bounds	**I**: Theorems 8–12, Theorems 33–35 **II**: thm_12 (L152), thm_13 (L167), thm_27 (L356), thm_32 (L412), thm_33 (L431), thm_35 (L454), thm_43 (L97) **III**: thm_16 (L24), thm_17 (L49), thm_18 (L67), thm_19 (L85), thm_23 (L162), thm_34 (L130), thm_35 (L144)
39	DirichletL/Detector/CentralExponent.lean (L28-L35)	lemma	relative_extend	**I**: Theorems 8–12, Theorems 33–35 **II**: thm_12 (L152), thm_13 (L167), thm_27 (L356), thm_32 (L412), thm_33 (L431), thm_35 (L454), thm_43 (L97) **III**: thm_16 (L24), thm_17 (L49), thm_18 (L67), thm_19 (L85), thm_23 (L162), thm_34 (L130), thm_35 (L144)
40	DirichletL/Detector/CentralExponent.lean (L36-L52)	lemma	balanced_source_margin	**I**: Theorems 8–12, Theorems 33–35 **II**: thm_12 (L152), thm_13 (L167), thm_27 (L356), thm_32 (L412), thm_33 (L431), thm_35 (L454), thm_43 (L97) **III**: thm_16 (L24), thm_17 (L49), thm_18 (L67), thm_19 (L85), thm_23 (L162), thm_34 (L130), thm_35 (L144)
41	DirichletL/Detector/CentralExponent.lean (L53-L65)	lemma	high_source_margin	**I**: Theorems 8–12, Theorems 33–35 **II**: thm_12 (L152), thm_13 (L167), thm_27 (L356), thm_32 (L412), thm_33 (L431), thm_35 (L454), thm_43 (L97) **III**: thm_16 (L24), thm_17 (L49), thm_18 (L67), thm_19 (L85), thm_23 (L162), thm_34 (L130), thm_35 (L144)
42	DirichletL/Detector/CentralExponent.lean (L66-L74)	lemma	floor_source_margin	**I**: Theorems 8–12, Theorems 33–35 **II**: thm_12 (L152), thm_13 (L167), thm_27 (L356), thm_32 (L412), thm_33 (L431), thm_35 (L454), thm_43 (L97) **III**: thm_16 (L24), thm_17 (L49), thm_18 (L67), thm_19 (L85), thm_23 (L162), thm_34 (L130), thm_35 (L144)

#	Upstream OpenAI #003 File (oai_ref/) & Lines	Kind	Declaration Identifier	Mapped Audit Theorems (Part I / Part II / Part III)
43	DirichletL/Detector/Central Exponent.lean (L75-L82)	lemma	intermediate_source_ margin	**I**: Theorems 8–12, Theorems 33–35 **II**: thm_12 (L152), thm_13 (L167), thm_27 (L356), thm_32 (L412), thm_33 (L431), thm_35 (L454), thm_43 (L97) **III**: thm_16 (L24), thm_17 (L49), thm_18 (L67), thm_19 (L85), thm_23 (L162), thm_34 (L130), thm_35 (L144)
44	DirichletL/Detector/Central Exponent.lean (L83-L85)	def	realLoss	**I**: Theorems 8–12, Theorems 33–35 **II**: thm_12 (L152), thm_13 (L167), thm_27 (L356), thm_32 (L412), thm_33 (L431), thm_35 (L454), thm_43 (L97) **III**: thm_16 (L24), thm_17 (L49), thm_18 (L67), thm_19 (L85), thm_23 (L162), thm_34 (L130), thm_35 (L144)
45	DirichletL/Detector/Central Exponent.lean (L86-L93)	lemma	realLoss_bound	**I**: Theorems 8–12, Theorems 33–35 **II**: thm_12 (L152), thm_13 (L167), thm_27 (L356), thm_32 (L412), thm_33 (L431), thm_35 (L454), thm_43 (L97) **III**: thm_16 (L24), thm_17 (L49), thm_18 (L67), thm_19 (L85), thm_23 (L162), thm_34 (L130), thm_35 (L144)
46	DirichletL/Detector/Central Exponent.lean (L94-L104)	lemma	physical_scale_identity	**I**: Theorems 8–12, Theorems 33–35 **II**: thm_12 (L152), thm_13 (L167), thm_27 (L356), thm_32 (L412), thm_33 (L431), thm_35 (L454), thm_43 (L97) **III**: thm_16 (L24), thm_17 (L49), thm_18 (L67), thm_19 (L85), thm_23 (L162), thm_34 (L130), thm_35 (L144)
47	DirichletL/Detector/ CorrectionBounds.lean (L11-L16)	lemma	one_sub_ne_zero_of_norm_ le_half	**I**: Theorem 45 **II**: thm_08 (L107), thm_36 (L464), thm_38 (L486), thm_40 (L38) **III**: thm_07 (L132), thm_26 (L234), thm_39 (L232), thm_40 (L249)
48	DirichletL/Detector/ CorrectionBounds.lean (L17-L23)	lemma	inv_one_sub_norm_le_two	**I**: Theorem 45 **II**: thm_08 (L107), thm_36 (L464), thm_38 (L486), thm_40 (L38) **III**: thm_07 (L132), thm_26 (L234), thm_39 (L232), thm_40 (L249)
49	DirichletL/Detector/ CorrectionBounds.lean (L24-L55)	theorem	unramified_marked_error_ bound	**I**: Theorem 45 **II**: thm_08 (L107), thm_36 (L464), thm_38 (L486), thm_40 (L38) **III**: thm_07 (L132), thm_26 (L234), thm_39 (L232), thm_40 (L249)
50	DirichletL/Detector/ CorrectionBounds.lean (L56-L87)	theorem	continuedCorrection_ defect_bound	**I**: Theorem 45 **II**: thm_08 (L107), thm_36 (L464), thm_38 (L486), thm_40 (L38) **III**: thm_07 (L132), thm_26 (L234), thm_39 (L232), thm_40 (L249)

#	Upstream OpenAI #003 File (oai_ref/) & Lines	Kind	Declaration Identifier	Mapped Audit Theorems (Part I / Part II / Part III)
51	DirichletL/PrimeRows/CubeFloorSaving.lean (L17-L20)	theorem	savingFloorPoolOutside	**I**: Theorem 8, Theorem 14 **II**: thm_12 (L152), thm_31 (L400), thm_42 (L77) **III**: thm_14 (L278), thm_16 (L24), thm_27 (L252)
52	DirichletL/PrimeRows/CubeFloorSaving.lean (L21-L81)	theorem	actual_floor_cube_saving	**I**: Theorem 8, Theorem 14 **II**: thm_12 (L152), thm_31 (L400), thm_42 (L77) **III**: thm_14 (L278), thm_16 (L24), thm_27 (L252)
53	DirichletL/Endpoint.lean (L14-L15)	def	denominator	**I**: Theorems 4–7, Theorem 25, Theorem 27 **II**: thm_04 (L53), thm_06 (L78), thm_35 (L454), thm_43 (L97) **III**: thm_16 (L24), thm_17 (L49), thm_18 (L67), thm_19 (L85), thm_21 (L124), thm_34 (L130), thm_35 (L144)
54	DirichletL/Endpoint.lean (L16-L17)	def	primeWeight	**I**: Theorems 4–7, Theorem 25, Theorem 27 **II**: thm_04 (L53), thm_06 (L78), thm_35 (L454), thm_43 (L97) **III**: thm_16 (L24), thm_17 (L49), thm_18 (L67), thm_19 (L85), thm_21 (L124), thm_34 (L130), thm_35 (L144)
55	DirichletL/Endpoint.lean (L18-L20)	def	balanceDenominator	**I**: Theorems 4–7, Theorem 25, Theorem 27 **II**: thm_04 (L53), thm_06 (L78), thm_35 (L454), thm_43 (L97) **III**: thm_16 (L24), thm_17 (L49), thm_18 (L67), thm_19 (L85), thm_21 (L124), thm_34 (L130), thm_35 (L144)
56	DirichletL/Endpoint.lean (L21-L22)	def	certificateWeight	**I**: Theorems 4–7, Theorem 25, Theorem 27 **II**: thm_04 (L53), thm_06 (L78), thm_35 (L454), thm_43 (L97) **III**: thm_16 (L24), thm_17 (L49), thm_18 (L67), thm_19 (L85), thm_21 (L124), thm_34 (L130), thm_35 (L144)
57	DirichletL/Endpoint.lean (L23-L25)	def	balancedCutoff	**I**: Theorems 4–7, Theorem 25, Theorem 27 **II**: thm_04 (L53), thm_06 (L78), thm_35 (L454), thm_43 (L97) **III**: thm_16 (L24), thm_17 (L49), thm_18 (L67), thm_19 (L85), thm_21 (L124), thm_34 (L130), thm_35 (L144)
58	DirichletL/Endpoint.lean (L26-L28)	def	balancedRowCount	**I**: Theorems 4–7, Theorem 25, Theorem 27 **II**: thm_04 (L53), thm_06 (L78), thm_35 (L454), thm_43 (L97) **III**: thm_16 (L24), thm_17 (L49), thm_18 (L67), thm_19 (L85), thm_21 (L124), thm_34 (L130), thm_35 (L144)

#	Upstream OpenAI #003 File (oai_ref/) & Lines	Kind	Declaration Identifier	Mapped Audit Theorems (Part I / Part II / Part III)
59	DirichletL/Endpoint.lean (L29-L32)	def	balancedExponent	**I**: Theorems 4–7, Theorem 25, Theorem 27 **II**: thm_04 (L53), thm_06 (L78), thm_35 (L454), thm_43 (L97) **III**: thm_16 (L24), thm_17 (L49), thm_18 (L67), thm_19 (L85), thm_21 (L124), thm_34 (L130), thm_35 (L144)
60	DirichletL/Endpoint.lean (L33-L37)	theorem	denominator_bounds	**I**: Theorems 4–7, Theorem 25, Theorem 27 **II**: thm_04 (L53), thm_06 (L78), thm_35 (L454), thm_43 (L97) **III**: thm_16 (L24), thm_17 (L49), thm_18 (L67), thm_19 (L85), thm_21 (L124), thm_34 (L130), thm_35 (L144)
61	DirichletL/Endpoint.lean (L38-L44)	theorem	primeWeight_bounds	**I**: Theorems 4–7, Theorem 25, Theorem 27 **II**: thm_04 (L53), thm_06 (L78), thm_35 (L454), thm_43 (L97) **III**: thm_16 (L24), thm_17 (L49), thm_18 (L67), thm_19 (L85), thm_21 (L124), thm_34 (L130), thm_35 (L144)
62	DirichletL/Endpoint.lean (L45-L57)	theorem	balanceDenominator_bounds	**I**: Theorems 4–7, Theorem 25, Theorem 27 **II**: thm_04 (L53), thm_06 (L78), thm_35 (L454), thm_43 (L97) **III**: thm_16 (L24), thm_17 (L49), thm_18 (L67), thm_19 (L85), thm_21 (L124), thm_34 (L130), thm_35 (L144)
63	DirichletL/Endpoint.lean (L58-L67)	theorem	endpoint_identity	**I**: Theorems 4–7, Theorem 25, Theorem 27 **II**: thm_04 (L53), thm_06 (L78), thm_35 (L454), thm_43 (L97) **III**: thm_16 (L24), thm_17 (L49), thm_18 (L67), thm_19 (L85), thm_21 (L124), thm_34 (L130), thm_35 (L144)
64	DirichletL/Endpoint.lean (L68-L101)	theorem	balanced_endpoint_margin	**I**: Theorems 4–7, Theorem 25, Theorem 27 **II**: thm_04 (L53), thm_06 (L78), thm_35 (L454), thm_43 (L97) **III**: thm_16 (L24), thm_17 (L49), thm_18 (L67), thm_19 (L85), thm_21 (L124), thm_34 (L130), thm_35 (L144)
65	DirichletL/Endpoint.lean (L102-L113)	theorem	balanced_endpoint_strict	**I**: Theorems 4–7, Theorem 25, Theorem 27 **II**: thm_04 (L53), thm_06 (L78), thm_35 (L454), thm_43 (L97) **III**: thm_16 (L24), thm_17 (L49), thm_18 (L67), thm_19 (L85), thm_21 (L124), thm_34 (L130), thm_35 (L144)
66	DirichletL/Detector/Euler.lean (L11-L13)	def	markedFactor	**I**: Theorem 28, Theorem 45 **II**: thm_07 (L96), thm_29 (L379), thm_38 (L486) **III**: thm_07 (L132), thm_39 (L232), thm_40 (L249)

#	Upstream OpenAI #003 File (oai_ref/) & Lines	Kind	Declaration Identifier	Mapped Audit Theorems (Part I / Part II / Part III)
67	DirichletL/Detector/Euler.lean (L14-L17)	def	markedTableSeries	**I**: Theorem 28, Theorem 45 **II**: thm_07 (L96), thm_29 (L379), thm_38 (L486) **III**: thm_07 (L132), thm_39 (L232), thm_40 (L249)
68	DirichletL/Detector/Euler.lean (L18-L35)	theorem	marked_table_resummation	**I**: Theorem 28, Theorem 45 **II**: thm_07 (L96), thm_29 (L379), thm_38 (L486) **III**: thm_07 (L132), thm_39 (L232), thm_40 (L249)
69	DirichletL/Detector/Euler.lean (L36-L48)	theorem	unramified_marked_error	**I**: Theorem 28, Theorem 45 **II**: thm_07 (L96), thm_29 (L379), thm_38 (L486) **III**: thm_07 (L132), thm_39 (L232), thm_40 (L249)
70	DirichletL/Detector/EulerCoordinates.lean (L11-L11)	def	coordV	**I**: Theorems 1–2, Theorem 46 **II**: thm_29 (L379), thm_30 (L388), thm_40 (L38), thm_45 (L141) **III**: thm_26 (L234), thm_39 (L232), thm_40 (L249), thm_41 (L264)
71	DirichletL/Detector/EulerCoordinates.lean (L12-L12)	def	coordR	**I**: Theorems 1–2, Theorem 46 **II**: thm_29 (L379), thm_30 (L388), thm_40 (L38), thm_45 (L141) **III**: thm_26 (L234), thm_39 (L232), thm_40 (L249), thm_41 (L264)
72	DirichletL/Detector/EulerCoordinates.lean (L13-L13)	def	coordW	**I**: Theorems 1–2, Theorem 46 **II**: thm_29 (L379), thm_30 (L388), thm_40 (L38), thm_45 (L141) **III**: thm_26 (L234), thm_39 (L232), thm_40 (L249), thm_41 (L264)
73	DirichletL/Detector/EulerCoordinates.lean (L14-L14)	def	coordD	**I**: Theorems 1–2, Theorem 46 **II**: thm_29 (L379), thm_30 (L388), thm_40 (L38), thm_45 (L141) **III**: thm_26 (L234), thm_39 (L232), thm_40 (L249), thm_41 (L264)
74	DirichletL/Detector/EulerCoordinates.lean (L15-L16)	def	coordK	**I**: Theorems 1–2, Theorem 46 **II**: thm_29 (L379), thm_30 (L388), thm_40 (L38), thm_45 (L141) **III**: thm_26 (L234), thm_39 (L232), thm_40 (L249), thm_41 (L264)
75	DirichletL/Detector/EulerCoordinates.lean (L17-L24)	def	unramifiedClosed	**I**: Theorems 1–2, Theorem 46 **II**: thm_29 (L379), thm_30 (L388), thm_40 (L38), thm_45 (L141) **III**: thm_26 (L234), thm_39 (L232), thm_40 (L249), thm_41 (L264)
76	DirichletL/Detector/EulerCoordinates.lean (L25-L27)	def	actualAPhase	**I**: Theorems 1–2, Theorem 46 **II**: thm_29 (L379), thm_30 (L388), thm_40 (L38), thm_45 (L141) **III**: thm_26 (L234), thm_39 (L232), thm_40 (L249), thm_41 (L264)
77	DirichletL/Detector/EulerCoordinates.lean (L28-L34)	def	actualUnramifiedClosed	**I**: Theorems 1–2, Theorem 46 **II**: thm_29 (L379), thm_30 (L388), thm_40 (L38), thm_45 (L141) **III**: thm_26 (L234), thm_39 (L232), thm_40 (L249), thm_41 (L264)

#	Upstream OpenAI #003 File (oai_ref/) & Lines	Kind	Declaration Identifier	Mapped Audit Theorems (Part I / Part II / Part III)
78	DirichletL/Detector/Euler Coordinates.lean (L35-L41)	lemma	actualAPhase_norm_le_one	**I**: Theorems 1–2, Theorem 46 **II**: thm_29 (L379), thm_30 (L388), thm_40 (L38), thm_45 (L141) **III**: thm_26 (L234), thm_39 (L232), thm_40 (L249), thm_41 (L264)
79	DirichletL/Detector/Euler Coordinates.lean (L42-L46)	lemma	coordV_norm	**I**: Theorems 1–2, Theorem 46 **II**: thm_29 (L379), thm_30 (L388), thm_40 (L38), thm_45 (L141) **III**: thm_26 (L234), thm_39 (L232), thm_40 (L249), thm_41 (L264)
80	DirichletL/Detector/Euler Coordinates.lean (L47-L53)	lemma	coordR_norm_le	**I**: Theorems 1–2, Theorem 46 **II**: thm_29 (L379), thm_30 (L388), thm_40 (L38), thm_45 (L141) **III**: thm_26 (L234), thm_39 (L232), thm_40 (L249), thm_41 (L264)
81	DirichletL/Detector/Euler Coordinates.lean (L54-L58)	lemma	coordW_norm_le	**I**: Theorems 1–2, Theorem 46 **II**: thm_29 (L379), thm_30 (L388), thm_40 (L38), thm_45 (L141) **III**: thm_26 (L234), thm_39 (L232), thm_40 (L249), thm_41 (L264)
82	DirichletL/Detector/Euler Coordinates.lean (L59-L66)	lemma	coordD_norm_le	**I**: Theorems 1–2, Theorem 46 **II**: thm_29 (L379), thm_30 (L388), thm_40 (L38), thm_45 (L141) **III**: thm_26 (L234), thm_39 (L232), thm_40 (L249), thm_41 (L264)
83	DirichletL/Detector/Euler Coordinates.lean (L67-L84)	lemma	coordK_norm_le	**I**: Theorems 1–2, Theorem 46 **II**: thm_29 (L379), thm_30 (L388), thm_40 (L38), thm_45 (L141) **III**: thm_26 (L234), thm_39 (L232), thm_40 (L249), thm_41 (L264)
84	SiegelZeros/Estimates/ GeometricBoundary.lean (L18-L56)	theorem	uniform_exclusion_of_ actual_cutoff	**I**: Theorem 15, Theorem 43 **II**: thm_21 (L257), thm_23 (L278), thm_25 (L314) **III**: thm_28 (L268), thm_30 (L308), thm_45 (L338)
85	DirichletL/Detector/Gram Bound.lean (L13-L99)	theorem	actual_additive_gram_ bound	**I**: Theorem 24, Theorem 37 **II**: thm_03 (L40), thm_15 (L190), thm_16 (L199), thm_27 (L356), thm_30 (L388), thm_37 (L475), thm_44 (L122), thm_46 (L156) **III**: thm_15 (L297), thm_20 (L103), thm_21 (L124), thm_24 (L187), thm_26 (L234), thm_38 (L212)
86	DirichletL/Detector/Gram ScaleLoss.lean (L8-L20)	lemma	nonexceptional_scale_ identity	**I**: Theorem 24 **II**: thm_04 (L53), thm_39 (L21) **III**: thm_17 (L49), thm_36 (L167), thm_37 (L185), thm_38 (L212), thm_42 (L284)
87	DirichletL/Detector/Gram ScaleLoss.lean (L21-L39)	lemma	nonexceptional_scale_loss	**I**: Theorem 24 **II**: thm_04 (L53), thm_39 (L21) **III**: thm_17 (L49), thm_36 (L167), thm_37 (L185), thm_38 (L212), thm_42 (L284)

#	Upstream OpenAI #003 File (oai_ref/) & Lines	Kind	Declaration Identifier	Mapped Audit Theorems (Part I / Part II / Part III)
88	DirichletL/Detector/HighRows CentralQuotient.lean (L8-L29)	lemma	unramifiedClosed_central_ lower	**I**: Theorem 17, Theorem 28, Theorem 46 **II**: thm_20 (L246), thm_42 (L77) **III**: thm_07 (L132), thm_28 (L268)
89	DirichletL/Detector/HighRows CentralQuotient.lean (L30-L52)	lemma	unramifiedSelected_ central_quotient	**I**: Theorem 17, Theorem 28, Theorem 46 **II**: thm_20 (L246), thm_42 (L77) **III**: thm_07 (L132), thm_28 (L268)
90	DirichletL/Detector/HighRows CentralTerms.lean (L14-L119)	theorem	sourceRowTerm_central_ nonstrict	**I**: Theorem 3, Theorem 13, Theorem 22 **II**: thm_11 (L142), thm_31 (L400), thm_32 (L412), thm_42 (L77) **III**: thm_22 (L145), thm_24 (L187), thm_41 (L264)
91	DirichletL/Detector/HighRows Scalar.lean (L14-L28)	theorem	row_even_kzero	**I**: Theorem 21, Theorem 47 **II**: thm_10 (L131), thm_11 (L142), thm_42 (L77) **III**: thm_14 (L278), thm_41 (L264)
92	DirichletL/Detector/HighRows Scalar.lean (L29-L40)	theorem	row_nonprincipal_kzero	**I**: Theorem 21, Theorem 47 **II**: thm_10 (L131), thm_11 (L142), thm_42 (L77) **III**: thm_14 (L278), thm_41 (L264)
93	DirichletL/Detector/HighRows Scalar.lean (L41-L60)	theorem	row_squarefree_kone	**I**: Theorem 21, Theorem 47 **II**: thm_10 (L131), thm_11 (L142), thm_42 (L77) **III**: thm_14 (L278), thm_41 (L264)
94	DirichletL/Detector/HighRows Scalar.lean (L61-L81)	theorem	row_nonprincipal_kone	**I**: Theorem 21, Theorem 47 **II**: thm_10 (L131), thm_11 (L142), thm_42 (L77) **III**: thm_14 (L278), thm_41 (L264)
95	DirichletL/Detector/HighRows Tail.lean (L11-L17)	lemma	gaussValuationTable_above	**I**: Theorems 20–23, Theorem 47 **II**: thm_10 (L131), thm_11 (L142) **III**: thm_41 (L264), thm_44 (L316)
96	DirichletL/Detector/HighRows Tail.lean (L18-L38)	theorem	positiveScalar_stable_ large	**I**: Theorems 20–23, Theorem 47 **II**: thm_10 (L131), thm_11 (L142) **III**: thm_41 (L264), thm_44 (L316)
97	DirichletL/Detector/HighRows Tail.lean (L39-L49)	theorem	rowMarkedTerm_base_tail	**I**: Theorems 20–23, Theorem 47 **II**: thm_10 (L131), thm_11 (L142) **III**: thm_41 (L264), thm_44 (L316)
98	DirichletL/Detector/HighRows Tail.lean (L50-L76)	theorem	rowInner_base_rational	**I**: Theorems 20–23, Theorem 47 **II**: thm_10 (L131), thm_11 (L142) **III**: thm_41 (L264), thm_44 (L316)
99	DirichletL/Detector/HighRows Unramified.lean (L13-L20)	lemma	rowMarkedTerm_unramified	**I**: Theorem 46 **II**: thm_19 (L236), thm_26 (L340) **III**: thm_07 (L132), thm_39 (L232)
100	DirichletL/Detector/HighRows Unramified.lean (L21-L35)	lemma	rowMarkedSeries_ unramified	**I**: Theorem 46 **II**: thm_19 (L236), thm_26 (L340) **III**: thm_07 (L132), thm_39 (L232)

#	Upstream OpenAI #003 File (oai_ref/) & Lines	Kind	Declaration Identifier	Mapped Audit Theorems (Part I / Part II / Part III)
101	DirichletL/Detector/HighRows Unramified.lean (L36-L53)	lemma	rowClosedMarked_ unramified	**I**: Theorem 46 **II**: thm_19 (L236), thm_26 (L340) **III**: thm_07 (L132), thm_39 (L232)
102	DirichletL/Detector/HighRows Unramified.lean (L54-L90)	theorem	sourceRowSeries_ unramified_euler	**I**: Theorem 46 **II**: thm_19 (L236), thm_26 (L340) **III**: thm_07 (L132), thm_39 (L232)
103	SiegelZeros/Intersection/ IsolatedBezoutFromRegular Selection.lean (L25-L48)	def	LocalIsolatedBezout Statement	**I**: Theorem 41 **II**: thm_23 (L278), thm_25 (L314) **III**: thm_28 (L268), thm_30 (L308), thm_45 (L338)
104	SiegelZeros/Intersection/ IsolatedBezoutFromRegular Selection.lean (L49-L103)	theorem	local_length_le_of_local_ isolated_bezout	**I**: Theorem 41 **II**: thm_23 (L278), thm_25 (L314) **III**: thm_28 (L268), thm_30 (L308), thm_45 (L338)
105	SiegelZeros/Intersection/ IsolatedBezoutFromRegular Selection.lean (L104-L127)	theorem	quotient_length_eq_of_ ringEquiv	**I**: Theorem 41 **II**: thm_23 (L278), thm_25 (L314) **III**: thm_28 (L268), thm_30 (L308), thm_45 (L338)
106	SiegelZeros/Intersection/ IsolatedBezoutFromRegular Selection.lean (L128-L129; instance polynomialComponent Prime_isPrime at L131-L132)	def	polynomialComponentPrime	**I**: Theorem 41 **II**: thm_23 (L278), thm_25 (L314) **III**: thm_28 (L268), thm_30 (L308), thm_45 (L338)
107	SiegelZeros/Intersection/ IsolatedBezoutFromRegular Selection.lean (L134-L141)	theorem	polynomialComponentPrime_ mem_minimalPrimes	**I**: Theorem 41 **II**: thm_23 (L278), thm_25 (L314) **III**: thm_28 (L268), thm_30 (L308), thm_45 (L338)
108	SiegelZeros/Intersection/ IsolatedBezoutFromRegular Selection.lean (L142-L145)	theorem	polynomialComponentPrime_ height	**I**: Theorem 41 **II**: thm_23 (L278), thm_25 (L314) **III**: thm_28 (L268), thm_30 (L308), thm_45 (L338)
109	SiegelZeros/Intersection/ IsolatedBezoutFromRegular Selection.lean (L146-L150)	def	polynomialTorusLocalEquiv	**I**: Theorem 41 **II**: thm_23 (L278), thm_25 (L314) **III**: thm_28 (L268), thm_30 (L308), thm_45 (L338)
110	SiegelZeros/Intersection/ IsolatedBezoutFromRegular Selection.lean (L152-L157)	theorem	polynomialTorusLocal Equiv_algebraMap	**I**: Theorem 41 **II**: private helper (audited in Part I) **III**: private helper (audited in Part I)
111	SiegelZeros/Intersection/ IsolatedBezoutFromRegular Selection.lean (L159-L174)	theorem	torus_localized_ideal_eq_ map_polynomial_localized	**I**: Theorem 41 **II**: thm_23 (L278), thm_25 (L314) **III**: thm_28 (L268), thm_30 (L308), thm_45 (L338)
112	SiegelZeros/Intersection/ IsolatedBezoutFromRegular Selection.lean (L175-L185)	def	polynomialTorusLocal QuotientEquiv	**I**: Theorem 41 **II**: thm_23 (L278), thm_25 (L314) **III**: thm_28 (L268), thm_30 (L308), thm_45 (L338)
113	SiegelZeros/Intersection/ IsolatedBezoutFromRegular Selection.lean (L186-L208)	theorem	polynomial_torus_local_ quotient_length_eq	**I**: Theorem 41 **II**: thm_23 (L278), thm_25 (L314) **III**: thm_28 (L268), thm_30 (L308), thm_45 (L338)
114	SiegelZeros/Intersection/ IsolatedBezoutFromRegular Selection.lean (L209-L246)	theorem	torus_local_length_le_of_ local_isolated_bezout	**I**: Theorem 41 **II**: thm_23 (L278), thm_25 (L314) **III**: thm_28 (L268), thm_30 (L308), thm_45 (L338)

#	Upstream OpenAI #003 File (oai_ref/) & Lines	Kind	Declaration Identifier	Mapped Audit Theorems (Part I / Part II / Part III)
115	SiegelZeros/Intersection/IsolatedBezoutFromRegularSelection.lean (L247-L252)	theorem	span_range_list_get	**I**: Theorem 41 **II**: thm_23 (L278), thm_25 (L314) **III**: thm_28 (L268), thm_30 (L308), thm_45 (L338)
116	SiegelZeros/Intersection/IsolatedBezoutFromRegularSelection.lean (L253-L266)	theorem	span_range_map_list_get	**I**: Theorem 41 **II**: thm_23 (L278), thm_25 (L314) **III**: thm_28 (L268), thm_30 (L308), thm_45 (L338)
117	SiegelZeros/Intersection/IsolatedBezoutFromRegularSelection.lean (L267-L286)	theorem	finiteLength_localized_minimal_quotient	**I**: Theorem 41 **II**: thm_23 (L278), thm_25 (L314) **III**: thm_28 (L268), thm_30 (L308), thm_45 (L338)
118	SiegelZeros/Intersection/IsolatedBezoutFromRegularSelection.lean (L287-L345)	theorem	affine_local_regular_list_bezout	**I**: Theorem 41 **II**: thm_23 (L278), thm_25 (L314) **III**: thm_28 (L268), thm_30 (L308), thm_45 (L338)
119	SiegelZeros/Intersection/IsolatedBezoutFromRegularSelection.lean (L346-L373)	theorem	localIsolatedBezout_of_actual_regular_selection	**I**: Theorem 41 **II**: thm_23 (L278), thm_25 (L314) **III**: thm_28 (L268), thm_30 (L308), thm_45 (L338)
120	DirichletL/Detector/Local.lean (L11-L12)	def	localFactor	**I**: Theorem 28, Theorem 31, Theorem 44 **II**: thm_07 (L96), thm_09 (L120), thm_38 (L486), thm_40 (L38) **III**: thm_07 (L132), thm_39 (L232), thm_40 (L249)
121	DirichletL/Detector/Local.lean (L13-L15)	def	localCorrection	**I**: Theorem 28, Theorem 31, Theorem 44 **II**: thm_07 (L96), thm_09 (L120), thm_38 (L486), thm_40 (L38) **III**: thm_07 (L132), thm_39 (L232), thm_40 (L249)
122	DirichletL/Detector/Local.lean (L16-L18)	def	continuedCorrection	**I**: Theorem 28, Theorem 31, Theorem 44 **II**: thm_07 (L96), thm_09 (L120), thm_38 (L486), thm_40 (L38) **III**: thm_07 (L132), thm_39 (L232), thm_40 (L249)
123	DirichletL/Detector/Local.lean (L19-L25)	theorem	continuedCorrection_eq_raw	**I**: Theorem 28, Theorem 31, Theorem 44 **II**: thm_07 (L96), thm_09 (L120), thm_38 (L486), thm_40 (L38) **III**: thm_07 (L132), thm_39 (L232), thm_40 (L249)
124	DirichletL/Detector/Local.lean (L26-L28)	def	compensatedReplacement	**I**: Theorem 28, Theorem 31, Theorem 44 **II**: thm_07 (L96), thm_09 (L120), thm_38 (L486), thm_40 (L38) **III**: thm_07 (L132), thm_39 (L232), thm_40 (L249)
125	DirichletL/Detector/Local.lean (L29-L37)	theorem	correction_defect	**I**: Theorem 28, Theorem 31, Theorem 44 **II**: thm_07 (L96), thm_09 (L120), thm_38 (L486), thm_40 (L38) **III**: thm_07 (L132), thm_39 (L232), thm_40 (L249)

#	Upstream OpenAI #003 File (oai_ref/) & Lines	Kind	Declaration Identifier	Mapped Audit Theorems (Part I / Part II / Part III)
126	DirichletL/Detector/Local.lean (L38-L48)	theorem	compensatedReplacement_eq_raw	**I**: Theorem 28, Theorem 31, Theorem 44 **II**: thm_07 (L96), thm_09 (L120), thm_38 (L486), thm_40 (L38) **III**: thm_07 (L132), thm_39 (L232), thm_40 (L249)
127	DirichletL/Detector/Local.lean (L49-L55)	theorem	compensatedReplacement_ramified	**I**: Theorem 28, Theorem 31, Theorem 44 **II**: thm_07 (L96), thm_09 (L120), thm_38 (L486), thm_40 (L38) **III**: thm_07 (L132), thm_39 (L232), thm_40 (L249)
128	DirichletL/Detector/Local.lean (L56-L67)	theorem	normalized_cancellation	**I**: Theorem 28, Theorem 31, Theorem 44 **II**: thm_07 (L96), thm_09 (L120), thm_38 (L486), thm_40 (L38) **III**: thm_07 (L132), thm_39 (L232), thm_40 (L249)
129	DirichletL/Detector/Local.lean (L68-L75)	theorem	continuedCorrection_defect	**I**: Theorem 28, Theorem 31, Theorem 44 **II**: thm_07 (L96), thm_09 (L120), thm_38 (L486), thm_40 (L38) **III**: thm_07 (L132), thm_39 (L232), thm_40 (L249)
130	DirichletL/Detector/Local.lean (L76-L87)	theorem	continued_normalized_cancellation	**I**: Theorem 28, Theorem 31, Theorem 44 **II**: thm_07 (L96), thm_09 (L120), thm_38 (L486), thm_40 (L38) **III**: thm_07 (L132), thm_39 (L232), thm_40 (L249)
131	DirichletL/Detector/Local.lean (L88-L98)	theorem	continued_ramified_compensation	**I**: Theorem 28, Theorem 31, Theorem 44 **II**: thm_07 (L96), thm_09 (L120), thm_38 (L486), thm_40 (L38) **III**: thm_07 (L132), thm_39 (L232), thm_40 (L249)
132	DirichletL/Detector/LowGramScale.lean (L8-L11)	lemma	compensated_gram_ratio	**I**: Theorem 18, Theorem 24, Theorem 35 **II**: thm_03 (L40), thm_28 (L368), thm_33 (L431), thm_39 (L21), thm_44 (L122), thm_46 (L156) **III**: thm_09 (L173), thm_15 (L297), thm_20 (L103), thm_27 (L252), thm_38 (L212)
133	DirichletL/Detector/LowGramScale.lean (L12-L36)	lemma	compensated_gram_scale_bound	**I**: Theorem 18, Theorem 24, Theorem 35 **II**: thm_03 (L40), thm_28 (L368), thm_33 (L431), thm_39 (L21), thm_44 (L122), thm_46 (L156) **III**: thm_09 (L173), thm_15 (L297), thm_20 (L103), thm_27 (L252), thm_38 (L212)
134	DirichletL/Detector/LowGramScale.lean (L37-L43)	lemma	source_gram_power	**I**: Theorem 18, Theorem 24, Theorem 35 **II**: thm_03 (L40), thm_28 (L368), thm_33 (L431), thm_39 (L21), thm_44 (L122), thm_46 (L156) **III**: thm_09 (L173), thm_15 (L297), thm_20 (L103), thm_27 (L252), thm_38 (L212)

#	Upstream OpenAI #003 File (oai_ref/) & Lines	Kind	Declaration Identifier	Mapped Audit Theorems (Part I / Part II / Part III)
135	DirichletL/Detector/LowGramScale.lean (L44-L53)	lemma	source_gram_sqrt_power	**I**: Theorem 18, Theorem 24, Theorem 35 **II**: thm_03 (L40), thm_28 (L368), thm_33 (L431), thm_39 (L21), thm_44 (L122), thm_46 (L156) **III**: thm_09 (L173), thm_15 (L297), thm_20 (L103), thm_27 (L252), thm_38 (L212)
136	DirichletL/Detector/LowSourceScales.lean (L10-L14)	lemma	source_scale_ratio	**I**: Theorem 24, Theorems 35–38 **II**: thm_01 (L16), thm_02 (L27), thm_39 (L21) **III**: thm_04 (L76), thm_17 (L49), thm_36 (L167), thm_37 (L185)
137	DirichletL/Detector/LowSourceScales.lean (L15-L19)	lemma	source_scale_square	**I**: Theorem 24, Theorems 35–38 **II**: thm_01 (L16), thm_02 (L27), thm_39 (L21) **III**: thm_04 (L76), thm_17 (L49), thm_36 (L167), thm_37 (L185)
138	DirichletL/Detector/LowSourceScales.lean (L20-L37)	lemma	source_compensated_scale_admissible	**I**: Theorem 24, Theorems 35–38 **II**: thm_01 (L16), thm_02 (L27), thm_39 (L21) **III**: thm_04 (L76), thm_17 (L49), thm_36 (L167), thm_37 (L185)
139	DirichletL/Detector/LowSourceScales.lean (L38-L61)	lemma	source_compensated_gram_scale	**I**: Theorem 24, Theorems 35–38 **II**: thm_01 (L16), thm_02 (L27), thm_39 (L21) **III**: thm_04 (L76), thm_17 (L49), thm_36 (L167), thm_37 (L185)
140	DirichletL/Detector/LowSourceScales.lean (L62-L71)	lemma	source_compensated_gram_sqrt	**I**: Theorem 24, Theorems 35–38 **II**: thm_01 (L16), thm_02 (L27), thm_39 (L21) **III**: thm_04 (L76), thm_17 (L49), thm_36 (L167), thm_37 (L185)
141	DirichletL/Detector/LowSourceScales.lean (L72-L78)	lemma	lowGramFactor_source_bound	**I**: Theorem 24, Theorems 35–38 **II**: thm_01 (L16), thm_02 (L27), thm_39 (L21) **III**: thm_04 (L76), thm_17 (L49), thm_36 (L167), thm_37 (L185)
142	DirichletL/Detector/LowSourceScales.lean (L79-L108)	lemma	eventually_compensated_source_scales	**I**: Theorem 24, Theorems 35–38 **II**: thm_01 (L16), thm_02 (L27), thm_39 (L21) **III**: thm_04 (L76), thm_17 (L49), thm_36 (L167), thm_37 (L185)
143	DirichletL/Parameters.lean (L12-L27)	theorem	compensated_geometry	**I**: Theorem 36, Theorem 48 **II**: thm_01 (L16), thm_05 (L65), thm_15 (L190), thm_33 (L431), thm_39 (L21) **III**: thm_17 (L49), thm_18 (L67), thm_19 (L85), thm_20 (L103), thm_35 (L144), thm_37 (L185)
144	DirichletL/Parameters.lean (L28-L42)	theorem	exists_height_cutoff	**I**: Theorem 36, Theorem 48 **II**: thm_01 (L16), thm_05 (L65), thm_15 (L190), thm_33 (L431), thm_39 (L21) **III**: thm_17 (L49), thm_18 (L67), thm_19 (L85), thm_20 (L103), thm_35 (L144), thm_37 (L185)
145	DirichletL/Parameters.lean (L43-L48)	theorem	exists_tail_order	**I**: Theorem 36, Theorem 48 **II**: thm_01 (L16), thm_05 (L65), thm_15 (L190), thm_33 (L431), thm_39 (L21) **III**: thm_17 (L49), thm_18 (L67), thm_19 (L85), thm_20 (L103), thm_35 (L144), thm_37 (L185)

#	Upstream OpenAI #003 File (oai_ref/) & Lines	Kind	Declaration Identifier	Mapped Audit Theorems (Part I / Part II / Part III)
146	DirichletL/Parameters.lean (L49-L66)	theorem	cumulative_frequency_bound	**I**: Theorem 36, Theorem 48 **II**: thm_01 (L16), thm_05 (L65), thm_15 (L190), thm_33 (L431), thm_39 (L21) **III**: thm_17 (L49), thm_18 (L67), thm_19 (L85), thm_20 (L103), thm_35 (L144), thm_37 (L185)
147	DirichletL/ParametersHighData.lean (L9-L51)	structure	HighData	**I**: Theorem 14, Theorem 19, Theorem 48 **II**: thm_17 (L210), thm_18 (L221), thm_31 (L400), thm_42 (L77) **III**: thm_24 (L187), thm_28 (L268), thm_44 (L316)
148	DirichletL/ParametersHighData.lean (L52-L114)	theorem	exists_high_data	**I**: Theorem 14, Theorem 19, Theorem 48 **II**: thm_17 (L210), thm_18 (L221), thm_31 (L400), thm_42 (L77) **III**: thm_24 (L187), thm_28 (L268), thm_44 (L316)
149	SiegelZeros/Selection/PivotBounds.lean (L17-L96)	theorem	source_pivot_bounds	**I**: Theorem 15, Theorem 43 **II**: thm_21 (L257), thm_22 (L268), thm_26 (L340) **III**: thm_28 (L268), thm_30 (L308), thm_45 (L338)
150	DirichletL/Detector/PrincipalRemainderBounds.lean (L16-L60)	lemma	active_prime_sum_bound	**I**: Theorem 18, Theorem 19, Theorem 39 **II**: thm_14 (L178), thm_33 (L431), thm_36 (L464), thm_37 (L475), thm_38 (L486), thm_41 (L58), thm_45 (L141) **III**: thm_05 (L98), thm_22 (L145), thm_26 (L234), thm_41 (L264)
151	DirichletL/Detector/PrincipalRemainderBounds.lean (L61-L63)	def	slotConstant	**I**: Theorem 18, Theorem 19, Theorem 39 **II**: thm_14 (L178), thm_33 (L431), thm_36 (L464), thm_37 (L475), thm_38 (L486), thm_41 (L58), thm_45 (L141) **III**: thm_05 (L98), thm_22 (L145), thm_26 (L234), thm_41 (L264)
152	DirichletL/Detector/PrincipalRemainderBounds.lean (L64-L70)	lemma	slotConstant_nonneg	**I**: Theorem 18, Theorem 19, Theorem 39 **II**: thm_14 (L178), thm_33 (L431), thm_36 (L464), thm_37 (L475), thm_38 (L486), thm_41 (L58), thm_45 (L141) **III**: thm_05 (L98), thm_22 (L145), thm_26 (L234), thm_41 (L264)
153	DirichletL/Detector/PrincipalRemainderBounds.lean (L71-L118)	theorem	window_sharp_bound	**I**: Theorem 18, Theorem 19, Theorem 39 **II**: thm_14 (L178), thm_33 (L431), thm_36 (L464), thm_37 (L475), thm_38 (L486), thm_41 (L58), thm_45 (L141) **III**: thm_05 (L98), thm_22 (L145), thm_26 (L234), thm_41 (L264)
154	DirichletL/Detector/PrincipalRemainderBounds.lean (L119-L121)	def	scalePower	**I**: Theorem 18, Theorem 19, Theorem 39 **II**: thm_14 (L178), thm_33 (L431), thm_36 (L464), thm_37 (L475), thm_38 (L486), thm_41 (L58), thm_45 (L141) **III**: thm_05 (L98), thm_22 (L145), thm_26 (L234), thm_41 (L264)

#	Upstream OpenAI #003 File (oai_ref/) & Lines	Kind	Declaration Identifier	Mapped Audit Theorems (Part I / Part II / Part III)
155	DirichletL/Detector/PrincipalRemainderBounds.lean (L122-L137)	lemma	scalePower_nonneg	**I**: Theorem 18, Theorem 19, Theorem 39 **II**: thm_14 (L178), thm_33 (L431), thm_36 (L464), thm_37 (L475), thm_38 (L486), thm_41 (L58), thm_45 (L141) **III**: thm_05 (L98), thm_22 (L145), thm_26 (L234), thm_41 (L264)
156	DirichletL/Detector/PrincipalRemainderBounds.lean (L138-L176)	lemma	continued_source_sharp_pointwise	**I**: Theorem 18, Theorem 19, Theorem 39 **II**: thm_14 (L178), thm_33 (L431), thm_36 (L464), thm_37 (L475), thm_38 (L486), thm_41 (L58), thm_45 (L141) **III**: thm_05 (L98), thm_22 (L145), thm_26 (L234), thm_41 (L264)
157	DirichletL/Detector/PrincipalRemainderBounds.lean (L177-L216)	lemma	full_sharp_pointwise	**I**: Theorem 18, Theorem 19, Theorem 39 **II**: thm_14 (L178), thm_33 (L431), thm_36 (L464), thm_37 (L475), thm_38 (L486), thm_41 (L58), thm_45 (L141) **III**: thm_05 (L98), thm_22 (L145), thm_26 (L234), thm_41 (L264)
158	DirichletL/Detector/PrincipalRemainderBounds.lean (L217-L247)	lemma	residue_sharp_pointwise	**I**: Theorem 18, Theorem 19, Theorem 39 **II**: thm_14 (L178), thm_33 (L431), thm_36 (L464), thm_37 (L475), thm_38 (L486), thm_41 (L58), thm_45 (L141) **III**: thm_05 (L98), thm_22 (L145), thm_26 (L234), thm_41 (L264)
159	DirichletL/Detector/PrincipalRemainderBounds.lean (L248-L257)	lemma	vertical_triple_eq_joint	**I**: Theorem 18, Theorem 19, Theorem 39 **II**: thm_14 (L178), thm_33 (L431), thm_36 (L464), thm_37 (L475), thm_38 (L486), thm_41 (L58), thm_45 (L141) **III**: thm_05 (L98), thm_22 (L145), thm_26 (L234), thm_41 (L264)
160	DirichletL/Detector/PrincipalRemainderBounds.lean (L258-L266)	lemma	vertical_pair_eq_joint	**I**: Theorem 18, Theorem 19, Theorem 39 **II**: thm_14 (L178), thm_33 (L431), thm_36 (L464), thm_37 (L475), thm_38 (L486), thm_41 (L58), thm_45 (L141) **III**: thm_05 (L98), thm_22 (L145), thm_26 (L234), thm_41 (L264)
161	DirichletL/Detector/PrincipalRemainderBounds.lean (L267-L279)	lemma	normalizer_norm_pos	**I**: Theorem 18, Theorem 19, Theorem 39 **II**: thm_14 (L178), thm_33 (L431), thm_36 (L464), thm_37 (L475), thm_38 (L486), thm_41 (L58), thm_45 (L141) **III**: thm_05 (L98), thm_22 (L145), thm_26 (L234), thm_41 (L264)
162	DirichletL/Detector/PrincipalRemainderBounds.lean (L280-L334)	theorem	full_scale_bound	**I**: Theorem 18, Theorem 19, Theorem 39 **II**: thm_14 (L178), thm_33 (L431), thm_36 (L464), thm_37 (L475), thm_38 (L486), thm_41 (L58), thm_45 (L141) **III**: thm_05 (L98), thm_22 (L145), thm_26 (L234), thm_41 (L264)

#	Upstream OpenAI #003 File (oai_ref/) & Lines	Kind	Declaration Identifier	Mapped Audit Theorems (Part I / Part II / Part III)
163	DirichletL/Detector/PrincipalRemainderBounds.lean (L335-L396)	theorem	residue_scale_bound	**I**: Theorem 18, Theorem 19, Theorem 39 **II**: thm_14 (L178), thm_33 (L431), thm_36 (L464), thm_37 (L475), thm_38 (L486), thm_41 (L58), thm_45 (L141) **III**: thm_05 (L98), thm_22 (L145), thm_26 (L234), thm_41 (L264)
164	DirichletL/Detector/PrincipalRemainderBounds.lean (L397-L431)	theorem	full_vertical_scale_bound	**I**: Theorem 18, Theorem 19, Theorem 39 **II**: thm_14 (L178), thm_33 (L431), thm_36 (L464), thm_37 (L475), thm_38 (L486), thm_41 (L58), thm_45 (L141) **III**: thm_05 (L98), thm_22 (L145), thm_26 (L234), thm_41 (L264)
165	DirichletL/Detector/PrincipalRemainderBounds.lean (L432-L467)	theorem	residue_vertical_scale_bound	**I**: Theorem 18, Theorem 19, Theorem 39 **II**: thm_14 (L178), thm_33 (L431), thm_36 (L464), thm_37 (L475), thm_38 (L486), thm_41 (L58), thm_45 (L141) **III**: thm_05 (L98), thm_22 (L145), thm_26 (L234), thm_41 (L264)
166	DirichletL/Detector/PrincipalRemainderBounds.lean (L468-L517)	theorem	ordered_remainders_scale_bound	**I**: Theorem 18, Theorem 19, Theorem 39 **II**: thm_14 (L178), thm_33 (L431), thm_36 (L464), thm_37 (L475), thm_38 (L486), thm_41 (L58), thm_45 (L141) **III**: thm_05 (L98), thm_22 (L145), thm_26 (L234), thm_41 (L264)
167	DirichletL/Detector/PrincipalRemainderBounds.lean (L518-L530)	lemma	source_scale_identity	**I**: Theorem 18, Theorem 19, Theorem 39 **II**: thm_14 (L178), thm_33 (L431), thm_36 (L464), thm_37 (L475), thm_38 (L486), thm_41 (L58), thm_45 (L141) **III**: thm_05 (L98), thm_22 (L145), thm_26 (L234), thm_41 (L264)
168	DirichletL/Detector/PrincipalRemainderBounds.lean (L531-L537)	lemma	source_w_scale_identity	**I**: Theorem 18, Theorem 19, Theorem 39 **II**: thm_14 (L178), thm_33 (L431), thm_36 (L464), thm_37 (L475), thm_38 (L486), thm_41 (L58), thm_45 (L141) **III**: thm_05 (L98), thm_22 (L145), thm_26 (L234), thm_41 (L264)
169	DirichletL/Detector/PrincipalRemainderBounds.lean (L538-L544)	lemma	source_z_scale_identity	**I**: Theorem 18, Theorem 19, Theorem 39 **II**: thm_14 (L178), thm_33 (L431), thm_36 (L464), thm_37 (L475), thm_38 (L486), thm_41 (L58), thm_45 (L141) **III**: thm_05 (L98), thm_22 (L145), thm_26 (L234), thm_41 (L264)
170	DirichletL/Detector/PrincipalRemainderBounds.lean (L545-L560)	lemma	eventual_annulus_threshold	**I**: Theorem 18, Theorem 19, Theorem 39 **II**: thm_14 (L178), thm_33 (L431), thm_36 (L464), thm_37 (L475), thm_38 (L486), thm_41 (L58), thm_45 (L141) **III**: thm_05 (L98), thm_22 (L145), thm_26 (L234), thm_41 (L264)

#	Upstream OpenAI #003 File (oai_ref/) & Lines	Kind	Declaration Identifier	Mapped Audit Theorems (Part I / Part II / Part III)
171	DirichletL/Detector/PrincipalRemainderBounds.lean (L561-L593)	theorem	source_remainders_power_bound	**I**: Theorem 18, Theorem 19, Theorem 39 **II**: thm_14 (L178), thm_33 (L431), thm_36 (L464), thm_37 (L475), thm_38 (L486), thm_41 (L58), thm_45 (L141) **III**: thm_05 (L98), thm_22 (L145), thm_26 (L234), thm_41 (L264)
172	DirichletL/Detector/PrincipalRemainderBounds.lean (L594-L596)	lemma	source_w_strict_exponent	**I**: Theorem 18, Theorem 19, Theorem 39 **II**: thm_14 (L178), thm_33 (L431), thm_36 (L464), thm_37 (L475), thm_38 (L486), thm_41 (L58), thm_45 (L141) **III**: thm_05 (L98), thm_22 (L145), thm_26 (L234), thm_41 (L264)
173	DirichletL/Detector/PrincipalRemainderBounds.lean (L597-L599)	lemma	source_z_strict_exponent	**I**: Theorem 18, Theorem 19, Theorem 39 **II**: thm_14 (L178), thm_33 (L431), thm_36 (L464), thm_37 (L475), thm_38 (L486), thm_41 (L58), thm_45 (L141) **III**: thm_05 (L98), thm_22 (L145), thm_26 (L234), thm_41 (L264)
174	DirichletL/Detector/PrincipalRemainderBounds.lean (L600-L640)	theorem	source_remainders_strict_saving	**I**: Theorem 18, Theorem 19, Theorem 39 **II**: thm_14 (L178), thm_33 (L431), thm_36 (L464), thm_37 (L475), thm_38 (L486), thm_41 (L58), thm_45 (L141) **III**: thm_05 (L98), thm_22 (L145), thm_26 (L234), thm_41 (L264)
175	DirichletL/Detector/ScalarTable.lean (L11-L14)	def	gaussValuationTable	**I**: Theorem 21, Theorem 47 **II**: thm_10 (L131), thm_11 (L142) **III**: thm_14 (L278), thm_41 (L264)
176	DirichletL/Detector/ScalarTable.lean (L15-L23)	theorem	actualSextic_gaussValuationTable	**I**: Theorem 21, Theorem 47 **II**: thm_10 (L131), thm_11 (L142) **III**: thm_14 (L278), thm_41 (L264)
177	DirichletL/Detector/ScalarTable.lean (L24-L49)	theorem	positiveScalar_actual_table	**I**: Theorem 21, Theorem 47 **II**: thm_10 (L131), thm_11 (L142) **III**: thm_14 (L278), thm_41 (L264)
178	DirichletL/Detector/ScalarTable.lean (L50-L64)	theorem	zero_index_scalar	**I**: Theorem 21, Theorem 47 **II**: thm_10 (L131), thm_11 (L142) **III**: thm_14 (L278), thm_41 (L264)
179	SiegelZeros/Conclusions/Theorem.lean (L11-L27)	theorem	exists_absolute_real_zero_gap	**I**: Theorem 16, Theorem 26, Theorem 43 **II**: thm_23 (L278), thm_24 (L288), thm_25 (L314), thm_43 (L97) **III**: thm_28 (L268), thm_29 (L290), thm_30 (L308), thm_43 (L299), thm_44 (L316), thm_45 (L338)

B Consolidated Cryptographic SHA-256 Manifest of the 13 Companion `Lean 4` Proof Modules

Table 19 records the exact cryptographic SHA-256 digests of all 13 standalone zero-`sorry Lean 4` modules (216 theorems, 1,022/1,022 killed hypothesis mutations) permanently archived in `ultari-proof-anatomy` (`doi:10.5281/zenodo.24437646`, Concept DOI `10.5281/zenodo.24241228`) [6].

Table 19: Consolidated cryptographic SHA-256 manifest of all 13 companion zero-`sorry Lean 4` proof modules (216 theorems).

Monograph Part	**Companion Lean 4 Module (`anatomy/...` in `doi:10.5281/zenodo.24437646`)**	**Thms**	**SHA-256 Digest**
Part I (Case 001)	`001-openai-003-qrh/proofs/qrh_continuation_and_rescaling.lean`	21	`7d64b243421117960431dc4e2ac86e4b3d086fae87af55746673e298976fa1e3`
Part I (Case 001)	`001-openai-003-qrh/proofs/qrh_exponent_and_parameter_bounds.lean`	27	`2e98aff37741ab5ae4b67c9e36da3816e09325c40d0abcf462a676e0e2ec6ae1`
Part II (Case 005)	`005-openai-003-qrh-mathematician-referee-audit/proofs/qrh_eight_tasks_critical_upgrade.lean`	10	`6ef57ba419b51e1905b3549077e314ed7605e3b40c43c146e9df567c1aefb9ef`
Part II (Case 005)	`005-openai-003-qrh-mathematician-referee-audit/proofs/qrh_mathematician_referee_audit.lean`	38	`922295600d2d133949cd47158f23e3c40a65a4aee9e2e19ea67ce80243c760e6`
Part III (Case 008)	`008-openai-003-qrh-11-12-and-cubic-sieve-synthesis/proofs/qrh_eleven_twelfths_and_cubic_large_sieve.lean`	15	`db8865fae7d724f17f28f803d4df09157767e3068eca7c64b0e70dfaae41a029`
Part III (Case 008)	`008-openai-003-qrh-11-12-and-cubic-sieve-synthesis/proofs/qrh_q_sqrt_921_farkas_and_unbundling_synthesis.lean`	15	`e8cd0d389dd1c111ad5d46dfac34ef2aa8234eaeafd939defe9cc02506d2f750`
Part III (Case 008)	`008-openai-003-qrh-11-12-and-cubic-sieve-synthesis/proofs/qrh_trilogy_induction_and_algebraic_bridge.lean`	15	`d6ee86e9b16f2ab31332fc0c655affe055b6ba9f3539f16a46bf66d8983ccc68`
Part IV (Case 015)	`015-classical-riemann-five-barriers/proofs/classical_burgess_and_kim_sarnak_barrier.lean`	12	`776e09813a00b76adaa702a1905b0bec3c7c83d94959021447682fd9d8f9c0e1`
Part IV (Case 015)	`015-classical-riemann-five-barriers/proofs/classical_dlvp_korobov_and_zero_free.lean`	15	`2a92e463b1b09c54bfd7981ccf5dff3619daae33fd178da0e52563726d58f341`
Part IV (Case 015)	`015-classical-riemann-five-barriers/proofs/classical_guth_maynard_and_qrh_gram.lean`	10	`fbd5c524ed2283a65763c1d6e4a83f09320f969f01ccf967ff96d2a9761494a3`
Part IV (Case 015)	`015-classical-riemann-five-barriers/proofs/classical_ingham_huxley_zero_density.lean`	10	`21dc3cf43f73fb819b42e5411d4905d2dc54f8477f64ac62c3d6491ee434b140`
Part IV (Case 015)	`015-classical-riemann-five-barriers/proofs/classical_levinson_conrey_and_mollifier_barrier.lean`	13	`3d065f7dc823c42c261932e4423714b9d85b3bef79e12db9bba189ba731faff5`
Part IV (Case 015)	`015-classical-riemann-five-barriers/proofs/classical_siegel_zero_and_ineffectiveness.lean`	15	`8e78df0cb546216bfaba0d362de06cb1735f4ecae50e1356b5510cfb361b1f9d`

References

[1] OpenAI, *Formalization of the Quasi-Riemann Hypothesis (*$\mathrm{Re}(s) > 7/8$*) and Siegel Zero Exclusion for Dirichlet and Hecke L-Functions in Lean 4* (`openai/math`, Family `#003`, commit `4eaee87`; `lean/OAI/NumberTheory/DirichletL/`, `SiegelZeros/`, and `CubicGauss/`), October 2026.

[2] L. Alpöge, *Formal proof of the Riemann hypothesis and Dirichlet generalized Riemann hypothesis in Lean 4* (`lean.tar.gz`, 175,187 files, 17,374,215 lines, `leanprover/lean4:v4.33.1`, `mathlib4` commit `0df444a360eaa60ab8c11dca51a86af692955474`), 20 November 2026.

[3] L. Alpöge, *Author's accompanying note on the Riemann hypothesis formalization* (`remark.pdf`, twenty chronological research-diary steps dated 6 October–16 November 2026), 20 November 2026.

[4] M. Jaswal, *The Riemann hypothesis for Dirichlet L-functions [after Levent Alpöge]*, Hexagon preprint `hexagon:2611.00799v1` (Zenodo `doi:10.5281/zenodo.24410057`), 21 November 2026.

[5] G. Park, *Full-Archive AST Stratification, Pinned `Mathlib` Boundary Audit, and Deep Hub Decompilation of the 17.37M-Line Alpöge–Claude Riemann Hypothesis Formalization*, Hexagon preprint `hexagon:2611.00881`, 22 November 2026.

[6] G. Park, *Ultari Proof Anatomy (v1.1.0): 216-Theorem Standalone Zero-`sorry` Lean 4 Audit Suite for OpenAI `#003` QRH Trilogy (`Cases 001, 005, 008`), the Five Classical Riemann Barriers (`Case 015`), and the Alpöge–Claude AST Atlas*, CERN Zenodo, `doi:10.5281/zenodo.24437646`, November 2026.

[7] A. Kontorovich et al., *`PrimeNumberTheoremAnd`, `quasi-rh`, and `oai-math-revised` (`PR #70`, commit `ca28f20`): Standalone Lean 4 formalizations of Wiener–Ikehara and community* 11/12 */ wrapper refactorings*, GitHub repositories `AlexKontorovich/PrimeNumberTheoremAnd` and `AlexKontorovich/quasi-rh`, 2024–2026.

[8] B. Liu, *Improved zero-free half-planes for the quasi-Riemann hypothesis* (`v1`: *Slightly improved zero-free half-planes for the quasi-Riemann hypothesis*), unrefereed preprint, `arXiv:2610.12234`, October 2026.

[9] Y. Xu and H. Sang, *Amplified moments and a refinement of the quasi-Riemann hypothesis*, unrefereed preprint, `arXiv:2610.15291`, October 2026.

[10] C.-J. de la Vallée Poussin, *Recherches analytiques sur la théorie des nombres premiers*, Ann. Soc. Sci. Bruxelles **20** (1896), 183–256.

[11] C. L. Siegel, *Über die Classenzahl quadratischer Zahlkörper*, Acta Arith. **1** (1935), 83–86.

[12] A. E. Ingham, *On the estimation of* $N(\sigma, T)$, Quart. J. Math. Oxford **11** (1940), 291–298.

[13] A. Selberg, *On the zeros of Riemann's zeta-function*, Skr. Norske Vid.-Akad. Oslo I **10** (1942), 1–59.

[14] N. M. Korobov, *Estimates of trigonometric sums and their applications*, Uspekhi Mat. Nauk **13** (1958), 185–192; I. M. Vinogradov, *A new estimate of the function* $\zeta(1+it)$, Izv. Akad. Nauk SSSR Ser. Mat. **22** (1958), 161–164.

[15] D. A. Burgess, *On character sums and L-series. II*, Proc. London Math. Soc. (3) **13** (1963), 524–536.

[16] A. Selberg, *On the estimation of Fourier coefficients of modular forms*, Proc. Sympos. Pure Math., vol. 8, Amer. Math. Soc., 1965, 1–15.

[17] M. N. Huxley, *On the difference between consecutive primes*, Invent. Math. **15** (1972), 164–170.

[18] N. Levinson, *More than one third of zeros of Riemann's zeta-function are on* $\sigma = 1/2$, Adv. Math. **13** (1974), 383–436.

[19] J.-M. Deshouillers and H. Iwaniec, *Kloosterman sums and Fourier coefficients of cusp forms*, Invent. Math. **70** (1982), 219–288.

[20] D. Goldfeld, *Gauss's class number problem for imaginary quadratic fields*, Bull. Amer. Math. Soc. **13** (1985), 23–37; B. H. Gross and D. B. Zagier, *Heegner points and derivatives of L-series*, Invent. Math. **84** (1986), 225–320.

[21] J. B. Conrey, *More than two fifths of the zeros of the Riemann zeta function are on the critical line*, J. Reine Angew. Math. **399** (1989), 1–26.

[22] D. R. Heath-Brown, *Kummer's conjecture for cubic Gauss sums*, Israel J. Math. **120** (2000), 97–124.

[23] J. B. Conrey and H. Iwaniec, *The cubic moment of central values of automorphic L-functions*, Ann. of Math. (2) **151** (2000), 1175–1216.

[24] H. H. Kim, *Functoriality for the exterior square of* GL_4 *and the symmetric fourth of* GL_2, J. Amer. Math. Soc. **16** (2003), 139–183, with Appendix 2 by H. H. Kim and P. Sarnak, 175–181.

[25] J. Bourgain, *Decoupling, exponential sums and the Riemann zeta function*, J. Amer. Math. Soc. **30** (2017), 205–224.

[26] I. Petrow and M. P. Young, *The Weyl bound for Dirichlet L-functions of cube-free conductor*, Ann. of Math. (2) **192** (2020), 437–486.

[27] L. Guth and J. Maynard, *New large value estimates for Dirichlet polynomials*, arXiv:2405.20552 (2024).